AFOSR-TR- 89-0048

THE EFFECT OF PRESSURE AND DEVIATORIC STRESS ON ROCK MAGNETISM

Approved for public release;
distribution unlimited.

APPLIED RESEARCH ASSOCIATES

NER New England Research

THE EFFECT OF PRESSURE AND DEVIATORIC STRESS ON ROCK MAGNETISM

sponsored by

AIR FORCE OFFICE OF SCIENTIFIC RESEAECH
BOLLING AIR FORCE BASE
WASHINGTON, D. C.

October 31, 1988

prepared by

Randolph J. Martin, III
New England Research, Inc.
P.O. Box 857
Norwich, VT 05055

UNCLASSIFIED
SECURITY CLASSIFICATION OF THIS PAGE

ADA204622

REPORT DOCUMENTATION PAGE

Form Approved
OMB No. 0704-0188

1a. REPORT SECURITY CLASSIFICATION UNCLASSIFIED	1b. RESTRICTIVE MARKINGS
2a. SECURITY CLASSIFICATION AUTHORITY	3. DISTRIBUTION/AVAILABILITY OF REPORT Approved for Public Release; Distribution Unlimited
2b. DECLASSIFICATION/DOWNGRADING SCHEDULE	
4. PERFORMING ORGANIZATION REPORT NUMBER(S)	5. MONITORING ORGANIZATION REPORT NUMBER(S) AFOSR-TR- 89 0048
6a. NAME OF PERFORMING ORGANIZATION APPLIED RSCH ASSOCIATE New England Research, Inc. — 6b. OFFICE SYMBOL (If applicable)	7a. NAME OF MONITORING ORGANIZATION AFOSR/NA
6c. ADDRESS (City, State, and ZIP Code) P.O. Box 857 Norwich, Vermont 05055	7b. ADDRESS (City, State, and ZIP Code) Bldg. 410 Bolling AFB, DC 20332-6448
8a. NAME OF FUNDING/SPONSORING ORGANIZATION AFOSR — 8b. OFFICE SYMBOL (If applicable) NA	9. PROCUREMENT INSTRUMENT IDENTIFICATION NUMBER ~~AFSC~~ F 49620-85-C-0135
8c. ADDRESS (City, State, and ZIP Code) Bldg. 410 Bolling AFB, DC 20332-6448	10. SOURCE OF FUNDING NUMBERS PROGRAM ELEMENT NO. 6.1102F — PROJECT NO. 2302 — TASK NO. C1 — WORK UNIT ACCESSION NO.
11. TITLE (Include Security Classification) THE EFFECT OF PRESSURE AND (U) DEVIATORIC STRESS ON ROCK MAGNETISM	
12. PERSONAL AUTHOR(S) Randolph J. Martin, III	
13a. TYPE OF REPORT Final Technical — 13b. TIME COVERED FROM 9/85 TO 8/31/88 — 14. DATE OF REPORT (Year, Month, Day) October 31, 1988 — 15. PAGE COUNT 100	
16. SUPPLEMENTARY NOTATION	
17. COSATI CODES FIELD / GROUP / SUB-GROUP	18. SUBJECT TERMS (Continue on reverse if necessary and identify by block number) Piezomagnetism, Remanent magnetization, Magnetic susceptibility, Rock physics

19. ABSTRACT (Continue on reverse if necessary and identify by block number)

A series of experiments has been carried out on a wide variety of rock types to examine the effect of pressure and stress on their magnetic properties. Specifically, the effect of loading path on thermoremanent magnetization (TRM) and magnetic susceptibility have been examined in detail. For samples with a TRM, initial loading produced a pronounced decrease in magnetization. As the specimen was unloaded, very little recovery in magnetization was observed resulting in a permanent demagnetization at the termination of the cycle. Furthermore, differential stress produced a larger demagnetization than hydrostatic pressure. Demagnetizations of approximately 20% were observed during pressurization, while the change in magnetization approached 40% of a differential stress of 200 MPa. If the specimen was reloaded over the same path to the same stress, the change in magnetization was much smaller than for the initial cycle, and only a small

20. DISTRIBUTION/AVAILABILITY OF ABSTRACT ☒ UNCLASSIFIED/UNLIMITED ☐ SAME AS RPT. ☐ DTIC USERS	21. ABSTRACT SECURITY CLASSIFICATION UNCLASSIFIED
22a NAME OF RESPONSIBLE INDIVIDUAL Major Steven C. Boyce	22b TELEPHONE (Include Area Code) (202) 767-4963 — 22c OFFICE SYMBOL AFOSR/NA

DD Form 1473 JUN 86

SECURITY CLASSIFICATION OF THIS PAGE
UNCLASSIFIED

additional increment of demagnetization was observed at the end of the cycle. If the peak stress was augmented, once the peak stress from the previous cycle was exceeded, the stress sensitivity increased noticeably. Upon unloading, there was a pronounced hysteresis and additional permanent demagnetization at zero stress.

In addition to considering the total intensity of the remanent moment, the components of magnetization parallel and normal to the axis of the cylindrical specimen were studied. As the inclination of the magnetic vector rotated away from the cylinder axis, changes in both components became more important. By continuously measuring the axial and transverse components of the remanent vector as a function of stress and pressure, it was possible to determine if significant rotations of the magnetic vector accompanied a reduction in intensity. For specimens loaded in hydrostatic compression, no rotation of the magnetic vector was evident and the rock simply demagnetized in direct proportion to the applied pressure.

During uniaxial compression, however, small rotations of the magnetic moment, on the order of three degrees, were observed during the loading portion of the initial cycle. During subsequent cycles conducted in uniaxial compression to the same peak stress, the orientation of the vector remained stable.

For a rock stressed in the presence of a fixed field, a decrease in magnetization resulted. Since the field is constant, the change in magnetization is directly proportional to the change in susceptibility. Consequently, in most discussions, susceptibility is discussed rather than the induced magnetization. Differential stress causes magnetic susceptibility to decrease monotonically with increasing load. Several experiments were carried out to examine the effect of hydrostatic pressure on susceptibility. The results of these tests clearly indicate that hydrostatic pressure does not influence magnetic susceptibility.

Most susceptibility experiments are carried out for geometries where the inducing field is parallel to the greatest principal stress direction. However, with the application of load, an anisotropy is introduced into the rock, and the transverse component of susceptibility must be considered. A series of experiments were carried out where the inclination of the inducing field was not coincident with the uniaxial stress axis. The results of these tests show that the two components of magnetization could be determined by analyzing the observed magnetization as a function of sample geometry.

The experimental results may be interpreted in terms of domain characteristics. Direct observation of domain behavior during cyclic loading has been carried out by *Boyd et al.*,(1984). They studied the motion and nucleation of magnetic domains as a function of applied stress. Tests on pseudosingle domain magnetite titanomagnetite assemblages showed that at very low stresses walls were nucleated. As the stress was augmented, additional domains nucleated and the domains adjusted to achieve a lower energy configuration. When the stress was removed, the domain pattern was irreversibly changed. *Halgedahl and Fuller* (1983) observed a similar effect due to the application of large magnetic fields. The piezomagnetic effect is discussed in terms of these observations.

Table of Contents

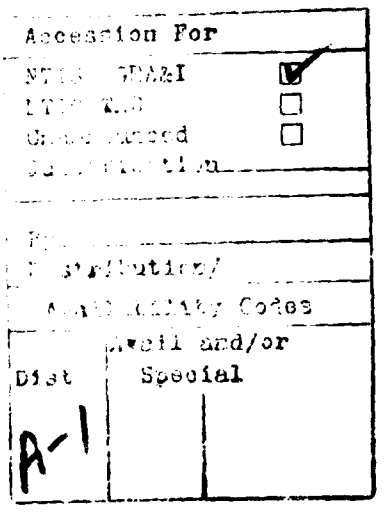

Summary

A series of experiments has been carried out on a wide variety of rock types to examine the effect of pressure and stress on their magnetic properties. Specifically, the effect of loading path on thermoremanent magnetization (TRM) and magnetic susceptibility have been examined in detail. For samples with a TRM, initial loading produced a pronounced decrease in magnetization. As the specimen was unloaded, very little recovery in magnetization was observed resulting in a permanent demagnetization at the termination of the cycle. Furthermore, differential stress pr duced a larger demagnetization than hydrostatic pressure. Demagnetizations of approximately 20% were observed during pressurization, while the change in magnetization approached 40% of a differential stress of 200 MPa. If the specimen was reloaded over the same path to the same stress, the change in magnetization was much smaller than for the initial cycle, and only a small additional increment of demagnetization was observed at the end of the cycle. If the peak stress was augmented, once the peak stress from the previous cycle was exceeded, the stress sensitivity increased noticeably. Upon unloading, there was a pronounced hysteresis and additional permanent demagnetization at zero stress.

In addition to considering the total intensity of the remanent moment, the components of magnetization parallel and normal to the axis of the cylindrical specimen were studied. As the inclination of the magnetic vector rotated away from the cylinder axis, changes in both components became more important. By continuously measuring the axial and transverse components of the remanent vector as a function of stress and pressure, it was possible to determine if significant rotations of the magnetic vector accompanied a reduction in intensity. For specimens loaded in hydrostatic compression, no rotation of the magnetic vector was evident and the rock simply demagnetized in direct proportion to the applied pressure.

During uniaxial compression, however, small rotations of the magnetic moment, on the order of three degrees, were observed during the loading portion of the initial cycle. During subsequent cycles conducted in uniaxial compression to the same peak stress, the orientation of the vector remained stable.

For a rock stressed in the presence of a fixed field, a decrease in magnetization resulted. Since the field is constant, the change in magnetization is directly proportional to the change in susceptibility. Consequently, in most discussions, susceptibility is discussed rather than the induced magnetization. Differential stress causes magnetic susceptibility to decrease monotonically with increasing load. Several experiments were carried out to examine the effect of hydrostatic pressure on susceptibility. The results of these tests clearly indicate that hydrostatic pressure does not influence magnetic susceptibility.

Most susceptibility experiments are carried out for geometries where the inducing field is parallel to the greatest principal stress direction. However, with the application of load, an anisotropy is introduced into the rock, and the transverse component of susceptibility must be considered. A series of experiments were carried out where the inclination of the inducing field was not coincident with the uniaxial stress axis. The results of these tests show that the two components of magnetization could be determined by analyzing the observed

magnetization as a function of sample geometry.

The experimental results may be interpreted in terms of domain characteristics. Direct observation of domain behavior during cyclic loading has been carried out by *Boyd et al.*,(1984). They studied the motion and nucleation of magnetic domains as a function of applied stress. Tests on pseudosingle domain magnetite titanomagnetite assemblages showed that at very low stresses walls were nucleated. As the stress was augmented, additional domains nucleated and the domains adjusted to achieve a lower energy configuration. When the stress was removed, the domain pattern was irreversibly changed. *Halgedahl and Fuller* (1983) observed a similar effect due to the application of large magnetic fields. The piezomagnetic effect is discussed in terms of these observations.

Introduction

For decades magnetic changes prior to tectonic and concurrent explosive events have been observed. *Smith and Johnston* (1976) observed a 1.8 gamma field change prior to the 1975 Thanksgiving day earthquake near Hollister, CA. *Mitzutani and Ishido* (1976) studied the magnetic changes associated with the Matsushiro earthquakes swarm in 1966. *Hasbrouck and Allen* (1972) reported large magnetic changes, up to 30 gammas, associated with the CANNIKIN explosion in Amchitka. These well documented changes in the earth's magnetic field suggest that some phenomena is perturbing the magnetization of the rocks prior to and coincidentally with a redistribution of the stress field in the vicinity of the observation. In the case of the Matsushiro swarm, *Ishido and Mitzutani* (1981) have proposed that the change in the magnetic field was primarily do to an electrokenetic effect associated with fluid flow in the epicentral region; *Martin et al* (1982) experimentally corroborated the electrokenetic effect. While fluid flow may explain some magnetic field changes, in the absence of flow the most probable reason for the anomalous behavior is a change in the local stress field.

Many investigators have observed changes in rock magnetization due to application of stress *(Ohnaha, and Kinoshita, 1968; Nagata, 1969; Nagata and Carleton, 1969; Ohnaha, 1969; Martin and Wyss, 1975; Jelenska, 1975; Kean et al., 1976; Martin et al., 1976; Martin, 1980).* The total magnetization of a rock is the vectorial sum of the remanent magnetization and the induced magnetization. The remanent magnetization is the magnetization a material possesses in the absence of an external field, whereas the induced magnetization is proportional to the applied field. Both remanent and induced magnetization change with applied stress, but only the induced magnetization is totally recoverable. When a rock with a remanent moment is initially loaded in compression, it begins to demagnetize; however, upon unloading the magnetization does not return to its initial value but exhibits a permanent demagnetization. The change of intensity at the termination of the stress cycle is a function of the maximum stress that the specimen experiences, the initial remanent moment, the magnetic grain size, and the orientation of the magnetic vector with respect to the greatest principal stress direction.

Martin and Wyss (1975) observed that when a sample was loaded cyclically in compression with the peak stress augmented for each cycle, the total magnetization of the specimen at the termination of each loading cycle decreased. This result is shown in Figure 1-1 for a gabbro sample from Rapidan, Virginia, loaded cyclically in uniaxial compression. The magnetization parallel to the loading axis is plotted as a function of stress. The remanent vector for this sample was parallel to the loading axis. Stress cycling continually reduced the zero

stress value of remanent magnetization. In a very real sense then the piezomagnetic effect reported in this study demonstrated the potential of remanent magnetization as a means of measuring the peak stress developed in the material. Quite simply, if the initial and final magnetization of a rock sample were known, a calibration similar to that in Figure 1-1 could be carried out and the peak stress that the rock has experienced readily determined. Furthermore, it demonstrates that while the first excursion to high stress results in permanent demagnetization upon unloading, subsequent stress cycling to the same stress level result in reproducible stress vs magnetization curves with little or no permanent demagnetization at the end of a loading cycle. The piezomagnetic effect is pronounced in rocks with pseudo-single-domain and multidomain magnetic grains with a low titanium content. The titanomagnetite grains that exhibit the optimum piezomagnetic effect have mean diameters between 10 and 20 microns and a Curie temperature of near 550°C. The piezomagnetic effect is controlled by movement of the domain walls within the magnetic minerals. On the first loading cycle, the movement of the domain walls has a large irreversible component *(Boyd et al., 1984).* Subsequent stress excursions to the same or lower level yield reversible domain wall motion. Second, the optimum piezomagnetic effect is observed when the greatest principal stress direction and the remanent moment are coincident or do not differ by more than 15° for five hundred MPa of stress. Rotation is typically away from the greatest principal stress direction. Finally, *Pike et al., 1981* noted that the demagnetization described above cannot distinguish between pressure and differential stress; it appears to respond to the total stress that has been applied to the material.

There has been an appreciable amount of effort devoted to the effect of stress on both remanent magnetization and susceptibility. In spite of this research, our understanding of the phenomena is still incomplete. While it has been adequately demonstrated, the domain wall nucleation and movement are responsible for the variation in magnetization in titano-magnetite grains, *(Halgedahl and Fuller, 1983; Boyd et al., 1984),* the relative contribution of stress path on remanent intensity or magnetic susceptibility has not been clearly established, either theoretically or experimentally. It would be of interest to know, for example, if hydrostatic stress produces magnetic changes equivalent to those observed due to a nonhydrostatic change in stress. Furthermore, it has been observed that the magnetic vector for both remanent magnetization and induced magnetization rotates with respect to the principal stress axis, as well as changing intensity with the application of differential stress. The question then arises, "How does the inclination of the magnetic vector with respect to the direction of the greatest principal stress direction affect the piezomagnetic response? In order to systematically examine these effects, a suite of experiments has been carried out over three different loading histories:

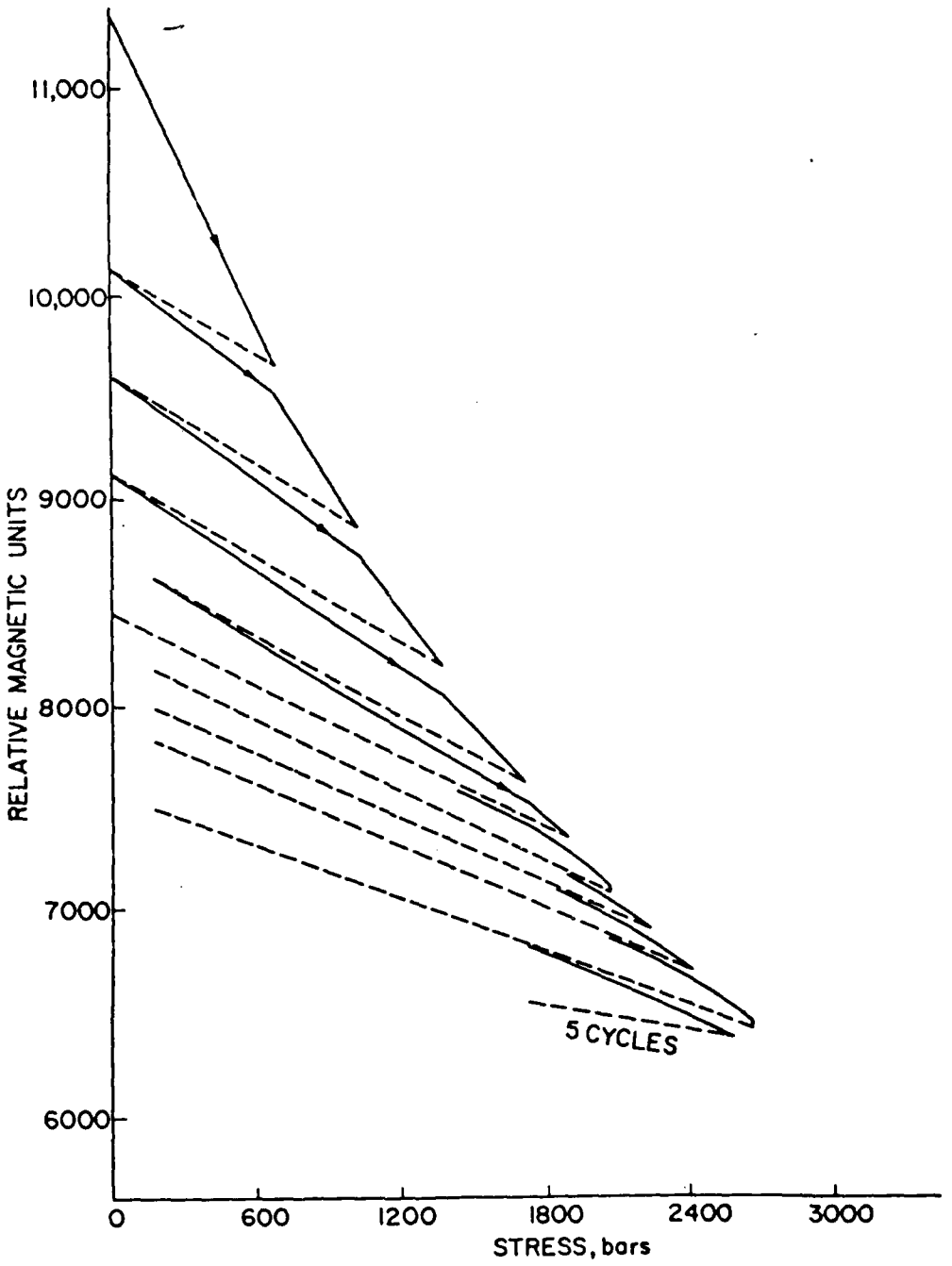

Figure 1-1 Change in the axial component of the remanent vector for a gabbro specimen cyclically loaded in uniaxial compression (from *Martin and Wyss*, 1975).

hydrostatic compression, confined compression, and uniaxial strain for well characterized rocks.

A number of additional fundamental gaps persist in our understanding of piezomagnetism. For example, with regards to remanence, it is of interest to know if the stress sensitivity increases with increasing initial magnetic intensity. Can permanent changes in rock magnetism due to differential stress be separated from those due to hydrostatic loading? What happens when the remanent magnetic vector is not parallel to the greatest principal stress direction; can the rotation of the magnetic vector be used to infer principal stress directions, as well as the magnitude of the stresses? With these questions in mind, a program was initiated aimed at resolving these topics and placing a stronger scientific foundation under the piezomagnetic response of rock.

Rock Properties and Experimental Procedure

In order to conduct meaningful piezomagnetic experiments on a rock with a significant percentage of titanomagnetite grains, the magnetic mineralogy must be well characterized. The magnetic properties of five rock types considered as potentially suitable for piezomagnetic studies are given in Table 1. These five rock types, a gabbro (Rapidan, VA), the Ralston diabase (Golden, CO), a basalt (Dotzero, CO), a granite (Westerly, RI), and an andesite (Mt. St. Helen's, WA) were selected for two important reasons. First, other investigators have used these rocks in previous studies (other than piezomagnetism); consequently there was existing database for these rocks. Second, homogeneous blocks of each rock could be readily obtained. Large blocks are necessary to obtain large numbers of reproducible specimens. In Table I, the magnetic susceptibility, the coercivity, the Curie temperature, the saturation magnetization, and the grain size for each of the five rocks is given. The *magnetic susceptibility* is the ratio of the observed magnetization to the applied magnetic field. As the field strength increases, the magnetization of the material increases with the susceptibility serving as a proportionality constant. At low field strengths, up to 100 Oe, the relationship between applied field and induced magnetization is linear and consequently, the magnetic susceptibility is treated as a constant.

The *coercivity* is a measure of resistance to movement of the domain walls of the magnetic minerals. When a specimen is alternatively driven to magnetic saturation in a positive and the a negative field, hysteresis is prominent. The value of the magnetic field at which the total magnetic induction, **B**, decreases to zero is termed the coercivity. ($\mathbf{B} = \mathbf{H} + 4\pi\mathbf{J}$, where **H** is the applied magnetic field and **J** is the magnetization of the rock).

The *Curie temperature* is the temperature at which the remanent magnetization drops to zero; i.e. the domains in the magnetic grains are randomly oriented. It has been shown that the Curie temperature is an excellent indicator of composition of titanomagnetite grains. Figure 1-2 gives the change in magnetization with increasing temperature for Rapidan gabbro. The magnetization decreases nearly linearly with increasing temperature up to 475°C and then rapidly decreasing to several tenths of an emu/g at 575°C. The temperature at which the magnetization precipitously decreases is reported as the Curie temperature.

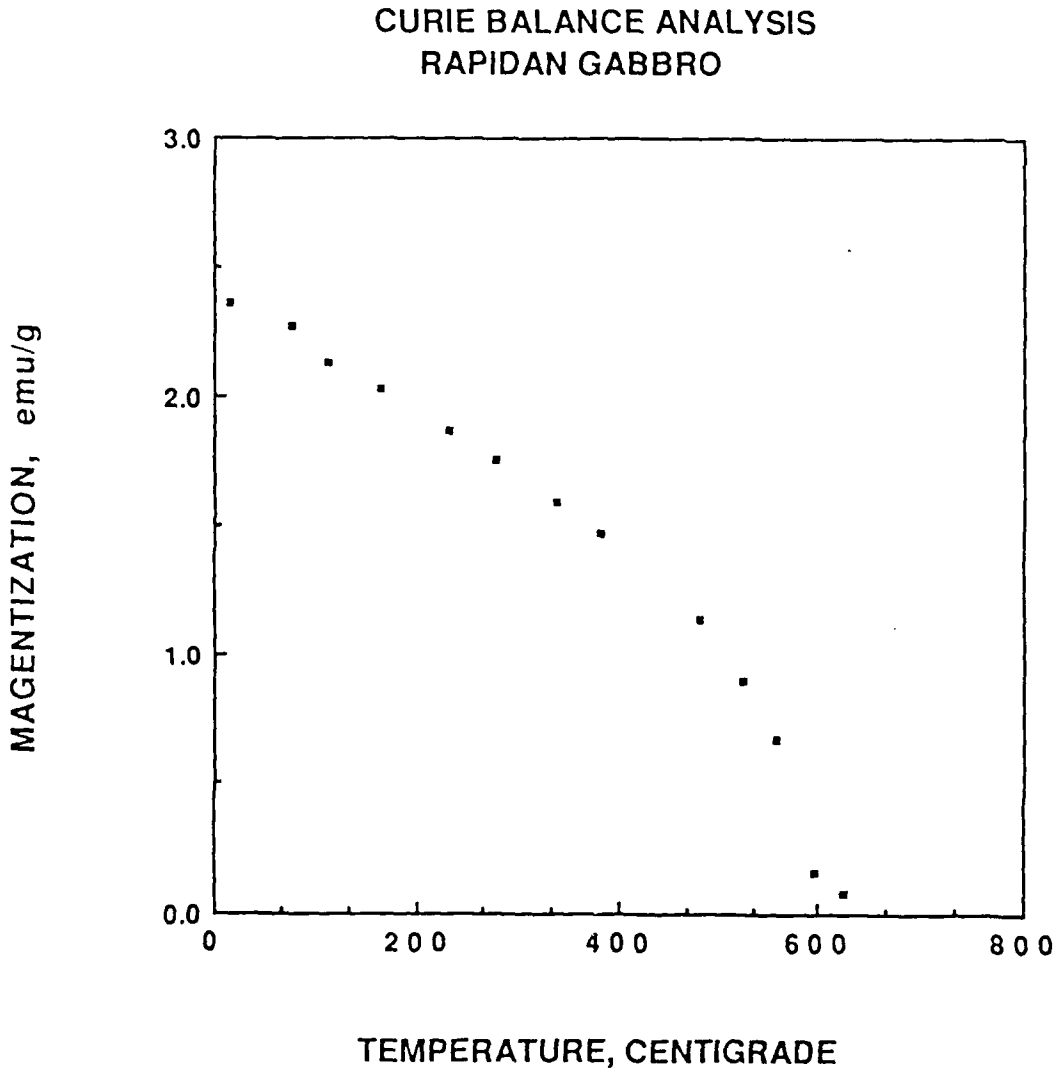

Figure 1-2 Change in magnetization of Rapidan gabbro as a function of temperature.

The Curie temperatures of all five rock types were very close, varying between 530 and 580°C. This indicates that the composition of the magnetic grains are similar. Titanomagnetite forms a solid solution series with end member of Fe_2TiO_4, ulvospinel, (Curie temperature 120°C) and Fe_3O_4, magnetite, (Curie temperature 580°C). As the composition moves from pure magnetite to ulvospinel, the Curie temperature decreases linearly with increasing titanium content. Based on the Curie temperatures observed on the five rock types listen in Table I, the composition of magnetic mineralogy is almost pure magnetite; only the magnetic carriers in the diabase contain a significant amount of titanium.

The *saturation magnetization* is the maximum magnetization that the sample acquired in an applied field of 15,000 Oe. Typically about 50 percent of the saturation magnetization develop with the application of a field of several hundred Oersted (Oe). The magnetic saturation reported is for the bulk sample, an aggregate of silicates minerals and titanomagnetite grains. For comparison, the saturation magnetization of iron (Fe) is 218 emu/g and for single crystal magnetite (Fe_3O_4) is 92 emu/g. Since the magnetic minerals constitute between 2 and 6 percent of the rocks by volume, saturation magnetization in the vicinity several emu/g are reasonable.

One of the most important characteristics of rocks exhibiting a piezomagnetic effect is the presence of pseudo-single-domain magnetic grains. Magnetic grains can be conveniently described as either single domain, pseudo-single-domain or multidomain. For a fixed titanomagnetite composition, as the grain size increases from 0.1 to 200 microns several pronounced changes occur: the number of domains increases, the coercivity decreases and the stability of the remanence decreases. For magnetite, single domain behavior is observed when the mean diameter is between 0.1 and 5 microns *(Dunlop, 1973, Day, 1973)*. The transition from pseudo-single-domain to multidomain grains occurs at grain sizes of 15 to 40 microns. Single domain have high coercivities (10^3 Oe) and stable or hard remanence. Multidomain grains exhibit low coercivities (several tens of Oe) and unstable or soft remanence. Pseudo-single-domain magnetization is observed in grains 1-30 microns and in size is characterized by coercivities of 100 Oe or so. Pseudo-single-domain grains are the stable carriers of the remanent moment. They remain largely unaffected by small changes in field strength (at temperatures well below the Curie temperature) but are responsible for the most reproducible piezomagnetic effects *(Nagata and Carleton, 1969; Ohnaka, 1969; Kean et al., 1976; Martin et al., 1976)*.

The five rocks listed in Table I possess pseudo-single-domain grains. The magnetization of the basalt and andesite is most certainly controlled by pseudo-single-domain magnetic minerals. The diabase, gabbro and granite contain pseudo-single-domain as well as

TABLE I

MAGNETIC PROPERTIES

ROCK TYPE and LOCALITY	SUSCEPTIBILITY emu/g/Oe x 10^{-3}	COERCIVITY Oe	SATURATION MAGNETIZATION emu/g	CURIE TEMPERATURE ^{o}C
Gabbro Rapidan,VA	1.79	47.5	2.36	579
Ralston Diabase Golden, CO	154	3	2.90	535
Andesite Mt. St. Helen's, OR	0.46	181	1.19	
Tuff Bandelier, NM	0.28	209	0.72	
Granite Westerly, RI	0.36	42	0.64	576
Basalt Dotzero, CO	1.45	183	3.92	570

multidomain titanomagnetite grains. This can be inferred from the distribution of magnetic grain diameters and the somewhat low coercivities of 42 and 47.5 Oe for the granite and gabbro respectively. The coercivity of the diabase is reported as nearly zero Oersteds. This is anomalously low and consequently the value is suspect. The determination of coercivity and saturation magnetization were made in facilities developed by L.N. Mulay at the College of Earth and Mineral Sciences, The Pennsylvania State University, University Park, Pennsylvania.

Of the five rocks listed in Table I, only three appear well suited for the study of piezoremanence: the basalt, the gabbro, and the diabase. All three have pseudo-single-domain grains, and a high saturation magnetization. Since one key aspect of this study is to examine the influence of remanent intensity on the piezomagnetic effect, a large saturation moment was essential. All five rock types were used for the influence of stress on magnetic susceptibility.

The composition of all the rocks studied was restricted to rocks in the titanomagnetite solid solution series. These oxides most commonly occur uniformly dispersed in igneous rocks. Their ready accessibility in a naturally occurring *ceramic type* host made them ideally suited for study.

It was of interest to know how the magnitude of the piezomagnetic effect depended on the initial remanent intensity and the mode of deformation. In most studies of remanent magnetism in rocks, the intensity developed as the rock cools through the Curie point in 0.5 Oe field (the Earth's magnetic field) is of primary importance. However, it is logical to ask if increasing the initial remanent intensity will increase the stress sensitivity? Is the piezomagnetic change greater when the remanent moment was larger? Does hydrostatic loading produce the same change per increment of stress as non-hydrostatic loading? In order to answer these questionS, rock cores were prepared in a uniform manner with varying remanent intensities and then stressed in a field free, non-magnetic test apparatus.

For the remanence experiments, the rock specimens were ground, right circular cylinders 4.13 cm in length and 1.79 cm in diameter. A thermoremanent magnetization (TRM) was developed in each sample. First, the sample was heated to 600°C, a temperature well above the Curie temperature. The specimens were heated in a furnace fitted into a two layer mu-metal shield which reduced the magnetic field inside the shield to less than 100 gammas (nT). The Furnace coils were wound non-inductively to prevent generating a magnetic field when the furnace was in operation. After the sample reached 600°C, the furnace was turned off. Simultaneously, two Helmholtz coils which surround the furnace and are inside the mu-metal shield were energized to magnetize the rock as they cooled through their Curie temperature. The coils had a radius of 8.89 cm and had a separation distance of 8.89 cm. Each coil

consisted of 371 turns of No. 22 copper magnet wire. Helmholtz coils generate a very uniform magnetic field along the axis of a two coil system. In order to develop a uniform remanent magnetization in each sample, the rock cores were located in the center of the cavity between the coils with the axis of the sample parallel to that of the magnetic field. A DC voltage was applied to the Helmholtz coils sufficient to produce a magnetic field of up to 100 Oe along the axis of the system using a Hewlett Packard 0-24 volt power supply.

To prevent the magnetic mineralogy from oxidizing as the samples were heated to 600°C, the oxygen fugacity in the furnace was controlled. For the titanomagnetite composition of the rocks used in this study, the stability field at 600°C requires a fugacity, f_{O_2}, between 10^{20} and 10^{23}. Tests were carried out using argon to control the fugacity. Argon was streamed into the furnace assembly at a rate of 1.0 l/min at a small positive pressure. (The gas was dried as it flowed through a desecant prior to entering the furnace.) This technique resulted in an oxygen fugacity of 10^{20} at 600°C, *(Larson et al., 1975)*.

Since the observed fugacity was on the low end of the stability field, samples were studied after high temperature excursions for signs of oxidation. Specifically, the Rapidan gabbro was examined in detail. Samples were heated to 600°C in the furnace under ambient atmospheric conditions and under a controlled oxygen fugacity and then compared with virgin samples. A visual inspection showed that the samples heated under controlled conditions were indistinguishable from the virgin samples, whereas the samples heated under atmospheric condition exhibited marked oxidation. Thin sections were prepared from these samples and compared with samples that had not been heated. There were no visible differences. Only the specimen heated under ambient laboratory conditions showed pronounced oxidation throughout the thin section. Based on this observation, all samples were heated in an argon environment.

Next, the remanent intensity and orientation of the magnetic moment was measured with an array of fluxgate magnetometers in a mu-metal shield. By varying the field developed by the Helmholtz coils up to 100 Oe remanent intensities up to 0.058 emu/cm^3 have been developed in the diabase and 0.148 emu/cm^3 have been achieved in the gabbro. The thermoremanent intensity of the diabase is nearly a factor of two lower than that for the gabbro although the TRM was induced at the same field strength. This is consistent with the fact that the magnetic susceptibility of the gabbro is slightly greater than twice that of the diabase. No attempt has been made to increase the remanent intensities beyond those developed in an inducing field of 100 Oe. The emphasis has been to study only samples that exhibit stable remanent moments. The orientation of the remanent vector is controlled by orienting the specimens within the furnace such that the core axis is inclined to the axis of the magnetic field.

All the deformation tests were conducted in a 200 MPa beryllium copper pressure vessel as shown in Figure 1-3. All the component parts of the pressure vessel were fabricated of beryllium copper hardened to R_C=39. Beryllium copper was used because it has a small remanent magnetization (10^{-6} emu/cm^3) and a low magnetic susceptibility. The pressure vessel was encased in a two-layer mu-metal shield which attenuated the external field to several hundred gammas. The pressure vessel, encased in the mu-metal shield, was bolted into a hydraulic press fitted with a beryllium copper end plate. The conventional mild steel end plate was replaced with a beryllium copper end plate because nonreproducible, viscous remanent magnetic variation *leaked* into the test vessel through the opening in the cap on the mu-metal shield, making reliable magnetic measurements difficult.

A schematic diagram of the sample assembly and flux gate magnetometer sensors is also shown in Figure 1- 3. Beryllium copper spacers were positioned at each end of the sample, and all three pieces were jacketed in 0.13 mm thick copper. The sealed sample was then clamped to the base plug, inserted in the pressure vessel, and a confining pressure of up to 200 MPa was imposed. A differential stress was applied to the sample by advancing the piston of the hydraulic cylinder driven with an air hydraulic booster. The force on the sample was measured to an accuracy of 1% with an external load cell.

The change in each component of the remanent magnetic vector of the sample was measured with unpotted flux gate magnetometer heads supported with a nylon holder. The magnetometers were Schonstedt DM-2220 digital magnetometers with a resolution of 1 gamma over the range of 0-2000 gamma. Two pairs of magnetometers were positioned as shown in Figure 1-3. One pair measured the axial and radial component of magnetization of the rock sample. The second set of magnetometers was positioned around a beryllium copper cylinder to monitor changes in the axial and radial component of the magnetic field inside the vessel during a loading cycle. The axial magnetometers were positioned as far away from each other as possible so that the magnetometers would not interact and the remanent magnetization of the sample would not bias the background field measurement in the beryllium copper vessel. The change in remanent magnetization of the rock as a function of stress could be simply obtained with the use of these four magnetometers. This was accomplished by subtracting the axial and radial magnetometer readings for the rock sample from axial and radial readings obtained in proximity to the beryllium copper cylinder. Magnetic susceptibility as a function of stress was measured with two similar transformer assemblies. For the case where the axis of the inducing field was parallel to that of the greatest principal compressive stress, the tests were conducted as a function of confining pressure in the beryllium copper pressure vessel of loading frame described above. A second set of susceptibility tests were run in uniaxial compression with

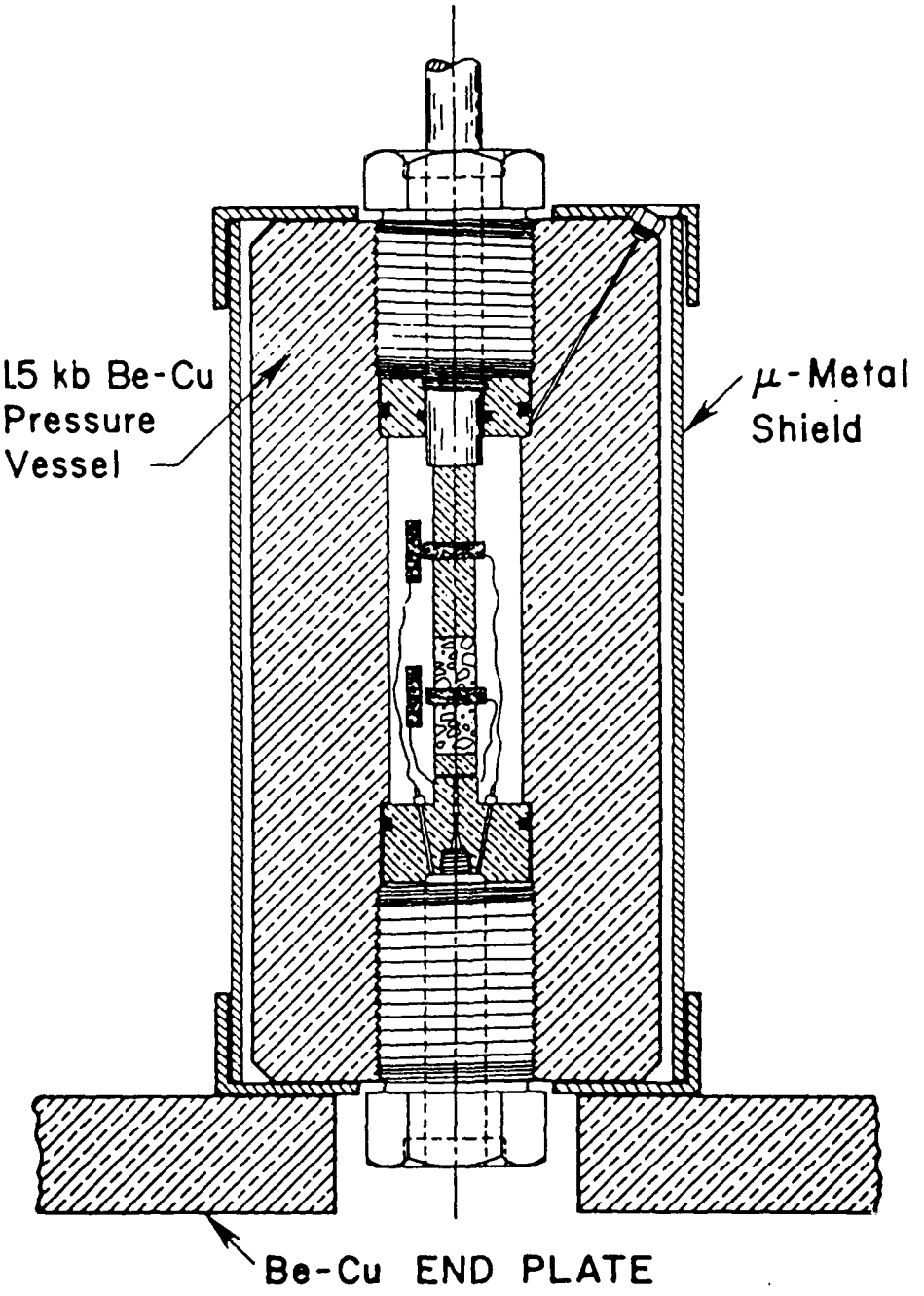

Figure 1-3 Scale diagram of the pressure vessel sample assembly and fluxgate magnetometer array used in studying the effect of pressure and differential stress on rock magnetism.

varying angular relations between the axis of the inducing field and the greatest principal stress direction. A different transformer array was fabricated for these tests.

All the high pressure susceptibility measurements were carried out on ground, right circular specimens 1.52 cm in diameter and 4.12 cm in length. A typical experiment consisted of step wise loading the sample to 90 to 95 percent of its fracture strength, and then unloading. Each stress increment was approximately 20 MPa. At each stress level the axial force, axial and circumferential strain, and either the axial susceptibility or the axial and radial components of the remanent magnetization were measured. The confining pressure was independently controlled and continuously monitored with a 200 MPa Heise gauge.

The susceptibility measurements were carried out in a bridge apparatus modified after the design of *Christie and Symons* (1969). Figure 1-4 is a schematic diagram of the susceptibility bridge. The bridge was a transformer balance in which the internal oscillator of a Princeton Applied Research (PAR) lock-in amplifier (Model 124A with model 116 differential preamplifier) was used to excite the primary coils of the measuring transformer and the reference transformer. The net in-phase signal picked up by the two secondary coils connected in series opposition was returned to the amplifier input where it passed through a transformer, a linear amplifier, a narrow-band filter, a phase-sensitive detector for comparison with the output phase, and finally to a d.c. voltmeter and a strip chart recorder. Each primary coil consisted of two Helmholtz coils with 1000 turns of No. 40 enameled wire wound on a nylon form 5.40 cm in diameter, separated by 4.13 cm and driven at a frequency of 1000 Hz with the PAR output adjusted to generate a field of 0.5 Oe. The secondary coil, positioned in the center of the coaxial Helmholtz coils, had 1000 turns of No. 40 enameled wire wound on a diameter of 3.00 cm.

The axial susceptibility is determined by first balancing the output of the secondary coils, and then inserting the sample into the axial cavity of one nylon coil form The sample generates an imbalance in the output of the secondary coils which is proportional to the susceptibility of the sample. The bridge was calibrated with a series of powders containing various percentages of titanomagnetite grains. The low field susceptibility of these powders was determined by the National Bureau of Standards, Boulder, Colorado.

With the sample emplaced, one sensing head was inserted into the pressure vessel while the reference coil assembly remained outside the pressure vessel. The vessel was pressurized to the desired confining pressure, the secondary coils were once again balanced, and then cyclic deformation tests were carried out. The amount of imbalance during loading and unloading is a measure of the change in axial susceptibility.

Samples were prepared for each susceptibility test in the following manner. Two strain

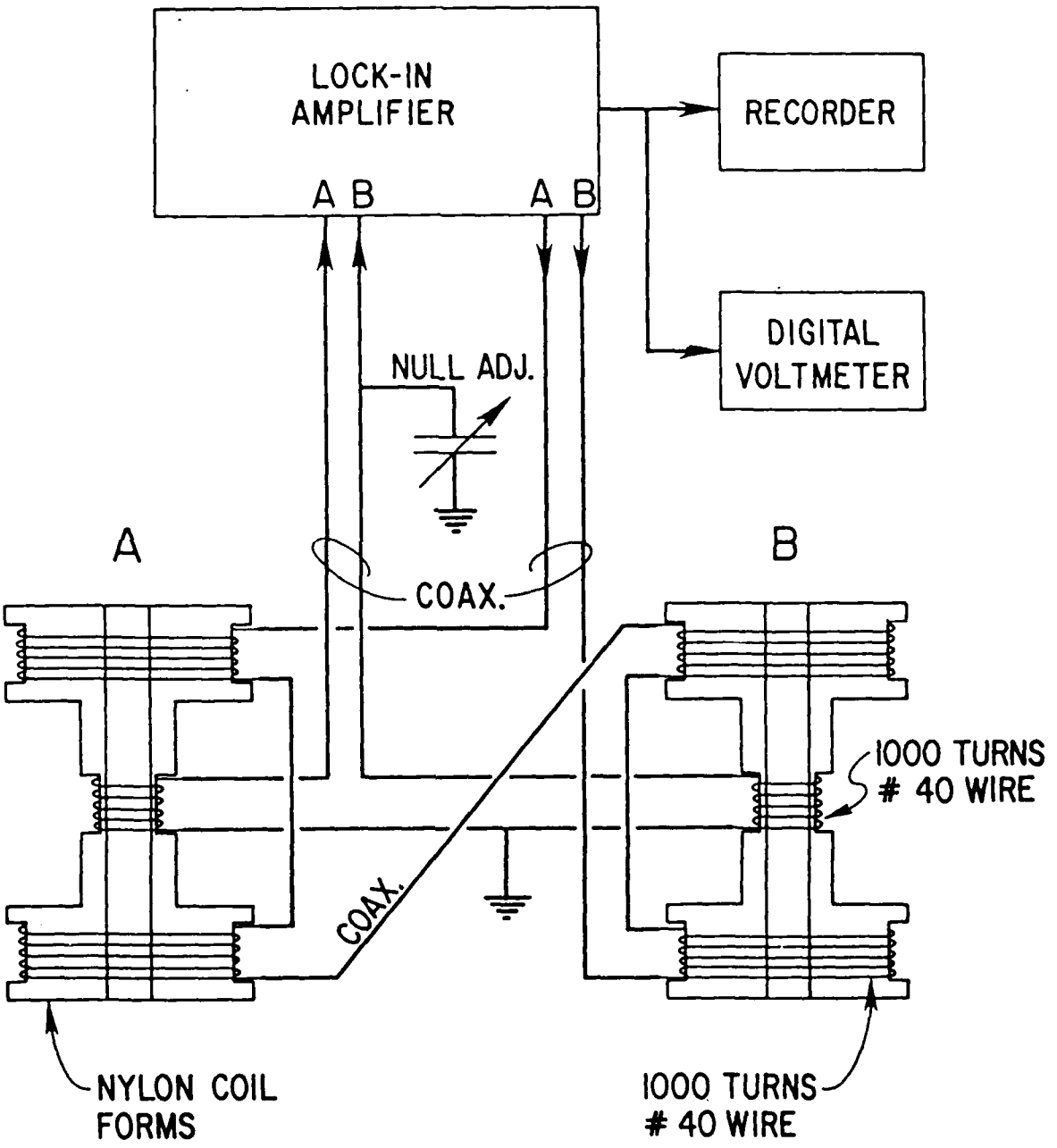

Figure 1-4 Schematic diagram of the transformer assembly used to measure magnetic susceptibility.

gauges were epoxied to the rock specimen, one axial and one circumferential. The sample was then wrapped with a thin sheet of teflon to reduce the friction between the jacket and the strain gauges, and inserted in a polyurethane jacket. Two lucolux spacers were positioned to keep conductive material away from the end of the sample. The jacket was then sealed by epoxying hardened steel plugs to the open ends of the jacket. A schematic diagram of the sample assembly and transformer is given in Figure 1-5.

For the susceptibility measurements where the axis of the inducing field and the direction of the greatest principal stress direction were not coincident, a modification of the apparatus described above was employed. The transformer surrounding the sample was capable of being inclined up to 35° with respect to the axis of uniaxial loading. In this transformer array, each primary coil consisted of 2 Helmholtz coils, with 1,000 turns of No. 30 enamel wire would on a nylon form 9.32 cm in diameter, separated by 5.59 cm, and driven at a frequency of 1,000 Hz with the lock-in amplifier output adjusted to generate a field of 0.5 Oe. The secondary coils, positioned in the center of the coaxial Helmholtz coils, had 1,000 turns of No. 30 enamel wire wound on a diameter of 6.99 cm. The sample and measuring transformer geometry are shown in Figure 1-6.

The reference transformer was isolated and the measuring transformer was inserted into the small deformational press. The air space in the coils of the measuring transformer allowed it to be inclined 35° with respect to the loading axis of the sample. The angle of inclination is shown in Figure 1-6. The inclination was measured to an accuracy of 0.25° using a protractor attached to the base of the measuring transformer. The samples were right circular cylinders 4.12 cm long and 1.52 cm in diameter and were positioned in the center of the measuring transformer coils. Lucolux end-caps were epoxied to the ends of the samples, and fillets of epoxy mixed with powered Al_2O_3 were formed over the interface to promote an even distribution of stress in the samples.

The force on the samples was measured to an accuracy of ±1% with an external load cell inserted between the piston of the press and the sample. The amplified output from the load cell, as well as that of the susceptibility bridge, was digitally recorded. Force was applied to the sample by advancing the piston of a hydraulic cylinder driven with an air hydraulic booster. The force was controlled by regulating the pressure of the gas in the booster. The samples were loaded and unloaded incrementally in steps of approximately 10 MPa. The strain in these experiments was not monitored.

The procedure was the same for each sample. Before the sample was inserted into the press, the output of the bridge was balanced (nulled) and the coils of the measuring transformer inclined at angles of 0, 5, 25, and 35°. The output of the bridge at each orientation was recorded. The sample was then inserted into the air space of the coils of the measuring transformer and the output of the bridge was again recorded for the same rotation. The initial

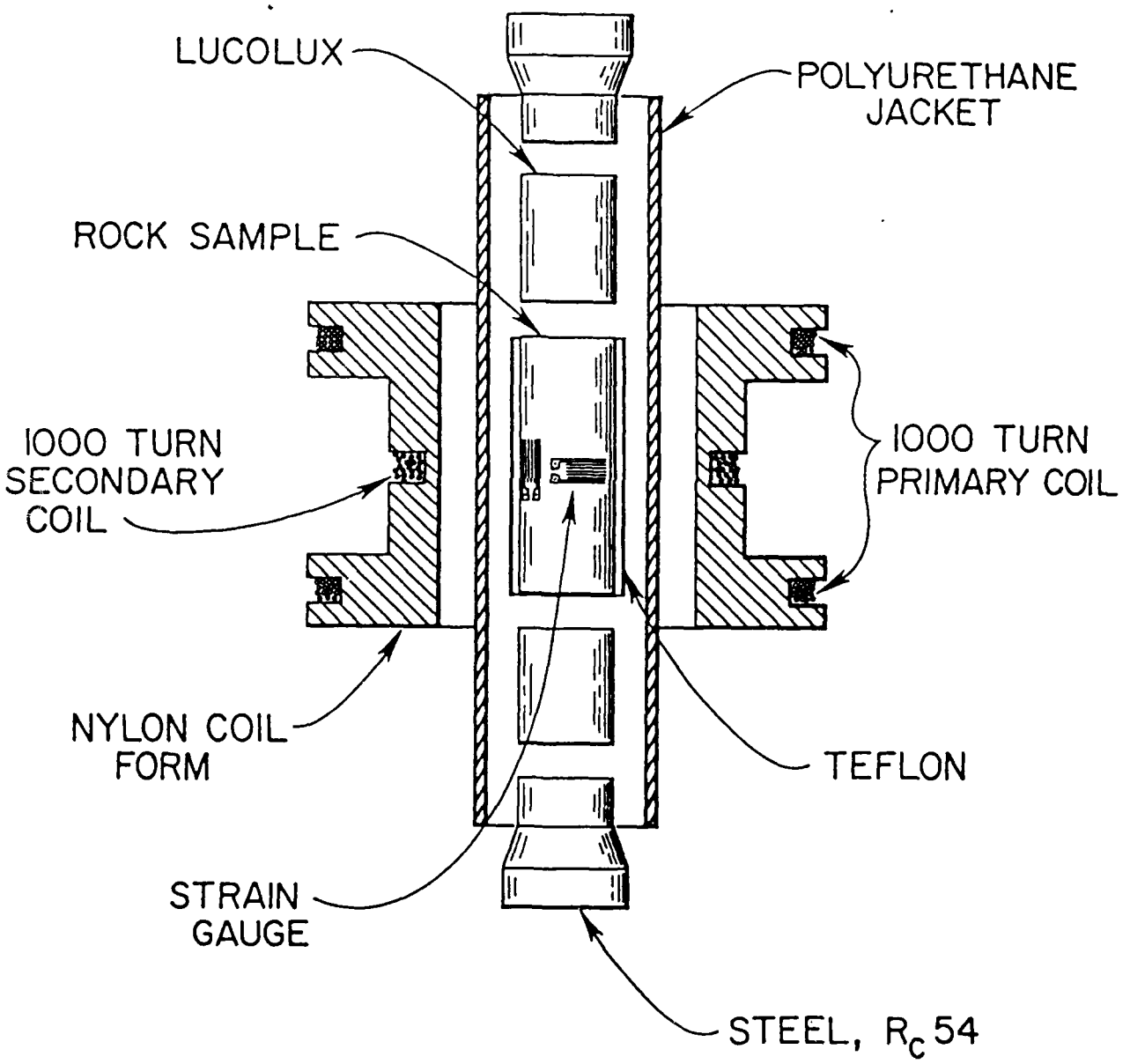

Figure 1-5 Schematic diagram of the sample geometry and the relationship between the rock sample and the sensing head for measuring magnetic susceptibility. The entire assembly fits into the beryllium copper pressure vessel shown in Figure 1-3.

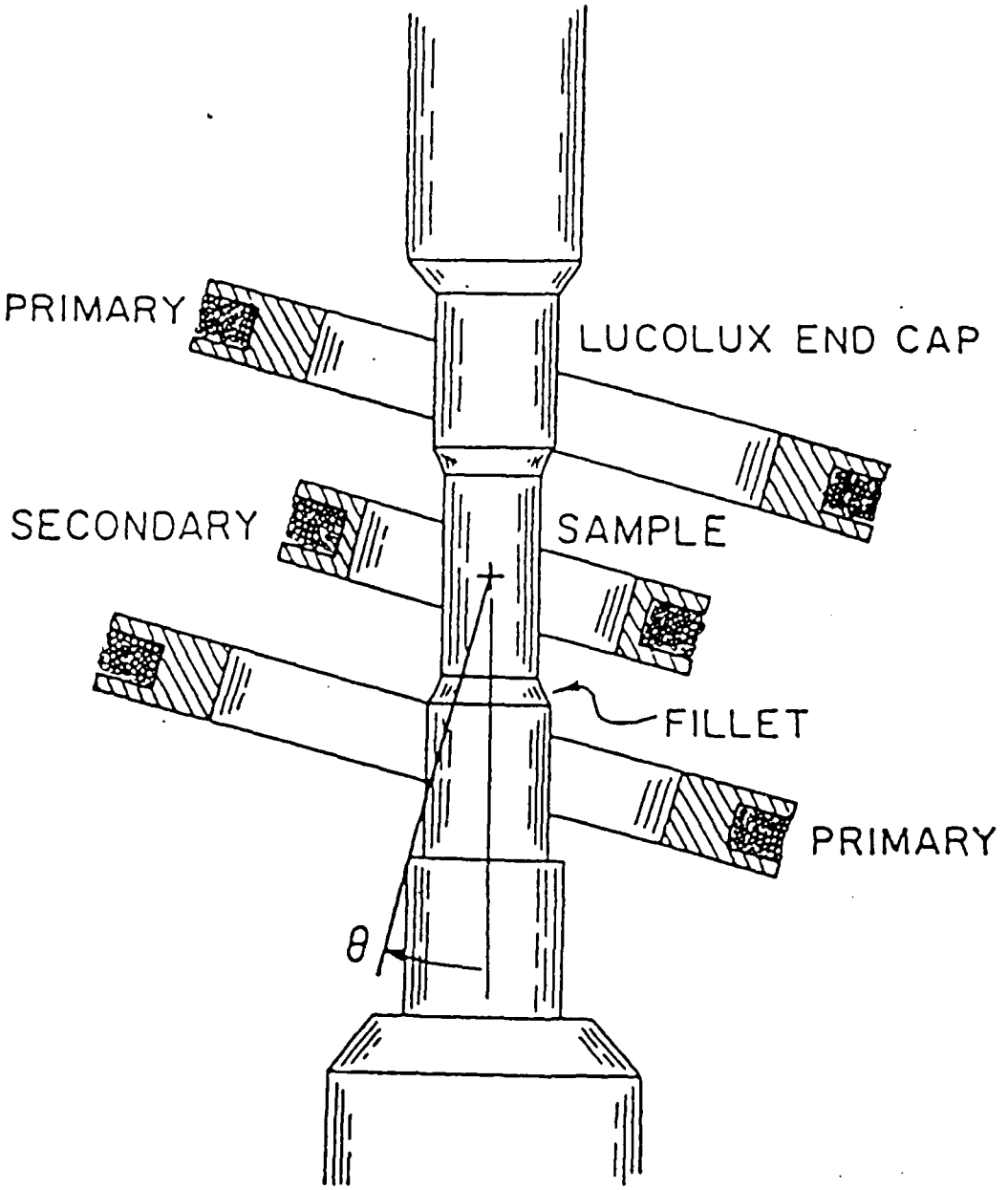

Figure 1-6 Diagram of the measuring transformer-sample arrangement. The angle, θ, is the angle between the axis of the coils and the loading axis of the sample. Lucolux end caps were attached to the samples and fillets of epoxy mixed with Al_2O_3 were spread over the joints.

susceptibility of the sample at each angle was then proportional to the difference in these voltages. The initial susceptibility of the sample appeared to increase as the angle was increased. This effect is related to the increased cross-sectional area of the sample in the plane of coils as the angle was increased.

The output of the bridge was balanced again and then the sample was cyclically loaded. The bridge was driven out of balance as the force on the sample was increased. The amount of imbalance was a measure of the change in susceptibility. The susceptibility as a function of stress was measured for inclinations of the inducing field with respect to the stress axis of 0, 15, 25, and 35°.

The steel tie rods of the press deflected the magnetic flux lines for inclinations of 15, 25, and 35° and biased the measurements made at these orientations. The effect of the tie rods also increased with stress. To correct for this, a Lucolux sample having negligible susceptibility was inserted into the press and loaded. The output of the bridge with the Lucolux sample was recorded and used to separate the effects of the press from those of the rock samples. This "dummy" sample was cycled before and after each experiment on the three rock types to estimate the correction to the measurements as a function of stress and orientation. There was only a small correction applied to the data measured at $\theta = 0°$. The error in the correction was negligible. A much larger correction is needed for the data at inclinations of 35°. The correction at 35° approached 20% of the output measured for rock samples.

The Influence of Stress Path on Thermoremanent Magnetization (TRM)

Piezomagnetic experiments have been carried out on specimens of a diabase from Golden, CO. and a gabbro from Rapidan, VA. The magnetic properties of these rocks are given in Table 1. Before testing a thermoremanent magnetization (TRM) was developed in each sample. For this suite of tests, the remanent vector was oriented parallel to the rock cylinder axis. Only samples with a magnetic vector within 4^{o} of the sample axis were selected for compressional tests. The sample geometry and sensor array is identical to that employed by *Martin et al.*,(1978) and described above. The confining pressure was maintained with a servocontrolled intensifier. A differential stress was applied to the sample by incrementally advancing the piston of the hydraulic cylinder driven with an air hydraulic booster. The force on the sample was measured to an accuracy of $\pm 1\%$ with an external load cell.

Cyclic loading experiments were carried out over three different paths while simultaneously monitoring two components of the remanent vector, the axial and circumferential strain on the specimen, the force, and the confining pressure. The loading conditions were:

1. Cyclic hydrostatic pressurization to 200 MPa in 10 MPa increments.
2. Confined compression at a confining pressure of 2.5 MPa to a peak stress of 200 MPa.
3. Uniaxial strain to a peak axial stress of 200 MPa. During each cycle, the radial strain was held constant to within 10 microstrains using a servocontrolled pressure intensifier. This required a continuous increase in confining pressure during loading. The specimen was both loaded and unloaded under uniaxial strain conditions. Frequently, during initial loading, cycles of 0 to 50 MPa, 0 to 100 MPa, and 0 to 200 MPa were run sequentially.

Experimental Results

At least three and often four stress cycles were conducted on each sample. Upon initial loading, regardless of the stress path, the remanent intensity diminished and a permanent demagnetization was observed at the termination of the cycle. With subsequent cycles of the same type to the same peak load, the slope of the magnetization vs. stress decreased and little or no permanent demagnetization was observed at the end of the cycle. A typical hydrostatic compression run on the Ralston diabase is shown in Figure 2-1. The intensity of the specimen normalized to its prestress value is plotted as a function of hydrostatic pressure. With the application of pressure to 50 MPa, the intensity monotonically decreased to approximately 90% of its initial value. As the sample was unloaded no recovery was observed. Repressurization

produced a slight decrease in magnetization up to 50 MPa, and then a greater pressure sensitivity up to the peak pressure of 100 MPa. During the reduction in pressure, the rock continued to demagnetize; the permanent demagnetization due to a 100 MPa pressure excursion was 19%. For the third pressure cycle no appreciable change in magnetization occurred until the previous peak value of 100 MPa was exceeded; once again an increased pressure sensitivity was exhibited as the pressure was augmented to 200 MPa. During unloading no recovery was observed and the remanent intensity retained only 70% of its initial value at the termination of the cycle.

The change in magnetization due to differential stress is also given in Figure 2-1. The normalized intensity is plotted as a function of stress difference for a confined compression test at 2.5 MPa. As the sample was loaded to 50 MPa, the thermal remanent magnetization decreased to 78% of its prestress value. As the load was removed from the sample, a small amount of additional demagnetization occurred; at the end of the cycle the intensity was 73% of its initial value. Reloading produced a minimal change in magnetization until the stress exceeded 50 MPa, then the rate of demagnetization increased perceptibly. As the sample was unloaded the demagnetization continued to decrease, resulting in a 40% reduction at the termination of the cycle. A final stress cycle to 200 MPa produced an effect similar to the 100 MPa cycle; the total demagnetization for the three cycles was 55%.

An examination of both experiments shows that for previously unstressed specimens with nominally the same initial intensity and orientation of the magnetic vector, differential stress produces a significantly greater demagnetization than simple hydrostatic compression, 54% vs. 30%. For both experiments the predominant magnetic changes occurred in the axial component of the remanent vector. No significant rotation of the magnetic vector was observed in either experiment.

In order to evaluate the piezoremanent response as a function of loading path, several mixed mode experiments were carried out to the same peak stress. The results of one of these tests on a diabase sample are given in Figure 2-2. The initial hydrostatic compression for this specimen is similar to the results shown in Figure 2-1; that is, the pressurization to 200 MPa yields a 32 to 35 % reduction in remanent intensity. Furthermore, pressurization to 200 MPa in one cycle produces the same demagnetization as pressurization to 200 MPa with sequentially larger minicycles. Figure 2-2 also gives the data for the second, third, and fourth stress cycles for the diabase specimen. The second cycle was run in hydrostatic compression, the third cycle in uniaxial strain, and the fourth cycle in uniaxial stress. In each case the remanent intensity, normalized to its prestress value, is plotted as a function of either pressure or axial stress. Cyclic repressurization to 200 MPa after initial loading to the same value results in an additional permanent demagnetization of only 3%. Furthermore, demagnetization per increment of applied pressure is much less than that observed during initial loading by a factor of five or so.

It was of interest to determine if a change in stress path would result in a further reduction in remanent intensity or if the irreversible demagnetization was accomplished in the first two

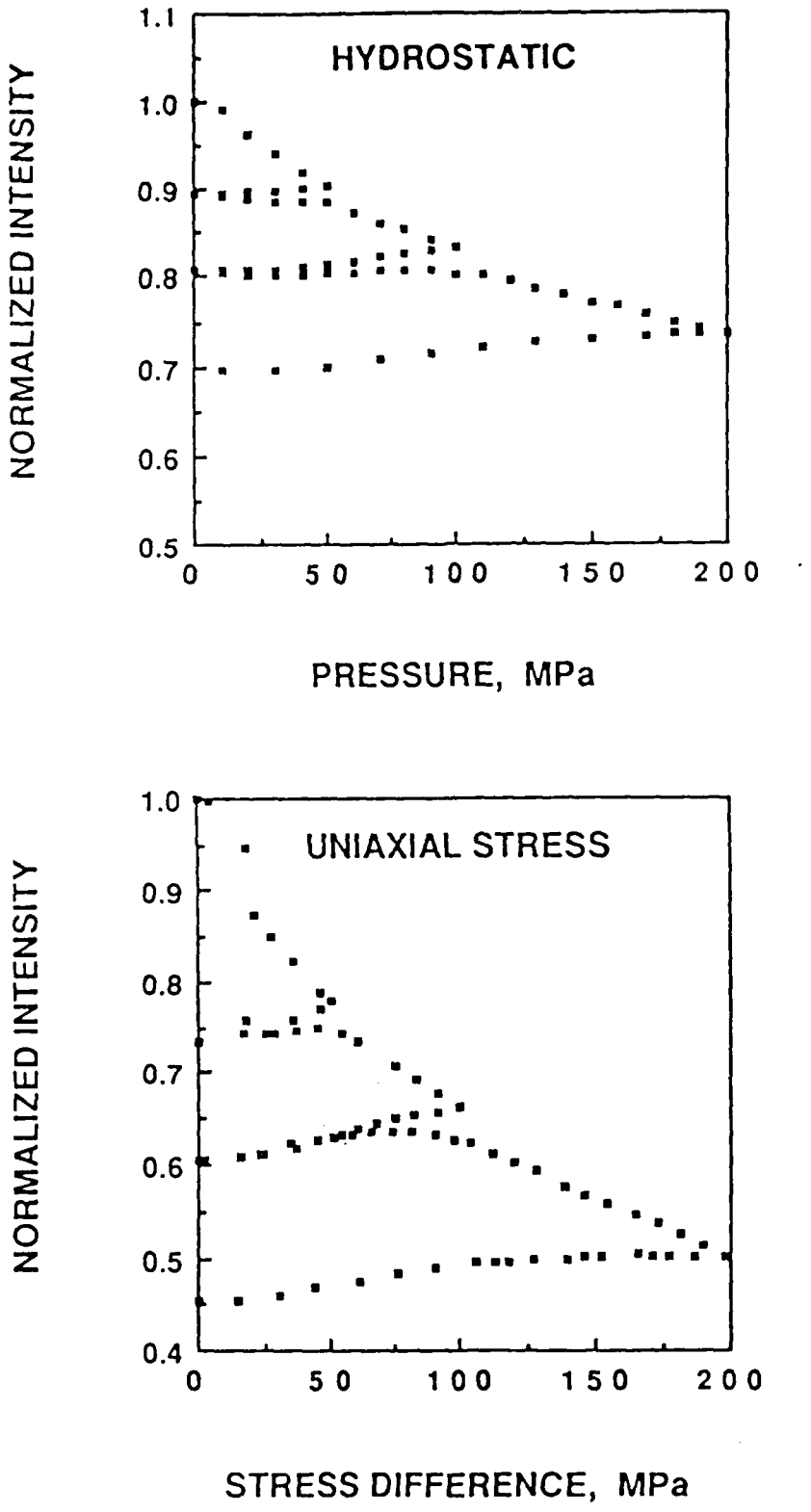

Figure 2-1. Normalized TRM is shown as a function of pressure or stress difference for the first loading cycle on diabase specimens. The initial intensities were 1.1 x 10^{-1} and 8.3 x 10^{-2} emu/cm3 respectively.

pressure cycles. Even a cursory examination of the data for a uniaxial strain test shows that additional demagnetization occurred as the loading path was altered. In fact, the total demagnetization dropped by 10% to 51% of its prestress value. Finally, the loading path was varied once again and cycle four was run in confined compression. A small confining pressure of 2.5 MPa was exerted on the sample to ensure proper seating of the copper jacket in strain gauges. The cyclic application of 175 MPa of differential stress resulted in a further demagnetization to 44% of the virgin TRM. A detailed examination of the uniaxial stress data shows an interesting but not totally unexpected result. The intensity actually increases up to a stress of approximately 80 MPa and then decreases continuously up to the peak stress for the cycle. No recovery was observed during unloading.

A similar sequence of experiments to those shown in Figure 2-2 was conducted on gabbro specimens from Rapidan, VA. The results are shown in Figure 2-3. Hydrostatic pressurization exhibits similar results to those observed on the Ralston diabase. Initial pressurization to 50 MPa caused the magnetization to decrease to 93% or so of its initial value with no recovery during the unloading sequence. The reapplication of pressure produced small changes in magnetization until the pressure exceeded 50 MPa, where upon the demagnetization rate increased. Subsequent pressure cycles to 100 and 200 MPa produced a final demagnetization of nearly 18%.

The same behavior displayed by the diabase for mixed mode cyclic loading was observed for the gabbro. The second hydrostatic cycle to 200 MPa resulted in an additional demagnetization of only 3% or so, while changing the loading path to uniaxial strain produced an additional 10% demagnetization, as well as a four fold increase in stress sensitivity with respect to the hydrostatic loading.

Figure 2-4 gives the data obtained on a gabbro specimen on which the initial loading was confined compression. Normalized remanent intensity is given as a function of differential stress for three loading cycles. The specimen was loaded in three progressively larger cycles to a peak stress of 200 MPa. The demagnetization observed at the peak stress was 60% or so of its prestressed value and the permanent demagnetization at zero stress due to an applied load of 200 MPa was 25%. The maximum demagnetization at 200 MPa of differential stress is nearly 20% greater than that observed at 200 MPa of hydrostatic pressure.

Two additional stress cycles were carried out on the same specimen; the second cycle was a uniaxial strain test while the third was a nominal uniaxial stress experiment. The reapplication of stress in cycle two produced a decrease in magnetization from 0.74 J_o to 0.64 J_o at 200 MPa, where J_o is equal to the initial remanent intensity. It is interesting to note that the value of the magnetization at the peak stress in Cycle 2 is the same as that observed at the peak stress in Cycle 1. There was a small hysteresis upon unloading and an additional demagnetization of approximately 2%. Cycle 3 was conducted under uniaxial stress conditions. The same was loaded to 200 MPa and failed prior to unloading. A comparison of the stress sensitivities observed during uniaxial strain and uniaxial stress indicates that they are very nearly the same. As a final point, no precursory changes in magnetization preceded fracture of the sample.

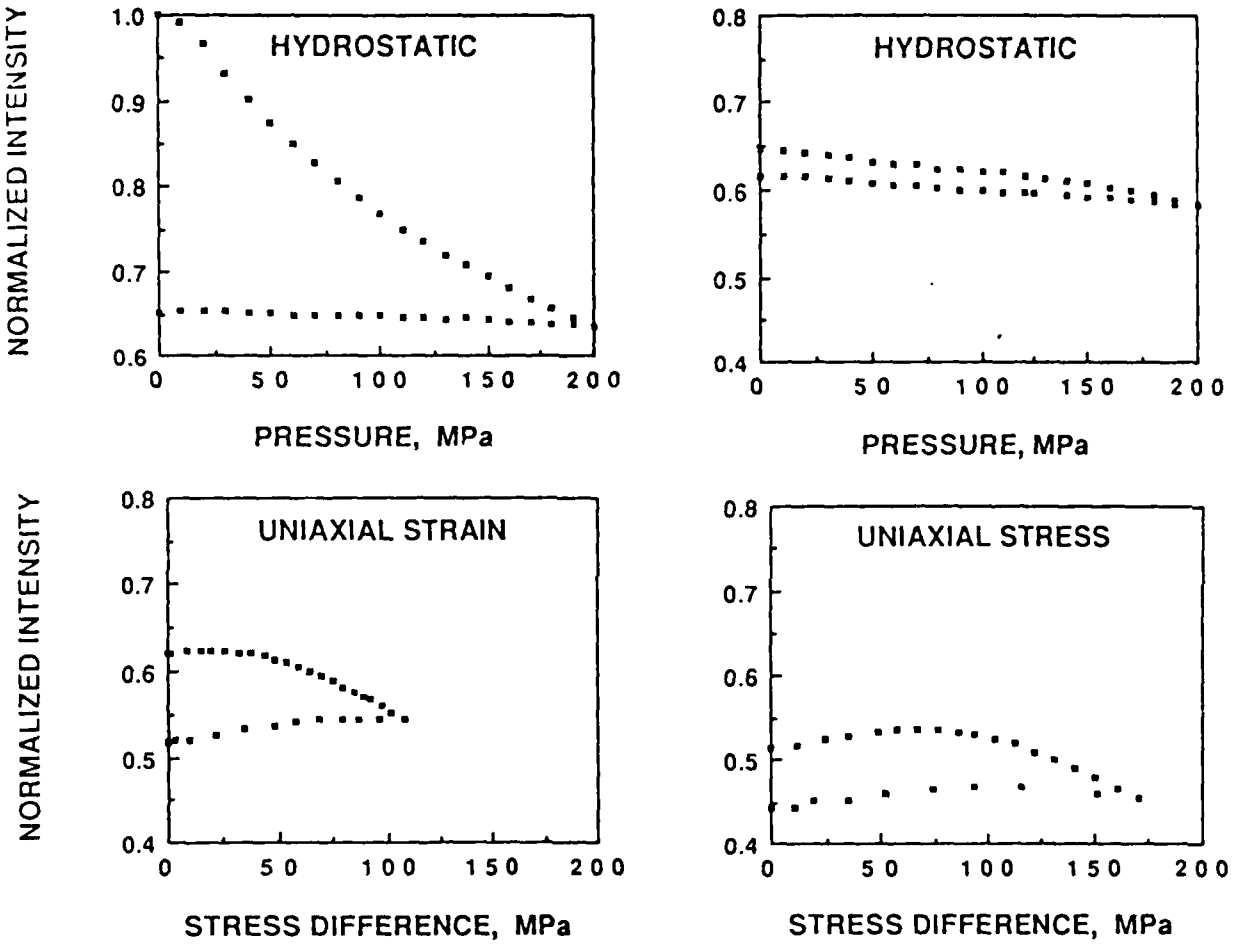

Figure 2-2. Normalized TRM is given as a function of pressure or stress difference for three stress paths on a diabase specimen. The initial TRM was 8.2 x 10-2 emu/cm3.

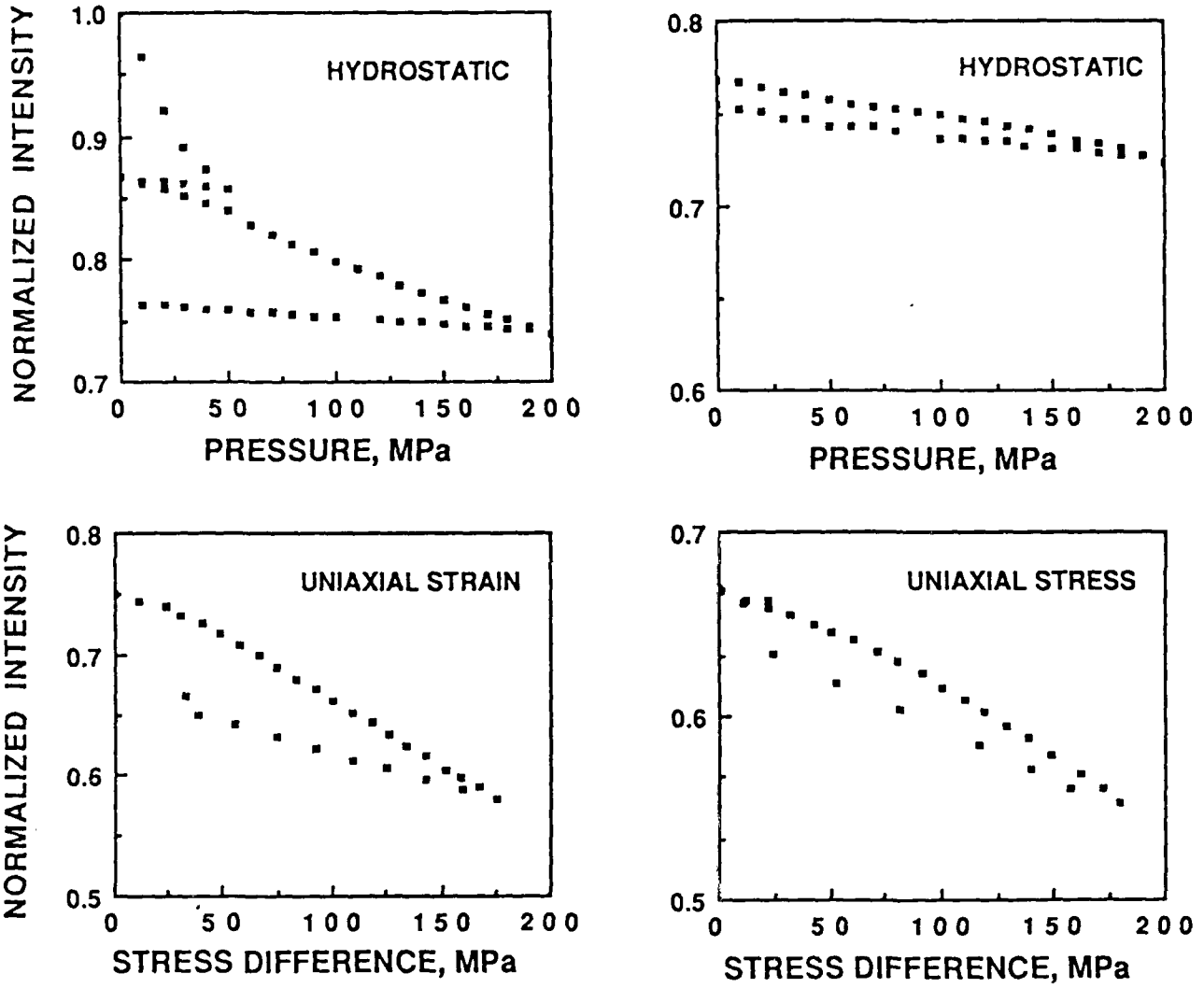

Figure 2-3. Normalized TRM is given as a function of pressure or stress difference for three stress paths on a gabbro specimen. The initial TRM was 1.5 x 10-1 emu/cm3.

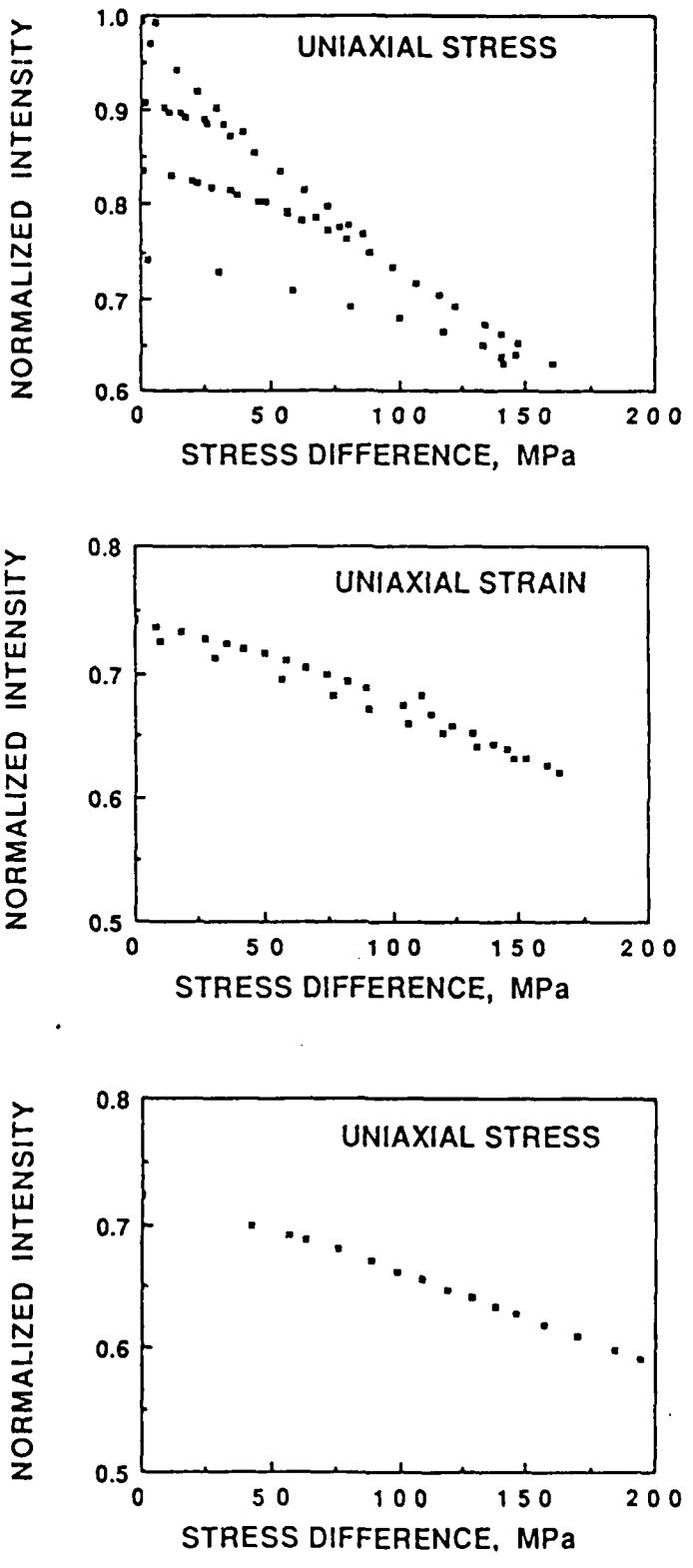

Figure 2-4. Normalized TRM is given as a function of pressure or stress difference for three stress paths on a gabbro specimen. The initial TRM was 1.4 x 10-1 emu/cm3.

Discussion

Experimental results presented above demonstrate that shear stress produces larger changes in remanent magnetization than hydrostatic stress. This is true both for initial loading on a previously unstressed sample, as well as for subsequent loading cycles. The initial demagnetization that is observed at the termination of the initial loading cycle is directly proportional to the peak stress that the rock has experienced. By progressively increasing the peak stress during cyclic loading, the permanent decrease in remanence increases monotonically, but certainly not linearly. The effect is greater when the specimen is loaded non-hydrostatically. In contrast, during multicycle experiments where the peak stress remains constant with increasing cycle number, the changes in magnetization tend to become reproducible after initial cycling with no additional permanent demagnetization at the end of the cycle. This is true as long as the stress path is not changed. For example, as is shown in Figure 2, the transition from hydrostatic loading to uniaxial strain conditions produced a significant change in the stress sensitivity, and a substantial increase in the permanent demagnetization.

Based on the results outlined above, it is obvious that stress has pronounced influence on the magnetization of materials. In the absence of a magnetic field, both hydrostatic and non-hydrostatic stress produce significant demagnetization of the remanent moment on initial cyclic loading. Subsequent loading cycles exhibit definite changes but no discernable permanent demagnetization. If the stress induced magnetic behavior observed in these experiments is due to the nucleation and movement of the domain, then it must be determined how the apparent divergent results reported above can be explained. The fact that the thermoremanent magnetization is permanently altered with the application of any state of stress may be directly attributable to the fact that the domain pattern is metastable.

Direct observation of domain behavior during cyclic loading has been carried out by *Boyd et al.*,(1984). They studied the motion and nucleation of magnetic domains as a function of applied stress. Tests on pseudosingle domain magnetite particles showed that at very low stresses walls were nucleated. As the stress was augmented, additional domains nucleated and the domains adjusted to achieve a lower energy configuration. When the stress was removed, the domain pattern was irreversibly changed. *Halgedahl and Fuller* (1983) observed a similar effect due to the application of large magnetic fields. As the inducing field was increased, domains nucleated and the spacial distribution of preexisting domains was altered. When the direction of the field was reversed, the domain pattern did not exhibit a reversible behavior but showed a pronounced hysteresis.

The results reported by *Boyd et al.*(1984) and *Halgedahl and Fuller* (1983) elegantly demonstrate that the nucleation and motion of domain walls adequately explain the observed

changes in magnetization due to the application of stress or the magnetic hysteresis observed as the inducing field is varied in a cyclic fashion. It is still unclear as to why hydrostatic pressure produces a smaller magnetic change than differential stress. It is even more puzzling if the low field susceptibility measurements are compared with the piezoremanent results. Changes in magnetic susceptibility are observed only during the application of a non-hydrostatic load with no permanent change at the termination of the cycle *(Martin, 1980)*. The difference in magnetization due to hydrostatic or differential stress is much more pronounced for susceptibility than for remanence. Obviously, in both cases domain nucleation, nucleation sites, and pattern readjustment are the controlling mechanisms for the observed changes. There is no comprehensive theory to explain the observations reported here as well as those of *Boyd et al.*(1984).

The nucleation sites are most likely high energy regions within the grain. As the stress increases, the energy barrier for nucleation is exceeded and the domain migrates to reduce its free energy. From this point of view it is relatively easy to understand why hydrostatic pressure produces a lower stress sensitivity than non-hydrostatic stress. Shear stress is much more efficient in moving imperfections such as dislocations or vacancies within the particle than hydrostatic pressure. Such a possibility explains the susceptibility results, but does not totally resolve the remanent changes. The first loading cycle on a specimen with undisturbed remanence produces permanent demagnetization. Most likely the initial remanence is unstable at room temperature and elevated pressure and readjusts to a more stable configuration. This produces a permanent change. Repeated application over the same path does not produce any further permanent variation. This situation is very similar to the susceptibility case.

The Influence of Remanent Vector Orientation with Respect to the Principal Stress Direction on the Piezomagnetic Effect

Rotations of the magnetic vector of up to 5° due to uniaxial stress on rocks have been previously reported *(Powell, 1960; Hall and Neale, 1960; Domen, 1962; Ohnaka, 1969; Martin et al, 1978; Martin, 1980; Pike et al, 1981; Lanham and Fuller, 1988). Carmichael* (1968) has theoretically examined the effect of uniaxial stress on the rotation of magnetization from the preferred axis (111) in magnetite and nickel. As stress is increased, the domain magnetizations are expected to be deflected toward the magnetoelastic minima and away from the magnetocrystalline preferred (111) orientations. Thus it seems that the effect of nonhydrostatic stress is to cause a rotation of the magnetic vector. *Stacey and Johnston*(1972) have also theoretically shown that for rocks, one component of the magnetic vector should increase while the other decreases with increasing stress, thus producing a rotation of the magnetic vector.

Kean et al. (1976) studied the effect of uniaxial compression on magnetic susceptibility. They found that the component of susceptibility parallel to the axis of compression decreased whereas the component normal to the loading axis increased. In addition, the relative contribution of remanent and induced effects to the total stress dependence on magnetization was determined. For the rocks studied, the susceptibility effect was slightly greater than the remanent effect.

The effect of stress and pressure as well on rock magnetization has been discussed in the previous section for the case where the magnetic vector is coincident with the greatest principal stress. In the earth it is very unlikely that the magnetic field will be aligned with the greatest principal stress direction. Consequently, it is of interest to consider situations where the change in stress may cause a rotation of the magnetic vector, as well as a change in magnetic intensity. In order to approach this problem realistically, the geometric relationship between stress and magnetization must be considered. It is well known that when a magnetic crystal is subjected to an inducing field, **H**, the material deforms. This phenomenon is termed *magnetostriction*. The relationship between the inducing field and the observed strain can be represented with a third rank tensor. For the sake of argument let us assume that the relationship between the change in magnetization and stress can also be related by a third rank tensor. This situation can only arise if there is a preexisting magnetization in the material. Given a magnetization of intensity, J_i, the relationship between stress, σ_{jk}, and magnetization can be written as:

$$J_i = d_{ijk}\,\sigma_{jk} \tag{1}$$

where d_{ijk} is the piezomagnetic tensor. For applied stress, σ_{jk}, a rock magnetization of J_i will be observed. This situation is directly analogous to the piezoelectric effect observed in many crystals (*Nye 1964*). For the two cases examined in this study, hydrostatic and uniaxial loading, the piezomagnetic effect due to an incremental change in stress, $\Delta\sigma_{jk}$, may be represented by

$$\Delta J_i = d_{ijk}\,\Delta\sigma_{jk} \tag{2}$$

For the case of hydrostatic pressure equation 2 reduces to

$$\Delta J_i = d_{ijk}\,\delta_{jk}\,p \tag{3}$$

where δ_{jk} is the Kronecker delta and p is the hydrostatic pressure. Since only two components of the magnetic vector are measured in these experiments, this equation simplifies to

$$\begin{aligned} \Delta J_1 &= (d_{111} + d_{122})\,p \\ \Delta J_2 &= (d_{211} + d_{222})\,p \end{aligned} \tag{4}$$

Similarly, for the nonhydrostatic case, equation 2 can be written as

$$\begin{aligned} \Delta J_1 &= d_{111}\,\sigma_{11} \\ \Delta J_2 &= d_{211}\,\sigma_{11} \end{aligned} \tag{5}$$

when only two components of magnetization are measured.

As a test of the applicability of representing the change in remanent magnetization, ΔJ_i, due to an increment of stress, $\Delta\sigma_{jk}$, as a third rank tensor, a suite of experiments were carried out for both magnetic susceptibility and remanent magnetization. The results of the remanent magnetization experiments will be discussed in this chapter, and the effect of stress on magnetic susceptibility will be covered in subsequent chapters. In order to test the applicability of treating piezoremanent magnetization as a third rank tensor, experiments were conducted on the Ralston diabase at a fixed remanent intensity (TRM) for various inclinations of the magnetic vector with respect to the core axis. A TRM was induced in each sample

with a nominal intensity of 1.9×10^{-1} emu/cm^3 at inclinations with respect to the core axis ranging from 4.9 to 75°. Each sample was prepared in the manner described previously, and subjected either to hydrostatic or uniaxial stress loading conditions to a level of 200 MPa. Several loading cycles were conducted on each sample; often the mode of loading was changed from cycle to cycle.

For the specimens that were hydrostatically loaded, the change in magnetic intensity should be the same irrespective of the orientation of the magnetic vector. If this is true, then as the orientation magnetic vector rotates with respect to the fixed coordinate system of the magnetometer array, the components of the magnetic vector should transform according to the following equations

$$\Delta J_A = \Delta J_{200} \cos \theta$$
$$\Delta J_R = \Delta J_{200} \sin \theta \qquad (6)$$

where ΔJ_A and ΔJ_R are the components of the magnetic vector measured in the axial and radial directions with respect to the magnetization reference system and ΔJ_{200} is the change in the TRM intensity at a pressure of 200 MPa..

Typical results of these experiments are given in Figures 3-1 and 3-2. The change in each component of remanent magnetization normalized to its prestress value is plotted as a function of confining pressure. Each specimen was pressurized to a peak load of 200 MPa in sequentially larger cycles: 0 to 50 MPa, 0 to 100 MPa, and 0 to 200 MPa. As the pressure increased, the TRM monotonically decreased. The change was not linear; the demagnetization was most pronounced at low pressures. Upon unloading, after reaching the peak pressure for the cycle, the magnetization was not reversible; each component showed a permanent decrease in magnetization at the termination of a cycle. For example, at the end of the 50 MPa cycle, the magnetization had decreased by 2.5% whereas the termination of the 200 MPa cycle, the magnetization had decreased by 12.5%. Furthermore, the relative change in magnetization as a function of pressure is the same for both specimens although the inclination of the magnetic vector was 72° for the data presented in Figure 3-1 and 48° for that shown in Figure 3-2.

A rotation of the magnetic vector occurs if the ratio of the radial to the axial component of the magnetic vector varies with pressure. In Figure 3-2, the ratio of the radial to the axial component of magnetization is shown as a function of confining pressure. The results indicate that the ratio remained relatively unchanged during the pressurization sequence, and surprisingly did not vary during unloading. The data indicates that any rotation of the remanent vector was less than 0.5°; this change may be an artifact of the data reduction technique. Thus, in spite of the fact that the intensity of magnetization decreased as much as 12%, no permanent change in the inclination of the magnetic vector was observed due to pressurization.

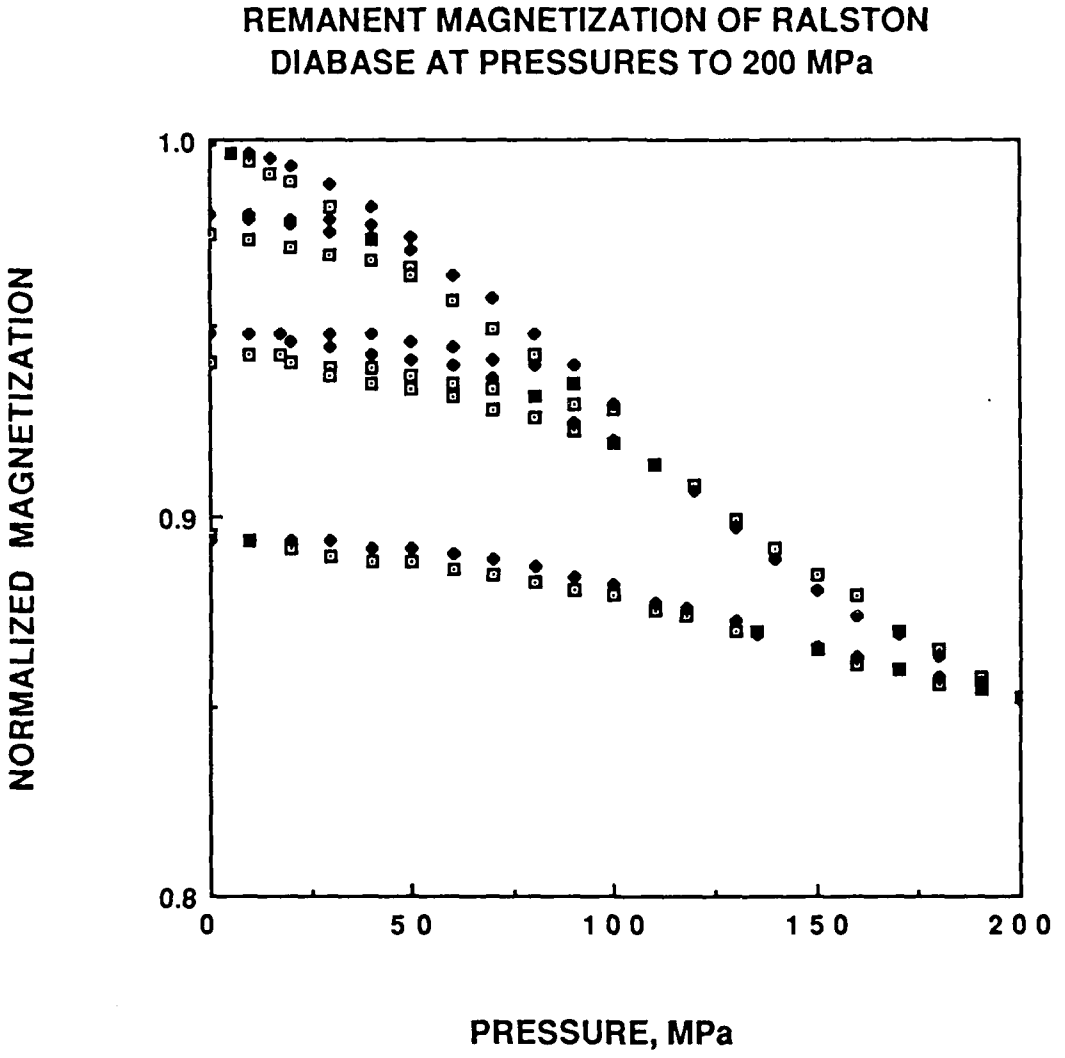

Figure 3-1 The axial (open symbols) and radial (solid symbols) components of the remanent vector normalized their initial values are plotted as a function of confining pressure for a diabase specimen. The initial intensity was 7.1×10^{-1} emu/cm^3; the inclination of the magnetic vector with respect to the sample axis was 72°.

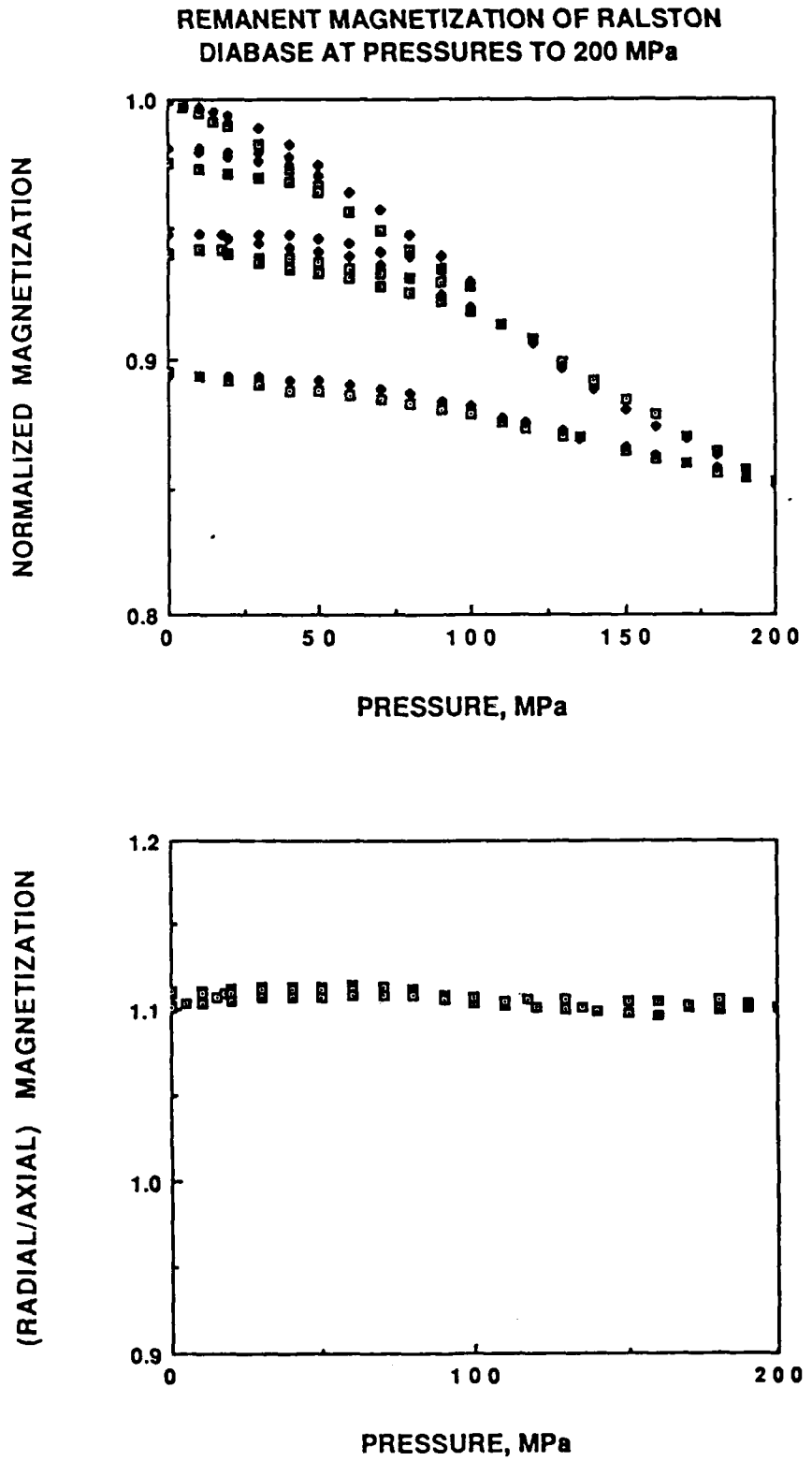

Figure 3-2 The axial (open symbols) and radial (solid symbols) components of the remanent vector normalized to their initial values are plotted as a function of pressure for a diabase specimen. The lower diagram displays the ratio of the radial to axial component of the magnetic vector as a function of pressure. The initial intensity was 1.6×10^{-1} emu/cm^3; the inclination of the magnetic vector with respect to the sample axis was 48°.

The changes in magnetization due to hydrostatic pressure in this set of experiments are very similar to those observed when the magnetic vector was coincident with the core axis *(Martin and Noel, 1988)*. As a specimen with a TRM was progressively loaded to higher pressures for successive cycles, the magnitude of the demagnetization at pressure increased, and the amount of permanent demagnetization measured at ambient conditions also increased. Since hydrostatic pressure does cause a rotation of the magnetic vector then the change in magnetization at the peak stress of 200 MPa should transform according to equation 6. Four hydrostatic experiments were carried out with initial inclinations of the magnetic vector ranging from 26 to 75°. The change in each component of magnetization due to a pressurization of 200 MPa is shown in Figure 3.3. For reference, the relationship given by equation 6 is shown for reference. An examination of the data shows that the axial component of magnetization at a confining pressure of 200 MPa can be fitted with an expression of the form given by equation 6. As the initial orientation of the magnetic vector rotated away from the sample axis, the axial component of magnetization decreased and the radial component increased in direct proportion.

The results of these experiments indicate that hydrostatic pressure causes the remanent magnetization to simply decrease in intensity but does not affect the orientation of the vector. Consequently, the sample geometry and the orientation of the magnetic vector with respect to the core axis do not affect the the observed change in magnetization due to hydrostatic pressure.

A similar suite of cyclic experiments were carried out under nominal uniaxial compression. Specimens of diabase with remanent vectors inclined at various angles to the stress axis were stressed to 200 MPa. A small confining pressure 2.5 MPa was applied to the sample to maintain alignment at the sample assembly. Typical results from these experiments are shown in Figures 3-4, 3-5, 3-6, and 3-7. For each figure the axial and radial component of the remanent vector, normalized to its initial prestress value is plotted as a function of differential stress. In addition, the values of the two components of magnetization measured with the fluxgate magnetometer assembly are presented as a function of differential stress. The values have not been corrected for the separation between the sample and the magnetometer. Consequently, these are reported as relative remanent magnetization without units. For each sample, the stress was monotonically increased to 200 MPa and then reduced to zero. The results were very consistent. Each component decreased with increasing stress. Demagnetizations at 200 MPa of 35% or so were typical. Upon unloading, the magnetization did not recover significantly and a permanent demagnetization at the termination of the cycle was observed.The single exception was observed for the sample with its magnetic vector inclined 4.9° to the loading axis. While the axial component decreased with load, the radial component exhibited a slight increase (Figure 3-7).

An examination of the data normalized to its initial value shows that when the inclination of the magnetic vector is small, the component parallel to the greatest principal stress axis

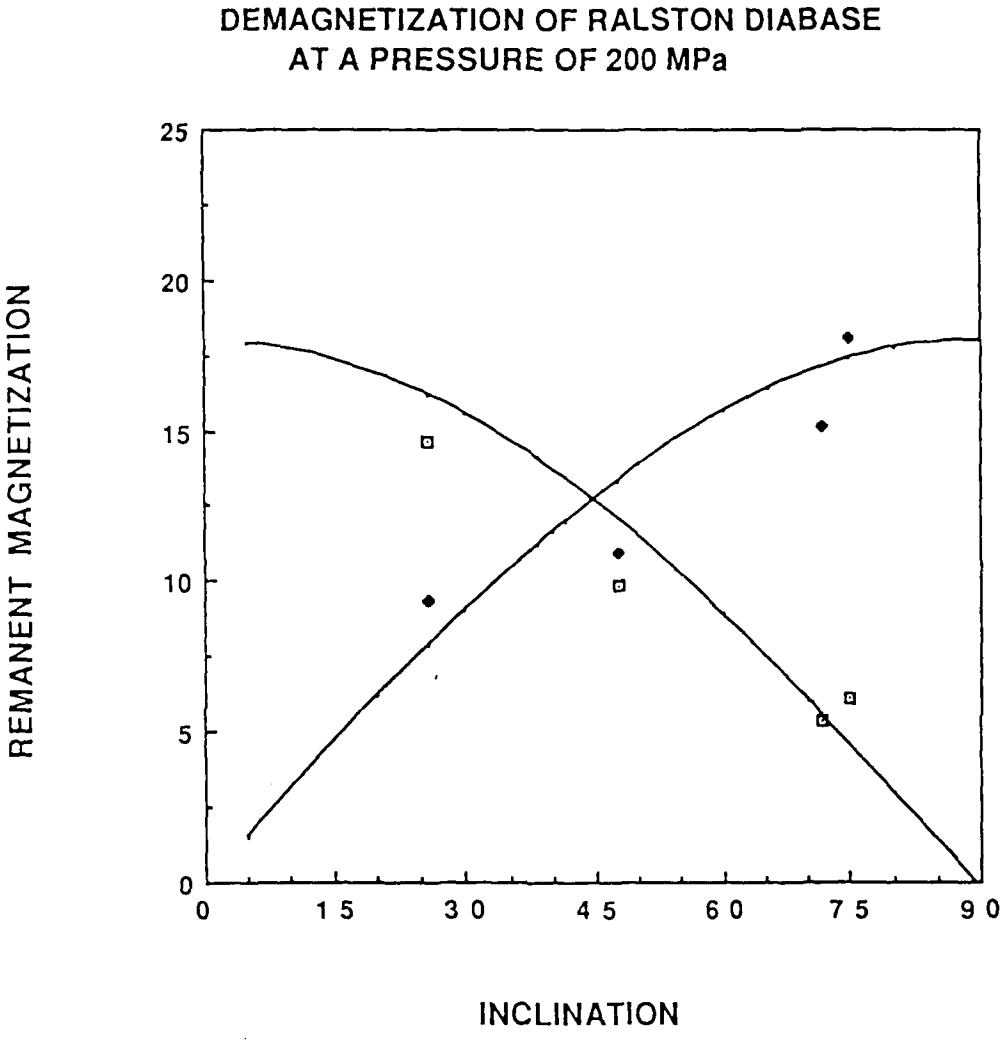

Figure 3-3 The change in each component of the remanent vector for diabase specimens at a pressure of 200 MPa is shown as a function of the inclination of the magnetic vector with respect to the sample axis. All the observations have been scaled to an initial remanent intensity (TRM) of 1.9×10^{-1} emu/cm^3. The open symbols indicate the axial component and the solid symbols indicate the radial component.

exhibits the greatest relative demagnetization (Figures 3-5, 3-6, and 3-7). However, for angles greater than 45^{o} or so, the normalized radial component shows a larger demagnetization than the normalized axial component (Figure 3-4). The initial value for the axial component is approximately 54 relative magnetic units, whereas the radial component is nearly 120 relative magnetic units. This observation suggests that for large inclinations that the transverse component of the remanent vector can exhibit larger changes than the component parallel to the stress direction.

The data collected as a function of inclination for uniaxial compression testing shows that there is a tendency for the component parallel to the greatest principal stress to exhibit the greatest demagnetization. In order to quantify this finding, the results for eight uniaxial compression tests with varying inclinations of the magnetic vector with respect to the principal stress direction were considered. First, all the data was scaled to a common intensity of 1.9×10^{-1} emu/cm^3. Then, the observed change in each component of magnetization at a stress of 200 MPa was plotted as a function of inclination. These results are shown in Figure 3-8. If this data set transforms according to a third rank piezomagnetic tensor, then for a fixed orientation and a constant stress level, the data should transform according to

$$\Delta J_A = (d_{111} \cos\theta + d_{211} \sin\theta)\, \Delta\sigma_{11}$$

$$\Delta J_R = (d_{211} \cos\theta + d_{111} \sin\theta)\, \Delta\sigma_{11} \qquad (7)$$

where ΔJ_A and ΔJ_R are components of the remanent magnetization measured with the fixed magnetometer array, and θ is the inclination of the magnetic vector with respect to the specimen axis. Using the data presented in Figure 3-7, the appropriate values for d_{111} and d_{211} were computed and substituted into equation 7. These curves are shown with solid lines in Figure 3-8. The results shown in Figure 3-8 indicate that the change in magnetization due to a uniaxial stress of 200 MPa transforms according to equation 7. The observations deviate only slightly from the curves developed based on the data set shown in Figure 3-7. The slight deviation of the observations from the projected curve are most likely due to small errors in the data used to compute the coefficients d_{111} and d_{211}. The increase in the transverse component of the magnetic vector for specimens with a vector nominally coincident with the principal stress axis was not universally observed. For example, a detailed examination of the data reported in the previous section showed that in some instances a small demagnetization occurred in a transverse direction as the stress was increased, whereas, in other cases, the magnetization showed a slight increase. This uncertainty with regard to the transverse component is reflected in the small discrepancies between the curves projected using equation 7 and the observed data. In spite of this uncertainty, the agreement between the theory and the observations is very good.

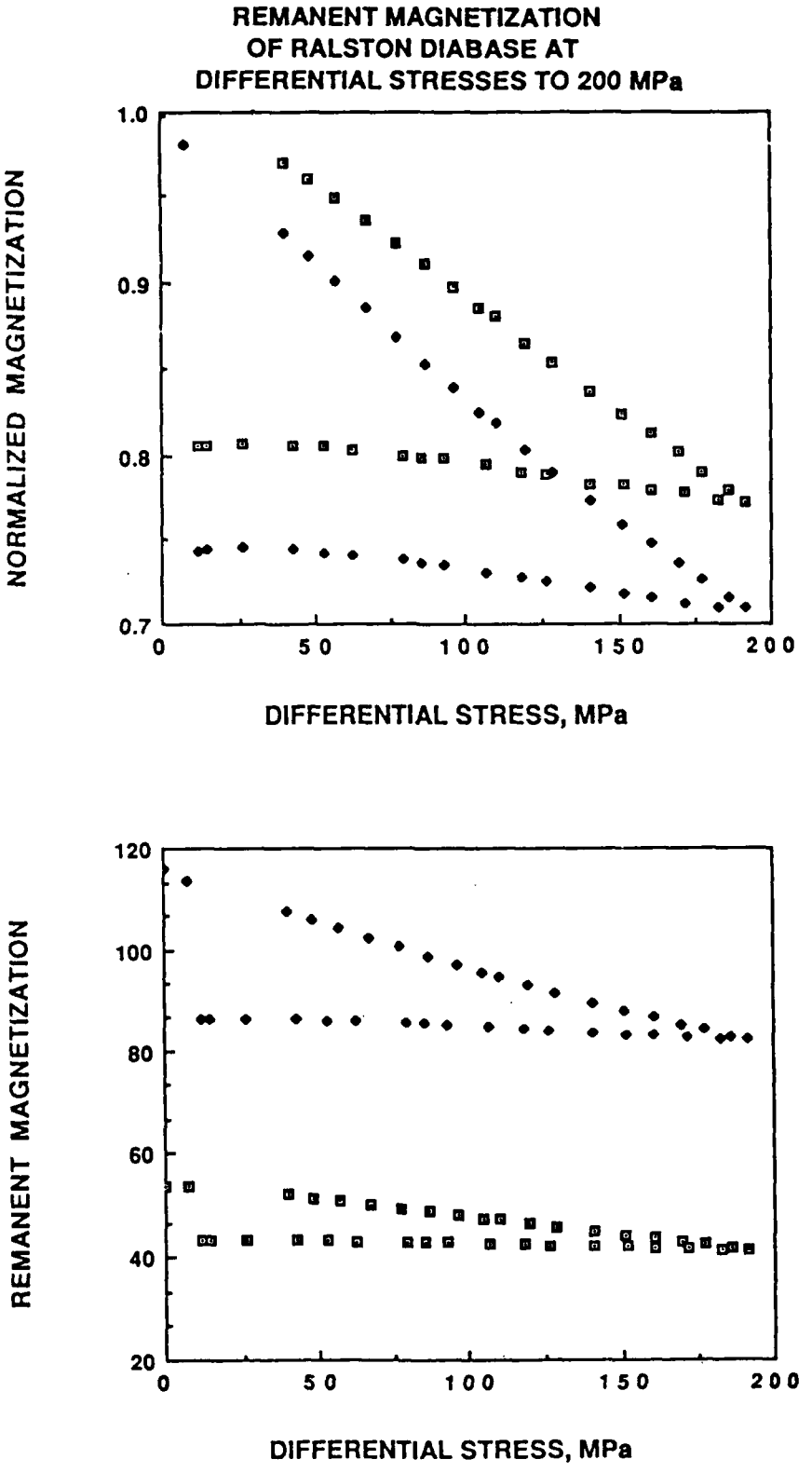

Figure 3-4 The axial (open symbols) and radial (solid symbols) components of the remanent vector normalized to their initial values (upper diagram) or without normalization (lower diagram) are plotted as a function of differential stress for a uniaxial stress experiment on a diabase specimen. The initial intensity (TRM) was 1.6×10^{-1} emu/cm^3; the inclination of the magnetic vector with respect to the sample axis was 65°.

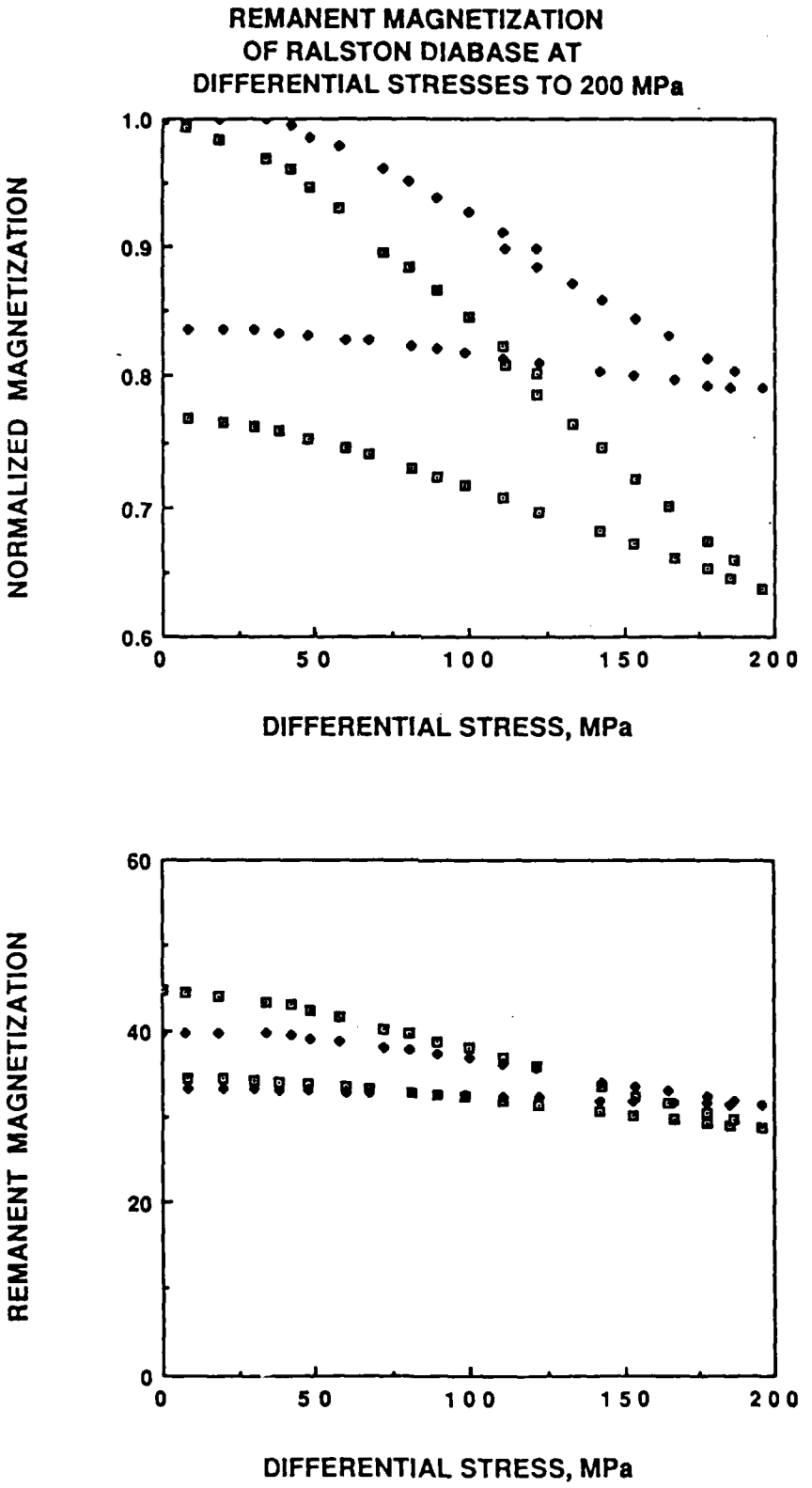

Figure 3-5 The axial (open symbols) and radial (solid symbols) components of the remanent vector normalized to their initial values (upper diagram) or without normalization (lower diagram) are plotted as a function of differential stress for a uniaxial stress experiment on a diabase specimen. The initial intensity (TRM) was 1.0×10^{-1} emu/cm^3; the inclination of the magnetic vector with respect to the sample axis was 41.5°.

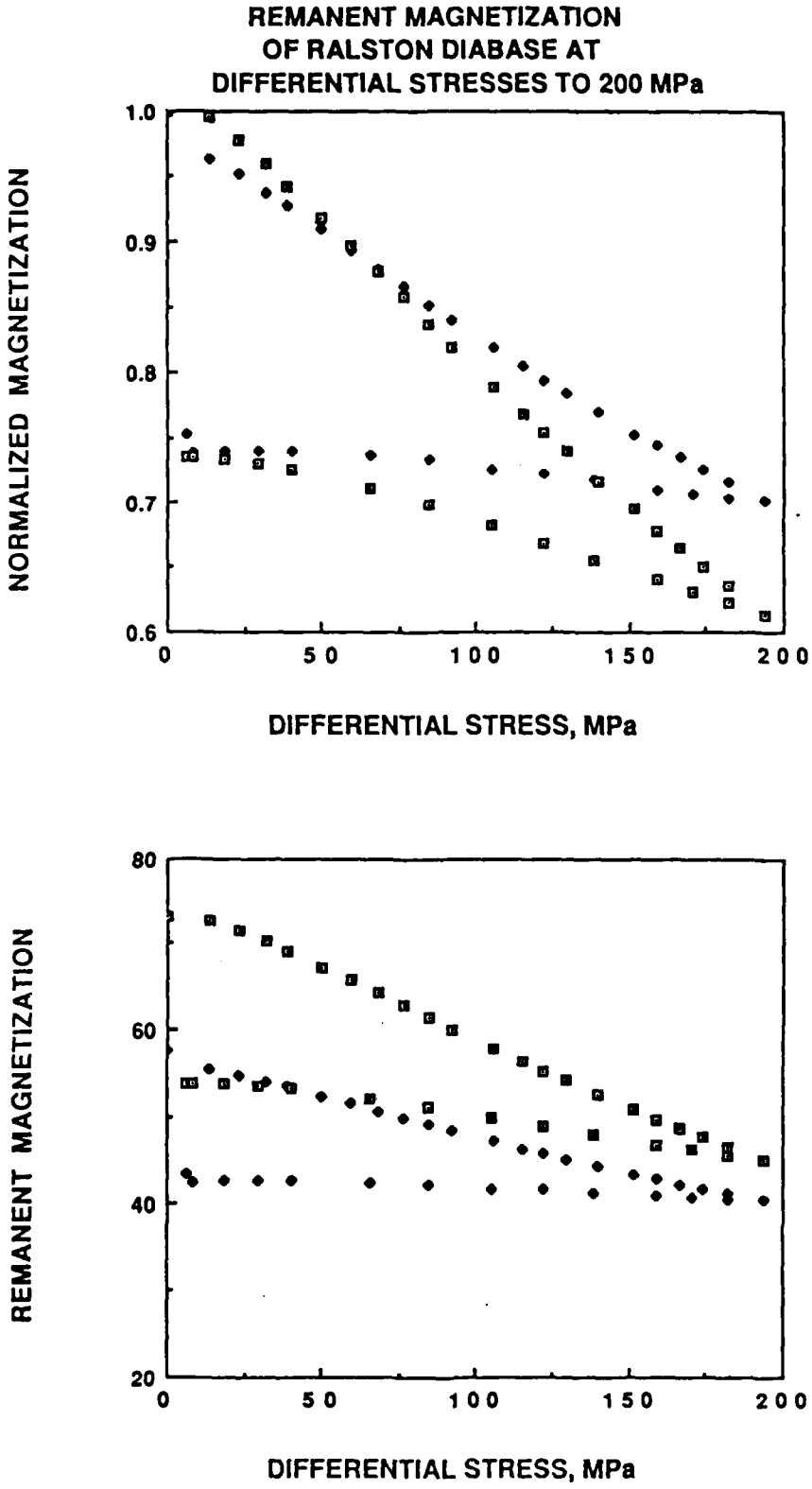

Figure 3-6 The axial (open symbols) and radial (solid symbols) components of the remanent vector normalized to their initial values (upper diagram) or without normalization (lower diagram) are plotted as a function of differential stress for a uniaxial stress experiment on a diabase specimen. The initial intensity (TRM) was 1.8×10^{-1} emu/cm^3; the inclination of the magnetic vector with respect to the sample axis was 38°.

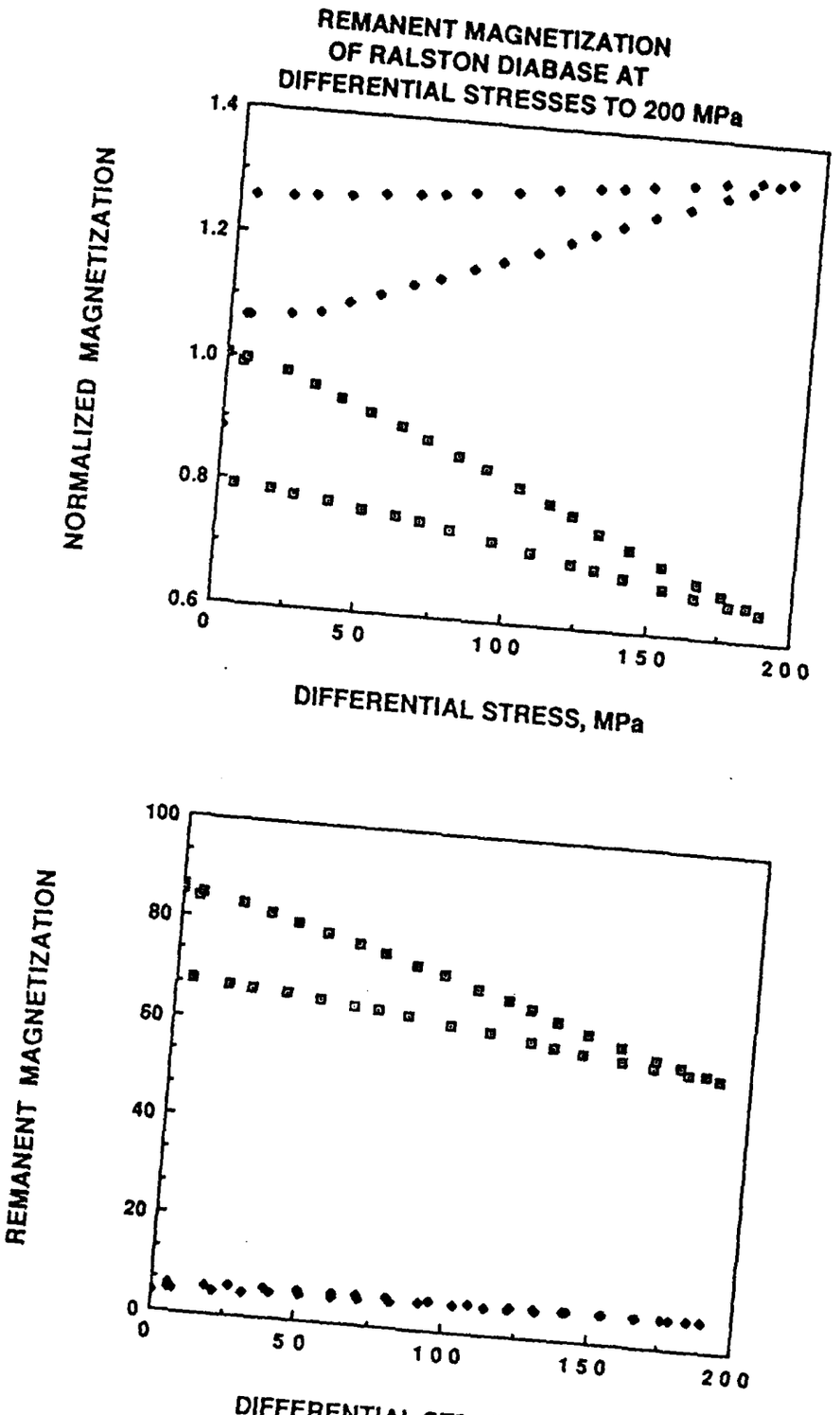

Figure 3-7 The axial (open symbols) and radial (solid symbols) components of the remanent vector normalized to their initial values (upper diagram) or without normalization (lower diagram) are plotted as a function of differential stress for a uniaxial stress experiment on a diabase specimen. The initial intensity (TRM) was 1.6×10^{-1} emu/cm^3; the inclination of the magnetic vector with respect to the sample axis was 4.9°.

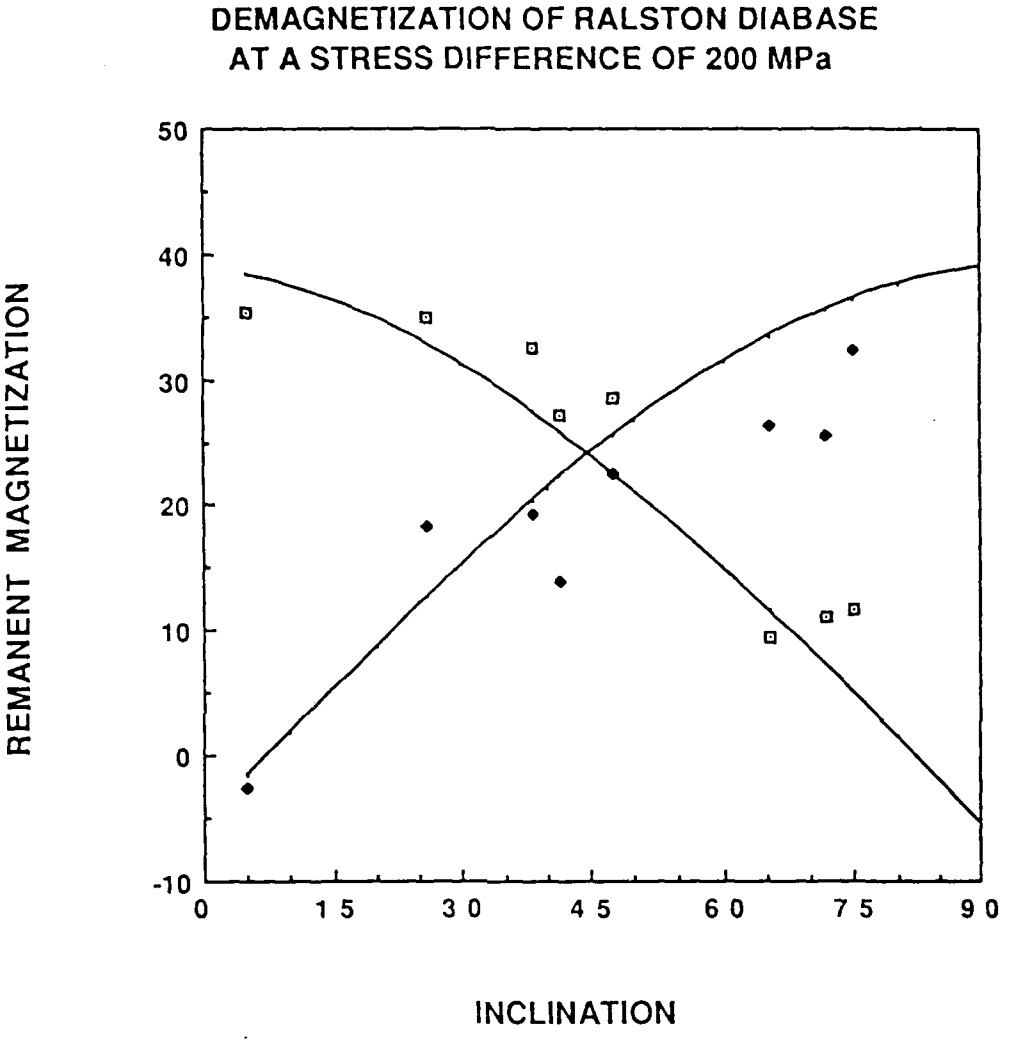

Figure 3-8 The change in the axial (open symbols) and radial (solid symbols) components of the remanent vector for diabase specimens at a differential stress of 200 MPa is plotted as a function of the inclination of the magnetic vector to the stress axis. All the observations have been scaled to an initial intensity of 1.9×10^{-1} emu/cm^3. The solid lines are the theoretical transformation for each component using equation 7.

The orientation of the magnetic vector changed with increasing stress for the diabase samples tested in this study. The vector rotated toward the stress direction, that is the inclination decreased with increasing stress. Upon unloading, there was typically no further change in the orientation of the vector. Results of a typical experiment are shown in Figure 3-9. Several cycles were carried out on a specimen with an initial inclination of 65°. As the stress increased, the vector rotated toward the principal stress axis by 2.7° at a peak stress of 200 MPa. The orientation of the vector did not recover during unloading. Subsequent cyclic loading to the same peak stress resulted in a small demagnetization as the stress was increased to 200 MPa with no permanent demagnetization at the termination of the cycle. The orientation of the remanent vector remained nearly constant during the second cycle.

The mathematical treatment of piezomagnetism as a third rank tensor described above is not strictly valid for the thermoremanent experiments because the magnetization is neither reversible when the specimen is unloaded, nor linear. However, it is interesting to note that the magnetization at any fixed stress level does transform according to the equations developed above, at least for the initial stress cycle. It may be more meaningful to treat the piezoremanent effect as a tensor only in very specialized instances where the loading conditions and stress history are known and well defined. In the previous chapter it was shown that a change in the loading regime results in a change in the magnetic response. The problem is compounded when the orientation of the stress axis varies with respect to the magnetic vector for various loading cycles. This suggests that each case must be treated individually, and the appropriate transformation developed in light of the previous stress history.

Multi-cycle experiments were also conducted on the suite of diabase samples. Typical results for experiments consisting of two stress cycles to a peak stress of 200 MPa are given in Figures 3-9 and 3-10. For these plots, the remanent intensity normalized to its initial prestress value is plotted as a function of differential stress. Demagnetizations of approximately 20% occurred during the first loading cycle. During the second loading cycle, the changes in magnetization were small. The magnetization at the peak stress of 200 MPa was very nearly the same as that observed during the initial loading procedure. As the specimen was unloaded, the magnetization exhibited only a slight hysteresis with less than several percent additional permanent demagnetization present at the end of the cycle. This observation is in substantial agreement with the results reported previously by *Martin et al, (1978) and Martin, (1980).* Furthermore, an examination of the data in Figure 3-9 showing the ratio of the radial to axial component of magnetization over the same stress range indicates that there was only a slight rotation of the magnetic vector during the second stress cycle. A rotation of less than 0.5° was observed over the loading path, and the inclination at the termination of the cycle was the same as that before the stress was applied.

A similar result was observed when specimens of diabase were repeatedly pressurized to the same peak pressure. Figure 3-11 shows the results of an experiment in which the

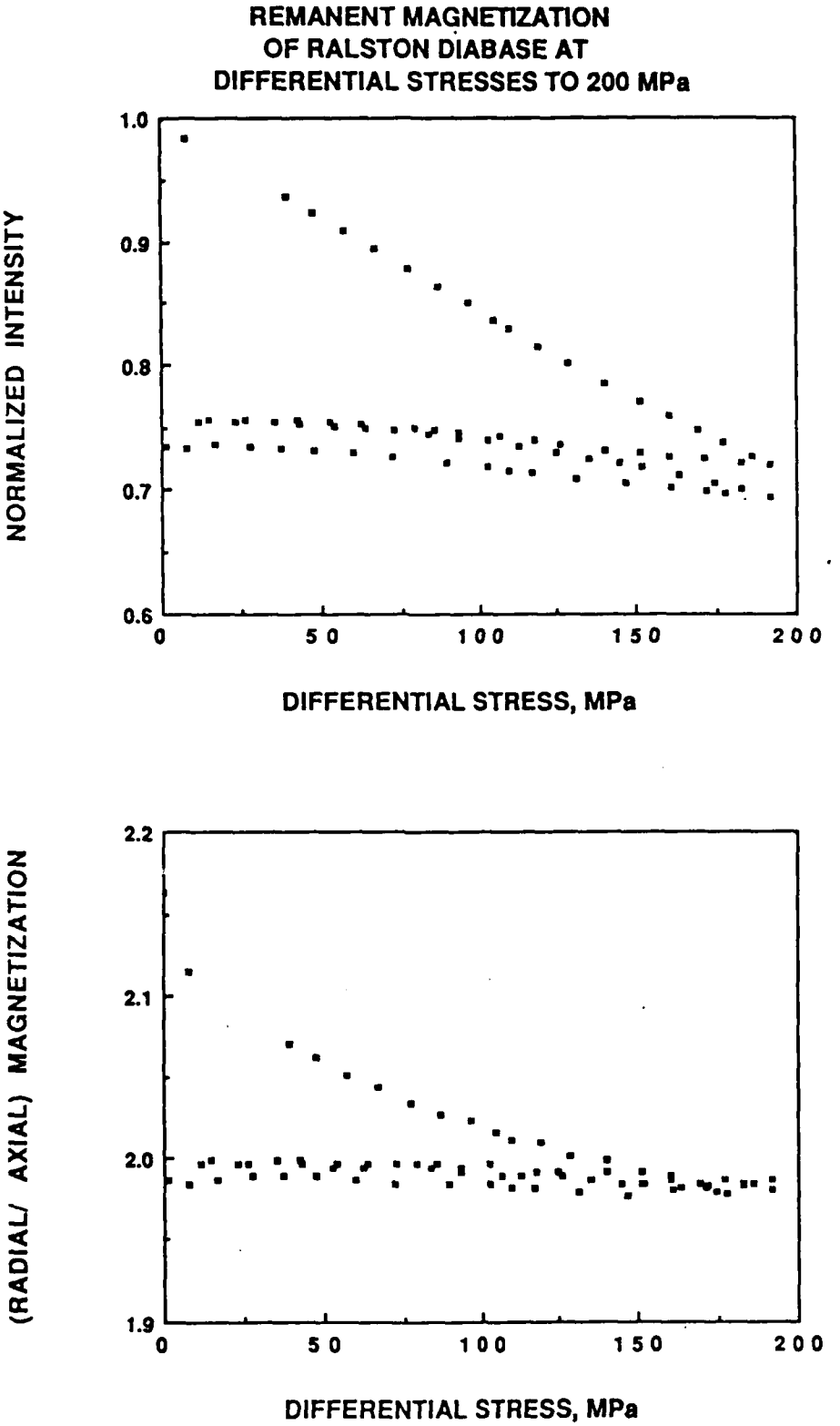

Figure 3-9 The thermoremanent intensity normalized to its initial value is plotted as a function of differential stress for two loading cycles of a diabase specimen to a peak stress of 200 MPa. The ratio of the radial to the axial component of magnetization is also shown as a function of differential stress. The initial intensity was 1.6×10^{-6} emu/cm^3; the inclination of the remanent vector with respect to the sample axis was 65°.

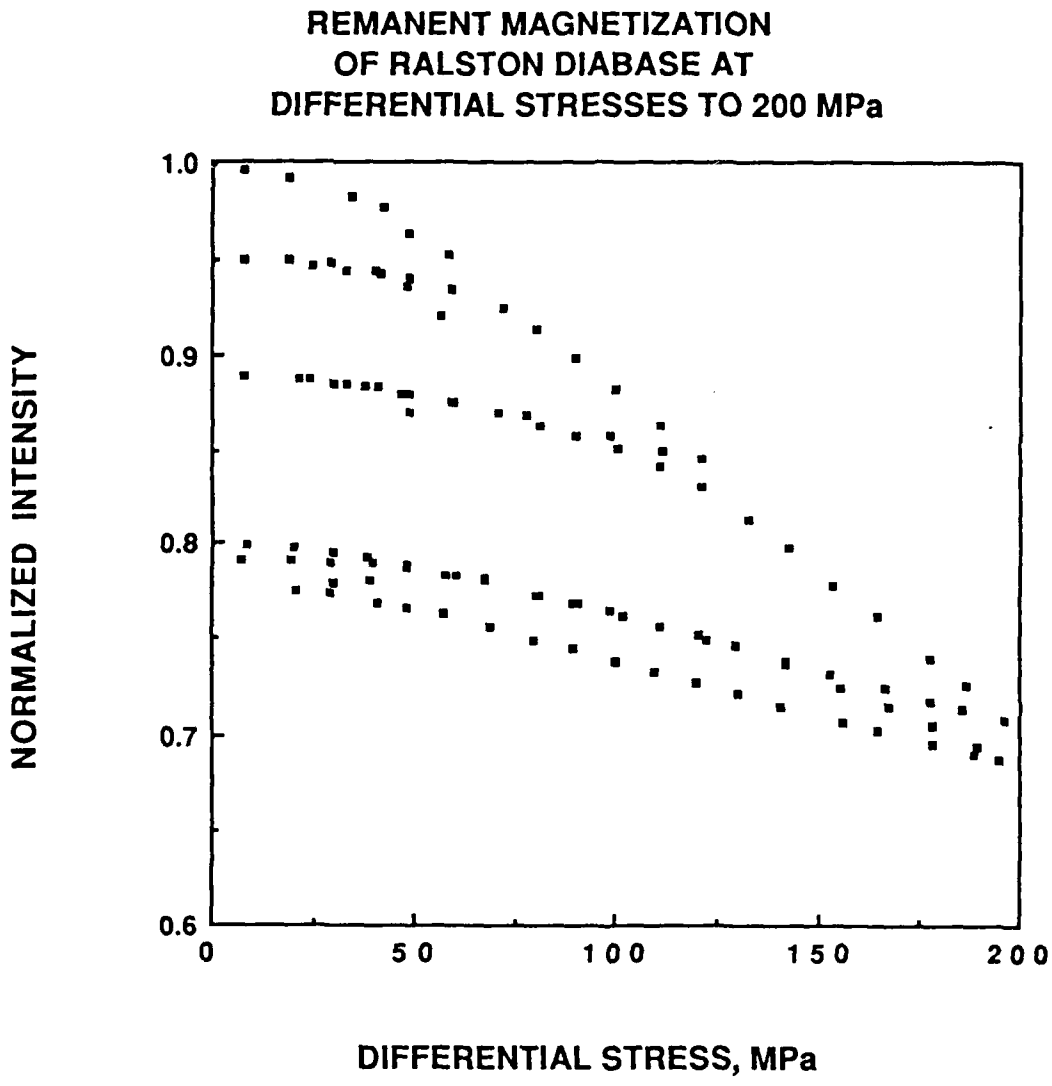

Figure 3-10 The thermoremanent intensity normalized to its initial value is plotted as a function of differential stress for two loading cycles of a diabase specimen. The initial intensity was 1.0×10^{-1} emu/cm^3; the inclination of the remanent vector with respect to the sample axis was 48°.

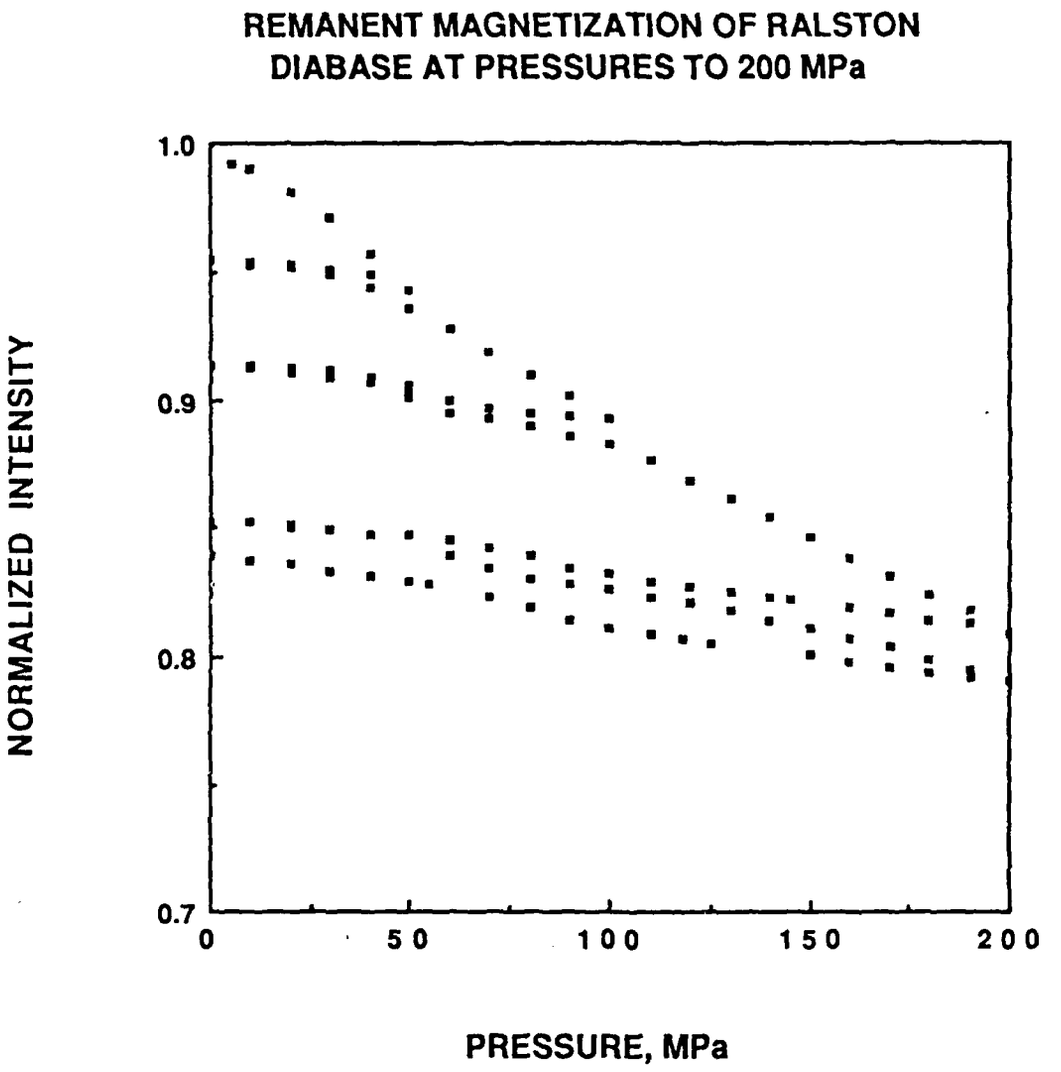

FIgure 3-11 The thermoremanent intensity normalized to its initial value is plotted as a function of pressure for two pressurization cycles on a diabase specimen. The initial intensity was 5.4×10^{-1} emu/cm^3; the inclination of the remanent vector with respect to the sample axis was 75°.

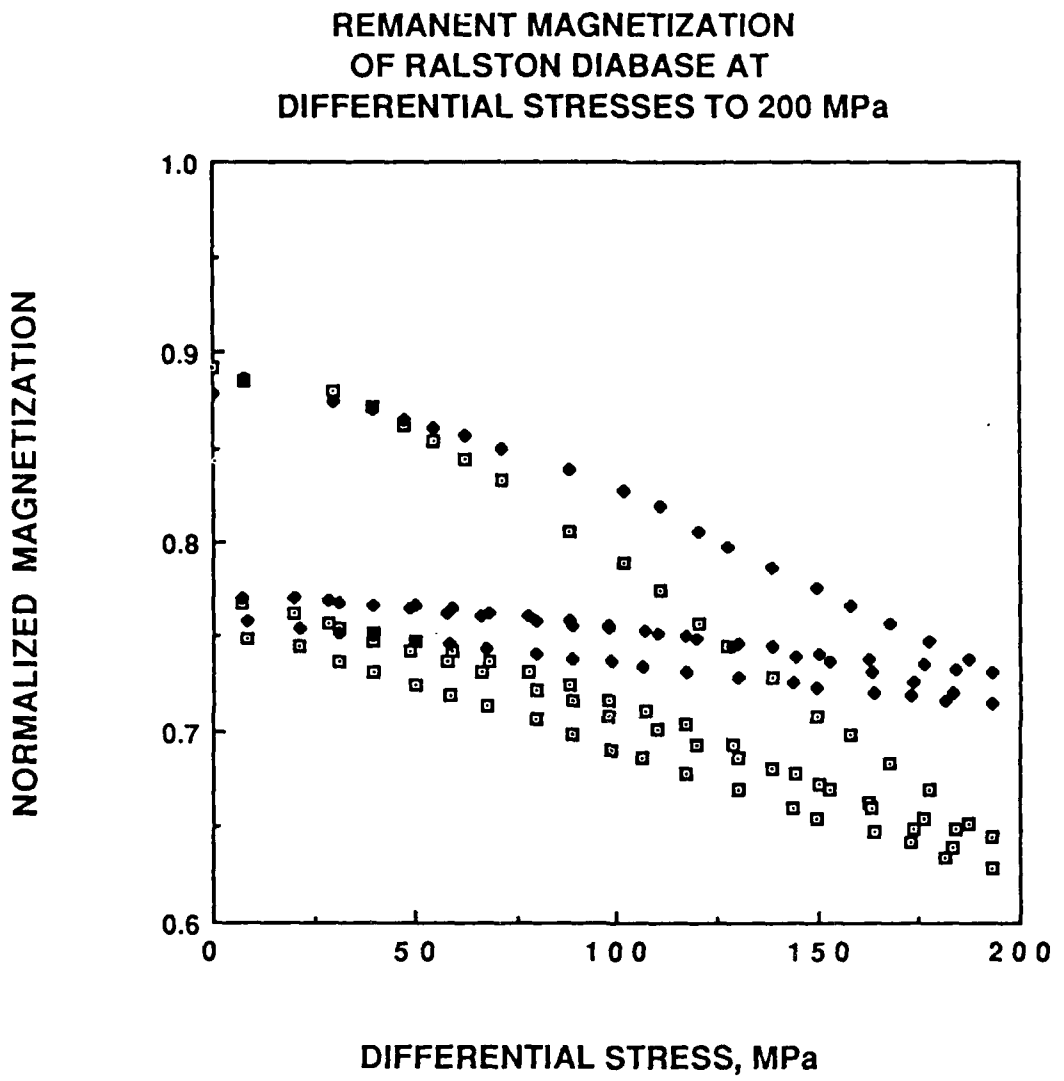

Figure 3-12 The axial (open symbols) and radial (solid symbols) components of the remanent vector normalized to their initial values are plotted as a function of differential stress for the second and third loading cycles on a diabase specimen. The first cycle was carried out in hydrostatic compression (see Figure 3-1). The initial intensity was 7.1×10^{-1} emu/cm^3; the inclination of the magnetic vector with respect to the sample axis was 72°.

specimen was initially pressurized to 200 MPa in three sequentially larger cycles and then cycled to 200 MPa for a second time. As the peak stress for sequential cycles was increased, the demagnetization observed at the termination of the cycle became progressively larger in direct proportion to the applied pressure. However, when the peak stress for sequential cycles was held constant, the change in magnetization with pressure displayed a much smaller change compared with the previous cycle, and no permanent demagnetization was observed at the end of the cycle. It should also be noted that the orientation of the remanent vector remained unchanged during each pressurization. These results are in agreement with the observations of *Martin and Noel (1988)* for cyclically pressurized specimens with the magnetic vector parallel with the specimen axis.

Finally, several mixed loading regime experiments were conducted. That is, after an initial pressurization cycle, several deformational cycles to the same peak stress were performed. Conversely, after an initial stress cycle to 200 MPa, several hydrostatic cycles were carried out on the same specimen. Figure 3-1 shows typical results for the pressurization-stress sequence. The initial pressurization cycle is shown in Figure 3-1. During the pressure cycle, each component of the remanent vector demagnetized to approximately 88% of its initial value. The relative change in each component during pressurization was the same. However, when the loading regime was changed to uniaxial stress, the axial component showed a larger relative change compared to the radial during a stress excursion to 200 MPa. Upon unloading, both components showed a pronounced hysteresis. At the termination of the cycle, an additional permanent demagnetization was observed. Both components decreased by an additional 12% to 76% of their initial value. A third cycle was carried out to the same peak stress. The loading-unloading curve for each component was nearly identical with the preceding cycle, with only a small hysteresis. No additional permanent demagnetization was detected at the end of the cycle. In Figure 3-4, a specimen with an initial inclination of 65° was stressed to 200 MPa and then unloaded. The relative change in the radial component of the magnetic vector was greater than that for the axial. This was consistent with the transformation equations discussed above. In Figure 3-12, the axial component of the remanent vector showed a greater relative change than the radial. This is indeed puzzling since the initial inclination of the remanent vector was 72°. This observation strengthens the point that loading history is very important in describing any piezomagnetic effect, and essential if a mathematical representation of the magnetic behavior has to be developed.

Figures 3-13 and 3-14 present the results of two experiments which underwent an initial nonhydrostatic loading sequence followed by a pressurization cycle. For the results shown in Figure 3-13 two stress cycles to 200 MPa preceded the hydrostatic loading. The second stress cycle is very typical of the previously described results on the Ralston diabase. The second loading cycle over the same path exhibits a much smaller relative change in each component of the magnetic vector, with a small hysteresis during unloading and a slight

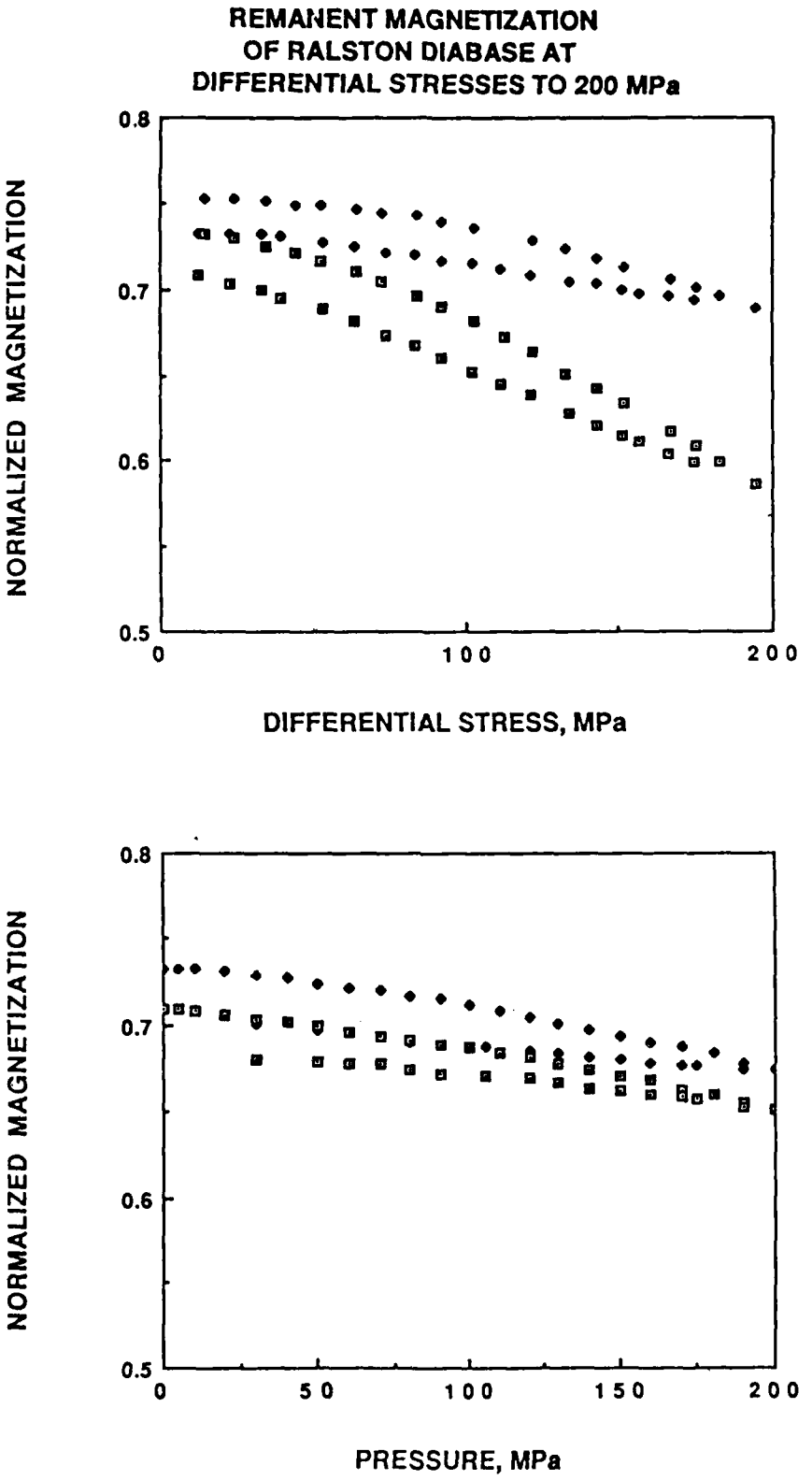

Figure 3-13 The axial (open symbols) and radial (solid symbols) components of the remanent vector normalized to their initial values are plotted as a function of differential stress (second loading cycle) for a diabase specimen. The first loading cycle is shown in Figure 3-6. The initial intensity was 1.8×10^{-1} emu/cm^3; the inclination of the magnetic vector with respect to the sample axis was 38°.

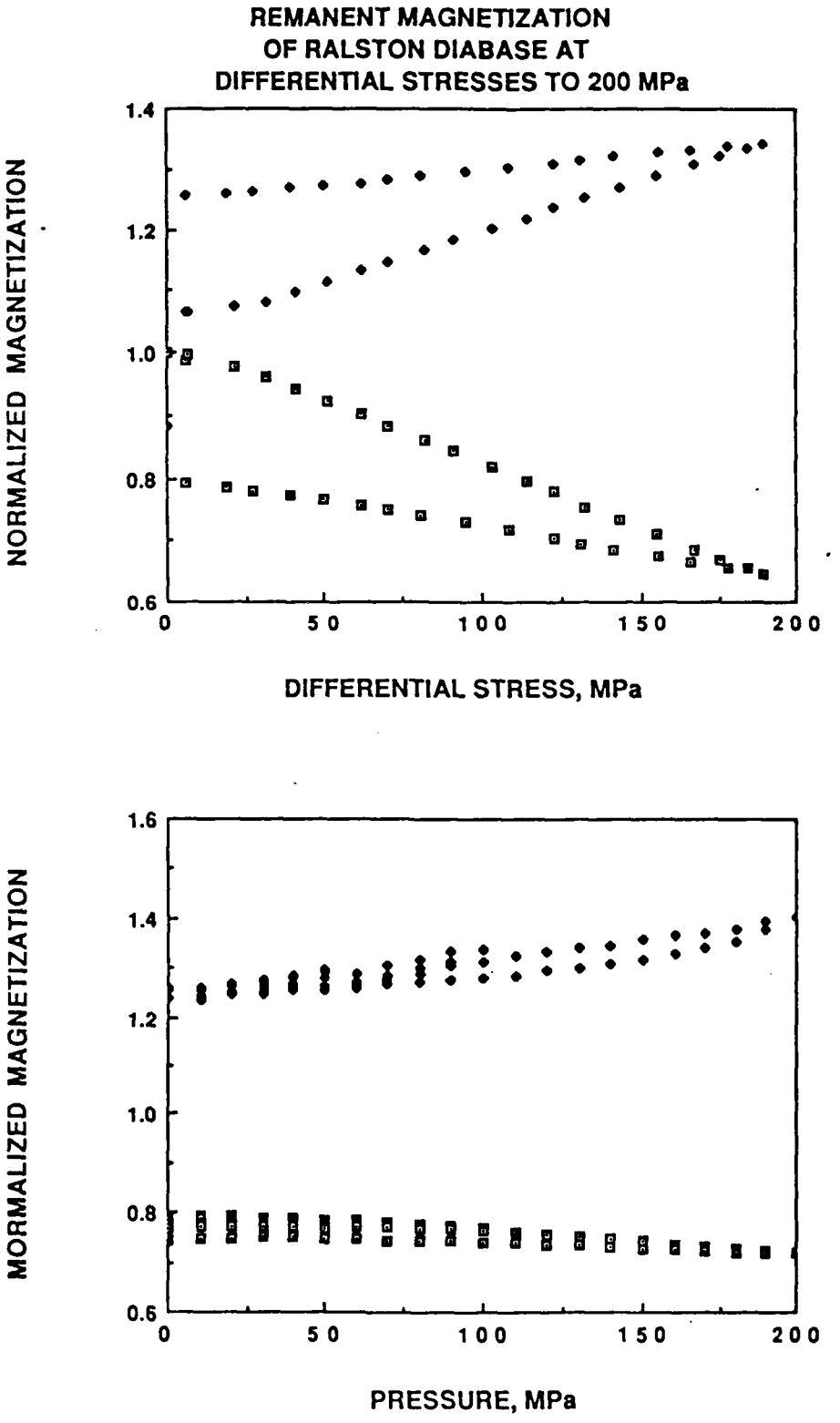

Figure 3-14 The axial (open symbols) and radial (solid symbols) components of the remanent vector normalized to their initial values are plotted as a function of differential stress (cycle 1) and pressure (cycle 2) for a diabase specimen. The initial intensity was 1.6 x 10^{-1} emu/cm^3; the inclination of the magnetic vector with respect to the sample axis was 4.9°.

additional permanent demagnetization at zero stress. When the same specimen was pressurized to 200 MPa, the relative change in each component of the magnetic vector was nearly identical. At a pressure of 200 MPa, the demagnetization of the axial component is much less than that observed during the previous cycle at a stress of 200 MPa. Once again, as the specimen was depressurized, a small hysteresis was observed, but the amount of permanent demagnetization at the termination of the cycle was imperceptible. A similar result is shown in Figure 3-14. In this case, only one stress cycle was conducted prior to pressurization. The initial stress cycle showed a relative increase in the transverse component of the remanent vector, and a decrease in the axial component. The initial orientation of the remanent vector in this specimen was 4.9°. During the pressurization cycle, the axial component showed a slight decrease while the radial component showed a consistent increase. It appears that a change in the loading regime does not cause a reversal change in the sign of the magnetization variation.

Discussion

The suite of experiments on Ralston diabase show that the effect of differential stress on remanent magnetization is significantly greater than that of hydrostatic compression. In addition, the remanent intensity simply decreased in magnitude due to pressurization, whereas, nonhydrostatic stress resulted in a small rotation in the magnetic vector, as well as a decrease in magnetic intensity. For both loading regimes, permanent demagnetization was observed at the termination of the initial stress or pressurization cycle. Furthermore, as the peak stress was augmented for sequential cycles, the magnetization at the peak stress decreased and the permanent demagnetization at the termination of the cycle increased. For subsequent stress cycles over the same path to the same peak load, the change in magnetization was not as great, the unloading was accomplished with minimal hysteresis and no permanent demagnetization was apparent at the end of the cycle.

The results obtained in this study are in substantial agreement with those reported previously by *Pike et al (1981), Ohnaka (1969), Martin et al (1978), and Martin and Noel (1988).* In each instance pressure or uniaxial stress produced a demagnetization which increased monotonically with load and resulted in a permanent demagnetization when the stress was removed. *Onaka (1969) and Martin et al (1978)* observed a rotation of the remanent moment during the application of stress and a permanent change in the inclination at the termination of the experiment.

Pike et al (1981) report a rotation of the magnetic vector for a granodiorite specimen cyclically pressurized to 150 MPa. The study presented here on Ralston diabase showed no rotation of the vector, either under pressure or at the completion of a cycle. Given the limited number of experiments carried out by *Pike et al (1981),* it is possible that the results are anomalous. Furthermore, the granodiorite experiments were carried out on a specimen with a remanent intensity an order of magnitude lower that the diabase specimens presented here. It is not known how intensity will affect the change in magnetization with pressure.

Perhaps the most interesting aspect of this series of experiments is that, at least for two well-defined loading regimes, the change in magnetization for various inclinations of the magnetic vector with respect to the loading axis (or core axis) can be represented with a simple transformation. For the hydrostatic case, the magnetic vector was inclined to the core axis and the components of remanent magnetization were measured with respect to the core axis. Since the effect of pressure was to simply reduce the remanent intensity, each component, measured at a fixed pressure, transformed according to equation 6. While it would be gratifying to treat this effect as a third ranked tensor, the practical reality is that we cannot. First, the demagnetization is neither linear with pressurization or reversible with depressurization. Consequently piezomagnetic coefficients cannot be rigorously defined

from these observations. The best that can be done is to demonstrate that for a specified pressure the magnetization does indeed rotate as a vector.

For the nonhydrostatic regime the problem is the same as observed during hydrostatic loading. The demagnetization is greater and the component of magnetization parallel to the loading direction tends to exhibit a greater demagnetization than the transverse component. At a fixed stress as the inclination of the magnetic vector with respect to the loading axis varies, each component can be represented by equation 7. The nonlinearity during loading and the pronounced hysteresis during unloading prevent the piezoremanent effect from being characterized as a tensor. Furthermore, the change in remanent magnetization depends on loading cycle as well as the loading regime; this suggests that each particular rock must be individually characterized. No general set of equations can be developed that will universally describe the observed behavior.

On the domain level the observed effect of pressure and stress can be explained in terms of domain nucleation and domain wall movement *(Boyd et al, 1984; Halgedahl and Fuller 1983)*. They observed that the application of stress or increasing the magnetic field produced domain nucleation and distortion of existing domains. Changing the stress or the magnetic field perturbs the free energy of the magnetic grain. Since the change in energy is greater when shear stress is applied to the system, as compared with hydrostatic pressure, it is understandable that the change in magnetization is greater. The fact that initial loading with either pressure or uniaxial stress, produces a permanent change in remanence can be explained by the fact that a portion of the TRM is metastable. That is, the remanence was induced at a high temperature in the presence of a magnetic field, the equilibrium condition for the TRM. The experiments conducted here are at room temperature and greater than atmospheric pressure. Consequently the application of stress establishes a new equilibrium state within the mineral grains. The domains readjust and nucleate in order to reach an equilibrium configuration. Hydrostatic pressure causes only dilatation of the magnetic mineralogy. Consequently the transition to the new energy state is accomplished without a rotation of the magnetic moment. For the non-hydrostatic case, shear stress causes a non uniform distortion of the magnetic carrier. Consequently small rotations are observed in conjunction with the demagnetization. Furthermore, if there is a relationship between the change in free energy of the system, which in this case is merely the strain energy, then the total change for an applied load should be a constant for all orientations of the magnetic vector with respect to the loading axis. A direct consequence will be the demonstrated transformation of the components of the magnetic vector shown in Figure 3-8.

The Effect of Pressure and Deviatoric Stress on Magnetic Susceptibility

While remanent magnetization persists in the absence of the applied field, induced magnetization is directly proportional to the magnitude of the inducing field. The constant that relates the applied field to the magnetization is called the susceptibility. *Kern (1961)* analyzed the effect of stress on magnetic susceptibility. Assuming a rock contained randomly oriented crystals with multi-domain grains, he developed a theory to explain the change in susceptibility due a deviatoric stress in terms of the magnetostriction parameters and the initial susceptibility of the magnetic carrier. His results indicated that the magnetic susceptibility should decrease in a nonlinear way with decreasing stress and predicted that the change in susceptibility could be represented by an equation of the form

$$K(\sigma) = \frac{K(0)}{1 + \beta\sigma} \qquad (1)$$

where K is the susceptibility, σ is the deviatoric stress, and β is the stress sensitivity. The stress sensitivity is given by

$$\beta = \frac{0.6\,(\lambda_{111} + \lambda_{100})}{J_s^2}\,K(0) \qquad (2)$$

where λ_{111} and λ_{100} are the magnetostriction constants for the titanomagnetite, and J_S is the saturation magnetization. Experimental results on a wide variety rock types by *Ohnaka and Kinoshita (1968),Nagata (1968), Kean et al (1986), Revol et al (1977) and Martin (1980)* observed that the susceptibility changes with stress were in substantial agreement with the theoretical model developed by Kern.

In spite of the apparent applicability of the model several questions remained unanswered. First, *Kern (1961)* predicted that hydrostatic pressure would not affect magnetic susceptibility. No measurements have been made to substantiate this hypothesis. Second, *Revol et al (1977)* observed a precursory susceptibility change for specimens stressed to failure. Since *Martin (1980)* demonstrated that changes in both remanent magnetization and susceptibility were independent of microcrack dilatancy which precede failure it seemed worthwhile to examine this topic in more detail. Finally, most of the reported effects of stress on magnetic susceptibility have been carried out where the inducing

field is parallel to the greatest principle stress axis. *Stacy and Johnston (1972)* suggested that the transverse component of the magnetic susceptibility tensor should increase with stress while the parallel component should decrease. In order to examine these unresolved problems, a series of susceptibility tests were carried out as a function of confining pressure, differential stress and the orientation of the inducing field with respect to the stress axis.

The susceptibility measurements were carried out on five rock types: Bandelier tuff, Dotzero basalt, Mt. St. Helen's andesite, Rapidan gabbro, and Westerly granite. The magnetic properties of these rocks are listed on Table I. The effect of pressure on susceptibility was carried out on gabbro, tuff, and granite samples. Pressure produced no appreciable changes in susceptibility. Typical results for tuff and granite specimens are given in Figures 4-1 and 4-2. The susceptibility normalized to its initial value at zero pressure is plotted as a function of pressure. The results for the Bandelier tuff show a slight increase in susceptibility at pressures lower that 40 MPa. No similar effect was observed for the gabbro or the granite. The corrections for the effect on the pressure on the susceptibility transformer is large and the observed increase is most likely due to difficulty in accurately determining the corrections that were applied to the data.

The Dotzero basalt, Bandelier tuff and Westerly granite were cyclically loaded at confining pressures ranging from 25 to 150 MPa. The samples were instrumented with strain gages. By monitoring the strains during deformation it was possible to cyclically load the specimens to approximately 85% of their fracture strength at each confining pressure. Typically the susceptibility decreased monotonically with increasing differential stress. Upon unloading, little or no hysteresis was observed and no permanent change in the susceptibility at zero stress was noted. Furthermore, the slope of the susceptibility versus the stress difference curve was independent of confining pressure. Increased confining pressure enabled the specimen to be loaded to higher differential stresses without failure but produced no change in the stress sensitivity. The results of a three cycle experiment on the Dotzero basalt are show in Figure 4-3. The sample was tested at progressively larger confining pressures of 25, 75 and 150 MPa. At a confining pressure of 125 MPa the susceptibility decreased by 9% at a stress of a 190 MPa. Upon unloading the susceptibility was reversible but showed a slight increase at zero stress. Stress cycling had increased the susceptibility by approximately 5%. This change is most likely due to compaction of the sample. The Dotzero basalt is one of the most porous of the rocks studied (7.4%), and showed a pronounced reduction in volume due to the pressurization and loading sequence in cycle one. For the second and third cycles the differential stress was increased to 275 and 350 MPa respectively. The corresponding susceptibility at these loads was 81 and 78% of the zero stress value. Unloading was reversible and the susceptibility for both cycles returned to its pre-stress value.

Four stress cycles conducted on the Bandelier tuff are shown in Figure 4-4. Two cycles were carried out at a confining pressure of 15 MPa; the second and third cycle were conducted at 75 and 150 MPa respectively. The results on the Bandelier are nearly identical

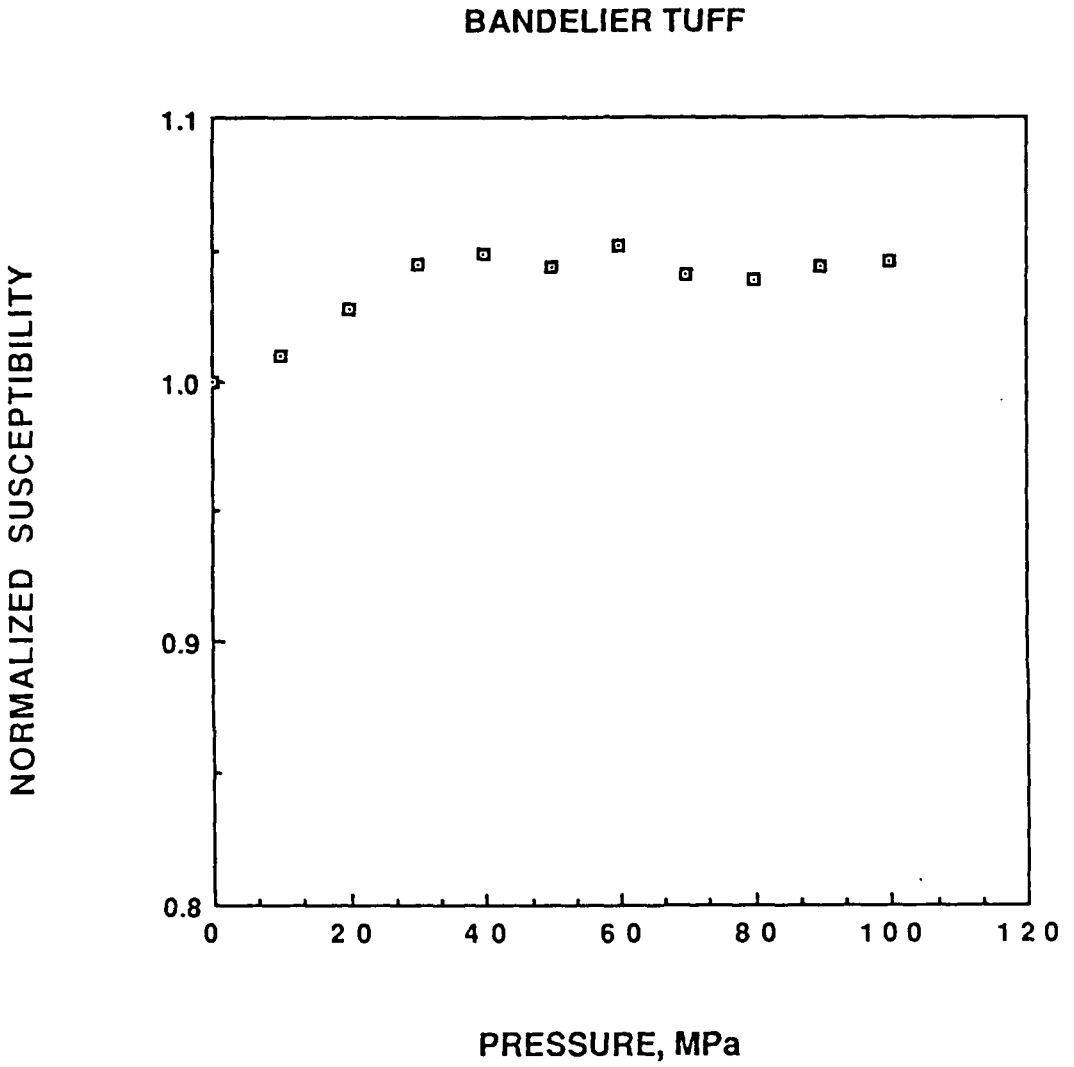

Figure 4-1 Magnetic susceptibility normalized to its initial value is plotted as a function of hydrostatic pressure for a specimen of Bandelier tuff. The initial susceptibility was 2.80×10^{-4} emu/g/Oe.

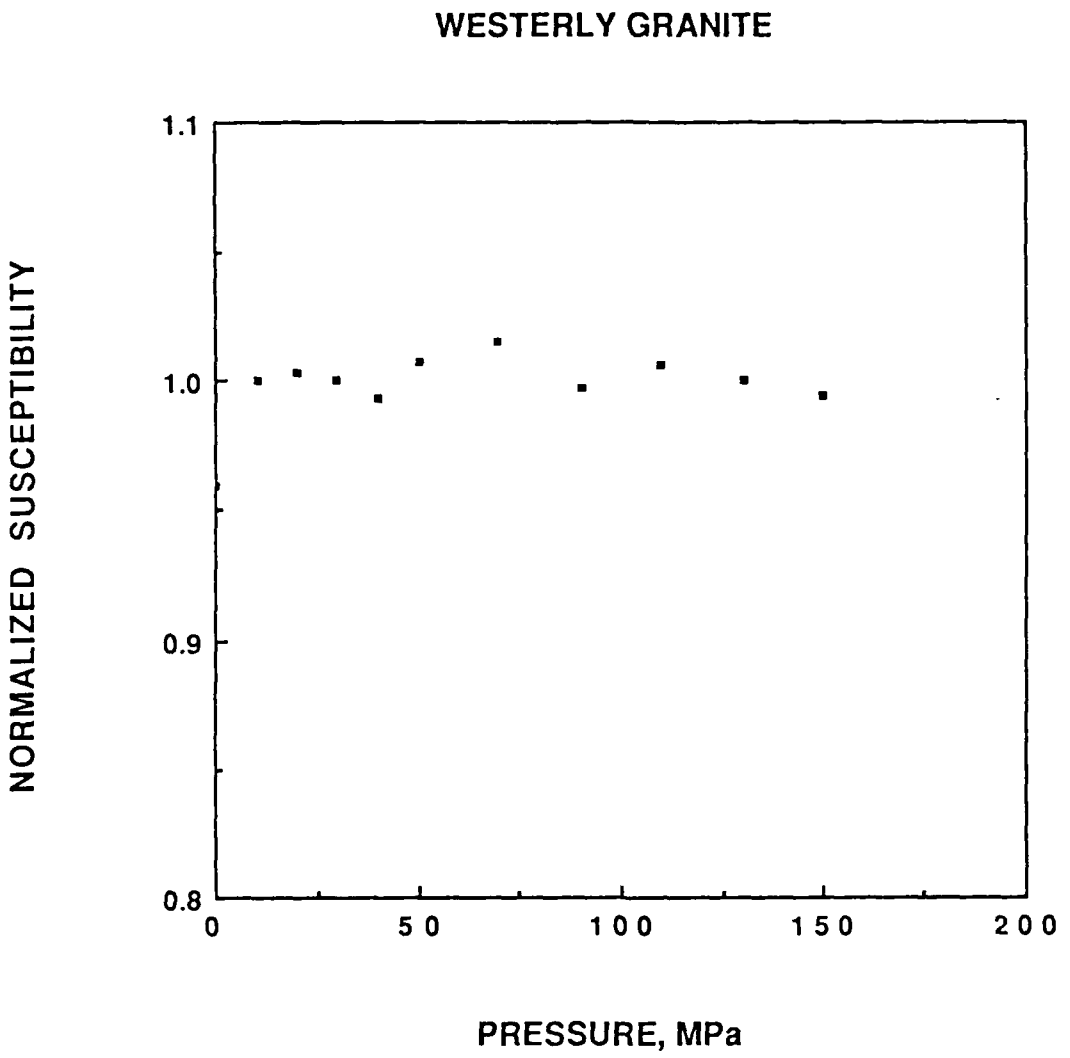

Figure 4-2 Magnetic susceptibility normalized to its initial value of hydrostatic pressure for a specimen of Westerly granite. The initial susceptibility was 3.6×10^{-4} emu/g/Oe.

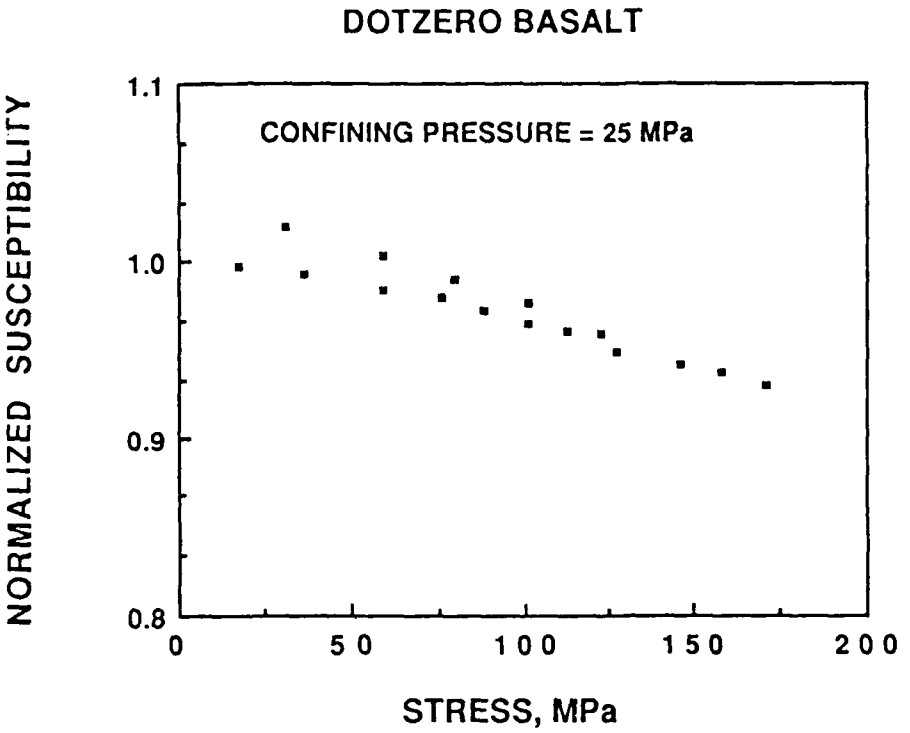

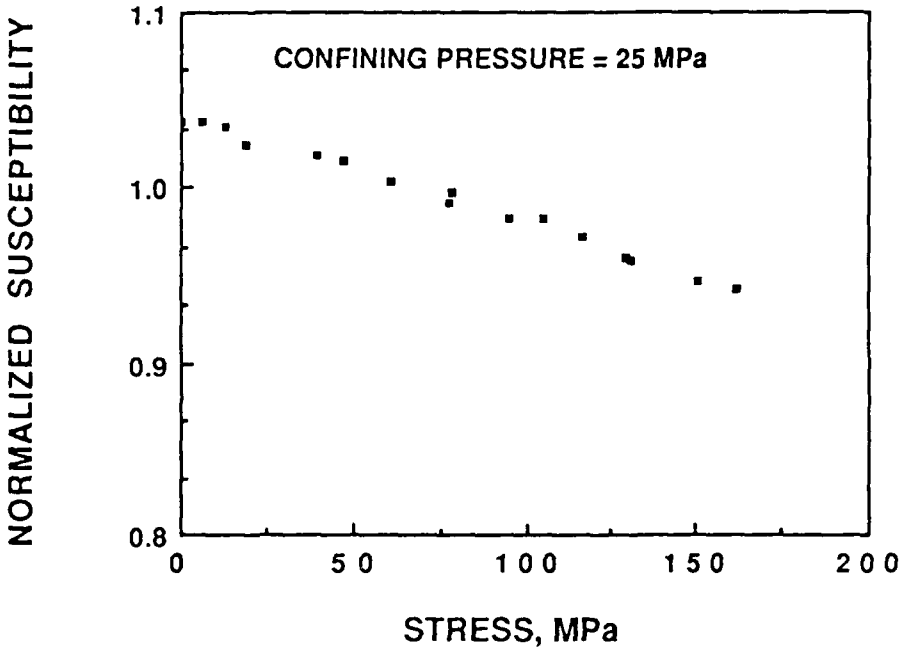

Figure 4-3 Magnetic susceptibility normalized to its initial value is plotted as a function of differential stress for three loading cycles on a Dotzero basalt specimen. The initial susceptibility was 1.45×10^{-3} emu/g/Oe.

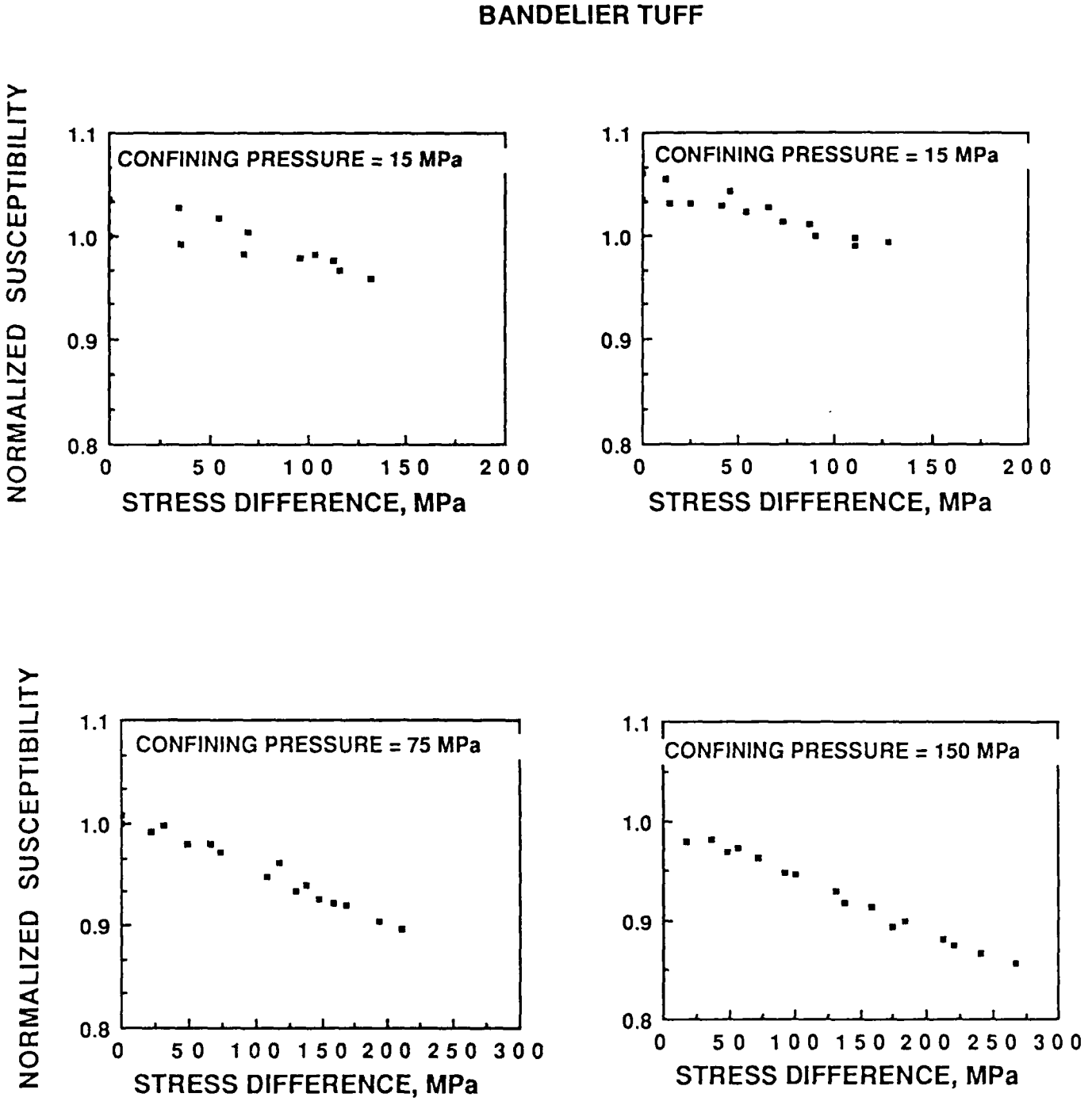

Figure 4-4 Magnetic susceptibility normalized to its initial value is plotted as a function of stress difference for four loading cycles on a Bandelier tuff specimen. The initial susceptibility was 2.8×10^{-4} emu/g/Oe.

to those observed on the Dotzero. The first loading cycles at low confining pressures showed a decrease in susceptibility with increasing load. Upon unloading the susceptibility at each stress level was greater than that observed on the loading cycle and the zero stress value of susceptibility was greater than the pretest value. The second and third cycles at higher confining pressures showed nearly the same stress dependence as the low pressure cycles but displayed a much smaller hysteresis and no change in the zero stress value of susceptibility. The porosity for the Bandelier tuff was 9.8%.

While the relatively porous and weak basalt and tuff specimens showed a small increase in susceptibility after loading, the low porosity (0.1-0.2%) Westerly granite and Rapidan gabbro did not exhibit this effect. The results of a typical experiment on Westerly granite are given in Figure 4-5. Three cycles were carried out at progressively higher confining pressures of 25, 75 and 150 MPa. The magnetic susceptibility normalized to its prestress value is plotted as a function of differential stress for each cycle. The susceptibility decreased nonlinearly with decreasing stress. A differential stress of 150 MPa produced a demagnetization of 20%, 400 MPa resulted in a 30% change and 900 MPa produced a 38% reduction in susceptibility. The susceptibility versus stress curve was identical for all loading segments regardless of confining pressure. However, the reproducibility during unloading decreased with increasing confining pressure. In all cases, the observed susceptibility at a fixed differential stress was greater during unloading than it was during loading. These deviations are definitely real and cannot be ascribed to experimental error that might arise due to friction in the O-ring seal of the pressure vessel. Errors of several percent can be attributed to the change in the direction of the frictional force exerted by the O-ring during unloading. In order to produce a truly reversible susceptibility versus stress curve the errors in computing the stress on the sample would have to approach 12 to 15%. This is well beyond the range of experimental error.

Finally, specimens of andesite granite, tuff and gabbro were loaded to failure at a fixed confining pressure of 25 MPa. *Revol et al (1979)* reported a significant recovery of the magnetic susceptibility prior to failure. They termed the change a precursory phenomenon. In the four failure experiments shown in Figure 4-6, the susceptibility decreased continuously until the sample failed. There is no evidence of anomalous or precursory behavior preceding fracture.

Discussion

The results of the susceptibility measurements carried out under hydrostatic pressure and confined compression corroborated the anticipated dependencies proposed by *Kern (1961)*. His analysis showed that deviatoric stress should result in a nonlinear decrease in susceptibility. He also predicted that confining pressure should produce no change in susceptibility. Since confining pressure produces only dilitational strains, the geometry, as

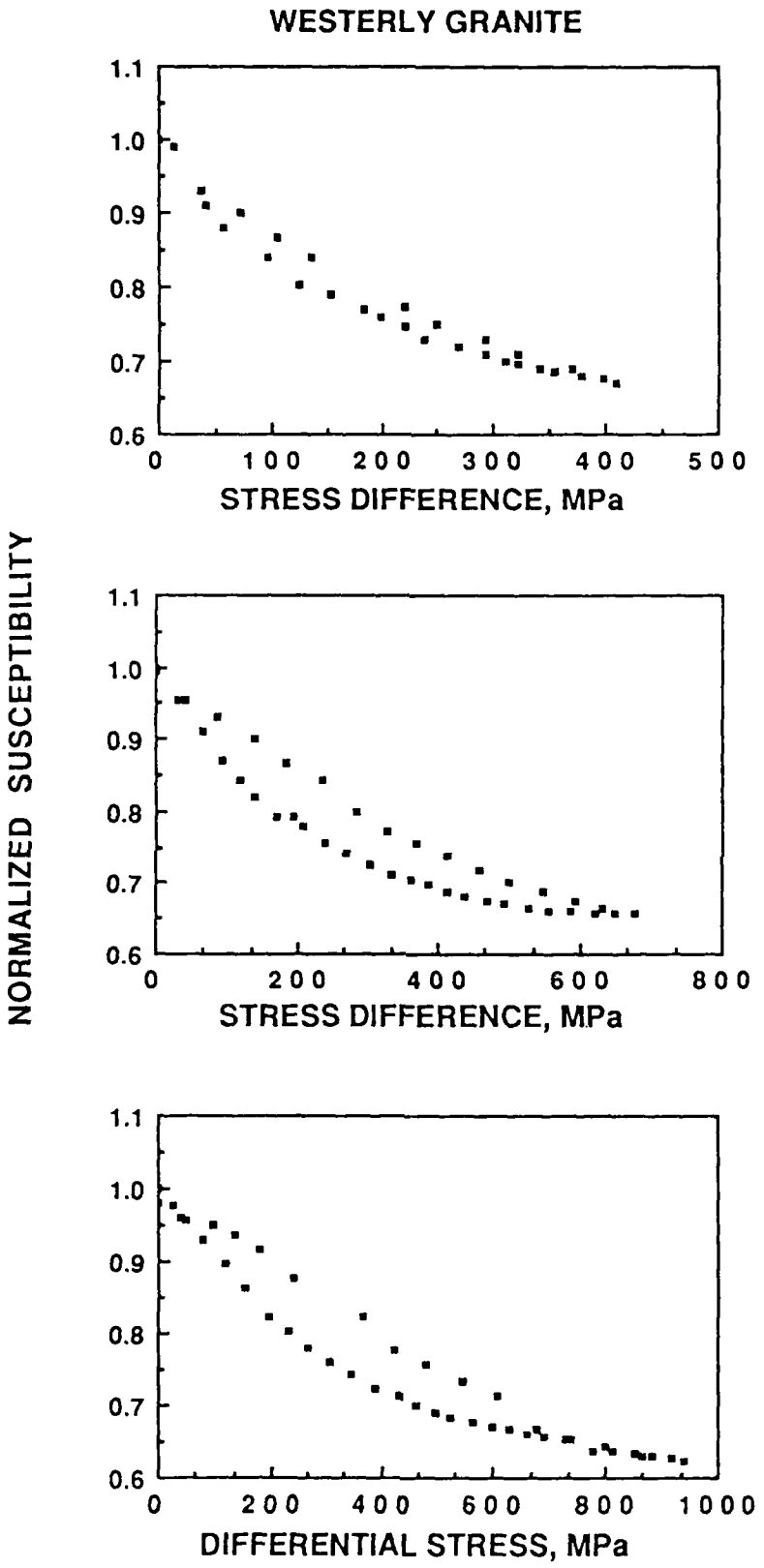

Figure 4-5 Magnetic susceptibility normalized to its initial value is plotted as a function of stress difference for three loading cycles on a Westerly granite specimen at confining pressures of 25, 75, and 150 MPa. The initial susceptibility was 3.6×10^{-4} emu/g/Oe.

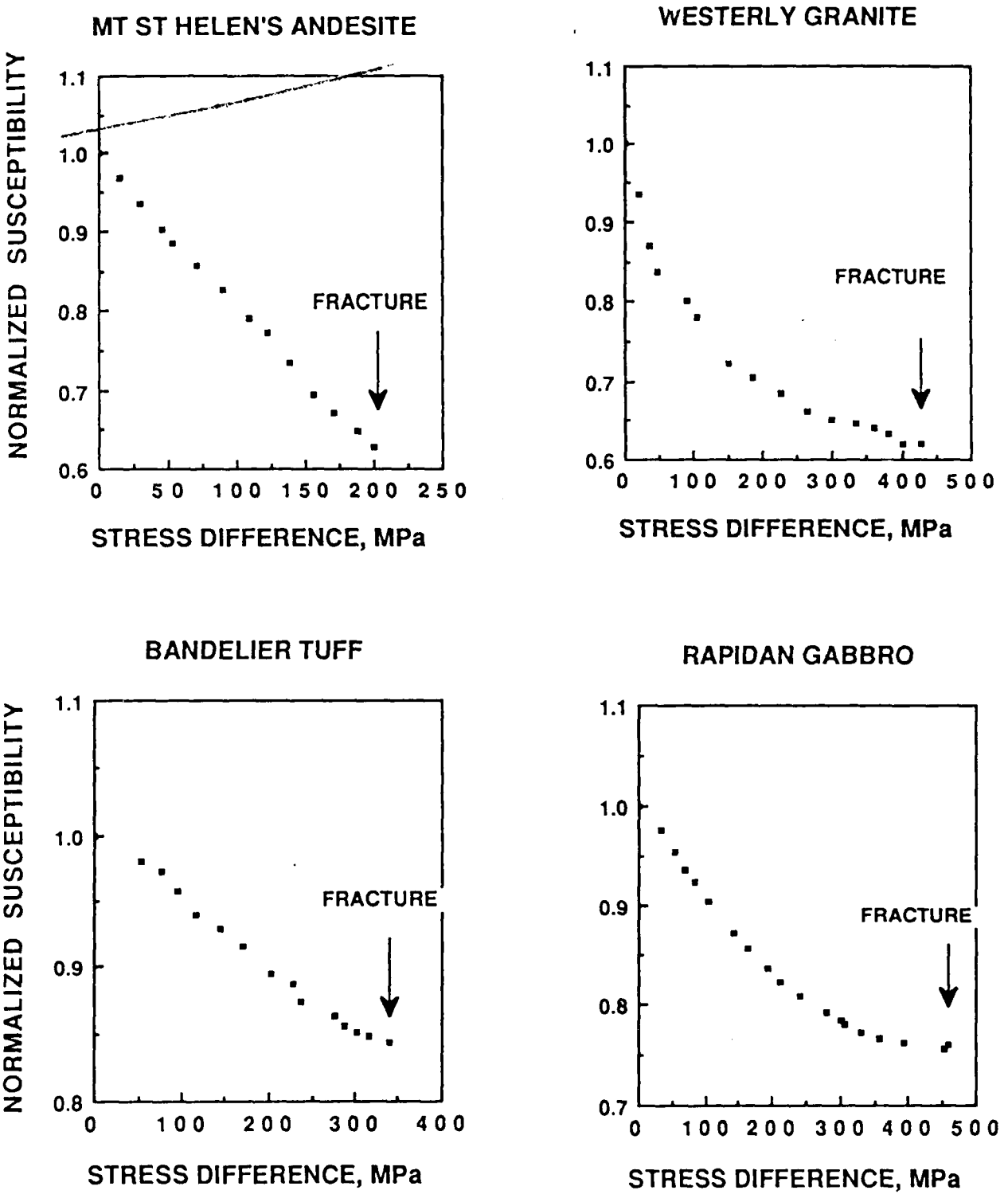

Figure 4-6 Normalized susceptibility is plotted as a function of stress difference for four specimens loaded to failure. The confining pressure on each rock core was 25 MPa.

well as the orientation of the magnetic carriers, should remain constant during pressurization. In the absence of shear strain energy, the susceptibility should not vary with pressure. This result may be approached in another way. If it is assumed that piezomagnetism can be represented with a third rank tensor of the form

$$\Delta J_i = d_{jk} \Delta \sigma_{jk} \qquad (3)$$

where ΔJ_i is the change in magnetization, (which is in turn equal to $K_{im}H_{m)}$, d_{ijk} is the piezomagnetic coefficient σ_{jk} is the deviatoric stress. *Nye (1964)* demonstrated, using symmetry arguments, that pressure should produce no change in magnetization if the material is isotropic. A series of measurements has shown that these rocks are isotropic in that the magnetization induced with the application of an external field is independent of orientation. For an isotropic material, all the piezomagnetic coefficients are zero. Consequently, no pressure dependence on magnetic susceptibility should be observed.

The decrease in susceptibility during the cyclic application of stress appears to be consistent over a wide range of rock types and magnetic mineralogies. The change is greatest at low stresses and decreases as the differential stress grows. At stresses approaching 1,000 MPa and greater, the decrease in susceptibility per increment of stress is indeed small and asymptotically approaches zero. In terms of the domain structure observed by *Boyd et al (1984)* and *Halgedahl and Fuller (1983)* and discussed in the previous sections, a physical explanation for the observations can be presented. In contrast with the effect of stress on remanent magnetization where the experiments were carried out in zero field, induced magnetization only exists in the presence of a field. Consequently, at zero stress, the domain structure is in an equilibrium configuration with respect to the applied field. As differential stress is applied to the system, the domains nucleate and distort in response to the change in energy. At extremely high stresses, the nucleation and rotation reaches a point at which it can no longer sustain further motion. Consequently, the change in susceptibility exhibits an extremely low stress dependence. This is analogous to the situation where the field on a crystal is increased until magnetic saturation occurs, increasing the field produces only a negligible increase in magnetization. In fact a very simple calculation for several of the rocks studied here shows that the strain energy of the magnetic mineralogy at 1,000 MPa is of the same order as the work done on a titanomagnetite crystal by an external field at saturation. It has already been pointed out by *Halgedahl and Fuller (1983)* that differential stress produces domain distortions and nucleations very similar to those observed with the application of stress. In light of this observation, it is reasonable to assume that there is an equivalence between the energy developed in a crystal due to the application of large fields, and the strain energy at high stresses. For this case the general energy function can be expressed as

$$dG = \varepsilon_{ij}\, d\sigma_{ij} + J_k dH_k$$

where G is an energy function, ε_{ij} is strain, σ_{ij} is stress, J_k is magnetization, and H_k is the

inducing field. For a constant field, the energy change is controlled by the stress-strain behavior, while at a constant stress, the energy change is due to a variation in the inducing field. Therefore, it appears that the stress sensitivity is controlled by the domain state in the magnetic carrier. Furthermore, saturation magnetization should occur at lower field strengths as the stress on the magnetic assemblage increases.

The Effect of Stress on Magnetic Susceptibility for Cases Where the Field Direction is Inclined to the Principal Stress Direction

INTRODUCTION

The effect of uniaxial stress on the magnetic susceptibility of rocks have been reported in several experimental studies *(Wilson, 1922; Grabovsky, 1947; Kalashnikov and Kapitza, 1952; Grabovsky and Parkomenko, 1953, Pakitza, 1955; Nagata and Kinoshita, 1965; Nagata, 1966; Ohnaka and Kinoshita, 1968; Kinoshita, 1968; Kean et al., 1976; Revol et al., 1977; and Martin, 1981).* In all cases, the longitudinal magnetic susceptibility, $K^p(\sigma)$, decreased 25-50% as stress was increased. The transverse susceptibility, $K^n(\sigma)$, showed either a slight increase or small decrease. The longitudinal and transverse susceptibilities were defined as the susceptibilities parallel and perpendicular to the stress greatest compressive stress direction, respectively. The best fit to the data generated in these experiments is given by the relations:

$$K^p(\sigma) = \frac{K_o}{1+\beta\sigma} \tag{1}$$

and

$$K^n(\sigma) = K_o\left(1+\frac{\beta\sigma}{2}\right) \tag{2}$$

where K_o is the initial isotropic susceptibility measured at zero stress and β is an empirical constant for each material.

Kean et al. (1976) used an apparatus which allowed the sample to be compressed while it was rotated in a fixed external field, measuring susceptibility versus direction for a series of rocks and titanomagnetite dispersions. The data generated in these experiments were fit by an empirical equation of the form

:

$$K(\theta,\sigma) = K_o\left[1-\frac{\beta\sigma}{4}(3\cos 2\theta + 1)\right] \tag{3}$$

where θ is the angle between the direction of the applied field **H** and the uniaxial stress

axis. *Kean et al.*(1976) also found that the stress-dependence of susceptibility was sensitive to the size and composition of the magnetic mineral grains. The stress sensitivity, i.e.the change in susceptibility measured for a given increment of stress, increased with both grain size and titanomagnetite content.

Martin (1981) conducted cyclic loading tests over an extended stress range and at confining pressures to 200 MPa. The longitudinal susceptibility typically decreased 50% as stress was increased, and there was very slight hysteresis upon unloading. The decrease in susceptibilty was not affected by either the opening of microcracks or changes in confining pressure, but appeared solely sensitive to the differential stress. This result suggests that changes in susceptibility may be a reliable indicator of perturbations in the stress fields of tectonically active regions.

Theoretical studies of the effects of stress on magnetic susceptibility have been reported by various authors. The literature has been dominated by domain-rotation or inverse-magnetostrictive models; an explanation of these types of models follows. When an external field **H** is applied to a magnetic mineral grain, the domains of the grain rotate so that their magnetizations, **M**, reinforce the applied field. In grains which are large enough to contain many domains, there is also movement of the boundaries between them (domain-wall translation). The combined effects of these two processes result in an increase in the volume of domain with magnetizations, **M**, parallel to the applied field, **H**, and the grain is said to be susceptible ($K = \mathbf{M} / \mathbf{H}$).

When a field is first applied to a magnetic grain, the dimensions of the grain change. This effect has been called magnetostriction. Most of the magnetostrictive change in length, ε (strain), is associated with the process of domain rotation. Experimental results have shown that there is a relation between the magnetostriction of a material and its magnetic behavior under stress. The reversible rotation of magnetic domains in a material under stress was called the inverse-magnetostrictive effect.

In rocks under compressive stress, the domains of the magnetic mineral grains are rotated away from the compressive stress axis. Consequently, the susceptibility parallel to the stress axis is reduced, while the susceptibility normal to the stress axis is increased. *Kern (1961), Stacey 91962), Stacey (1963), Nagata (1966), Kinoshita (1968), and Nagata (1970 a,b)* all assumed isotropic magnetostriction and obtained expressions for the stress-dependence of susceptibility. All the expressions were consistent with the experimental results, but the assumption of isotropic magnetostriction resulted in expressions which were not completely satisfactory.

Magnetic minerals are not isotropic but possess "easy" and "hard" directions of magnetization. The direction of "easy" magnetization is the direction of spontaneous magnetization in the absence of an external field. The degree of crystal anisotropy is represented by the constants K_1 and K_2, which are a measure of the work necessary to deflect the magnetizations away from the "easy" directions. It follows that the

magnetostrictions of the cubic magnetic minerals is also anisotropic and is specified by the constants λ_{100} and λ_{111} which are the changes in length in the (100) and (111) crystallographic directions, respectively.

Stacey and Johnston (1972) calculated expressions for $K^p(\sigma)$ and $K^n(\sigma)$ in terms of the crystal anisotropy constants K_1 and K_2 and the magnetostrictive constants λ_{100} and λ_{111} and obtained the following expressions:

$$K^p(\sigma) = \frac{K_o}{1 + S\sigma} \tag{4}$$

$$K^n(\sigma) = K_o\left(1 + \frac{S\sigma}{2}\right) \tag{5}$$

where S is the theoretically derived stress sensitivity:

$$S = \frac{\lambda_{100} + \lambda_{111}}{3NM_S^2 - 4(K_1 - 0.33\,K_2)} \tag{6}$$

N is the average demagnetizing factor, which depends mainly on grain shape, and M_S is saturation magnetization. This expression was an improvement over previous ones, which did not take into account the anisotropy of magnetostriction.

The results of experimental studies on the effects of stress on magnetic susceptibility have been widely reported, but the results have been deficient in several ways. In particular, most investigators looked at the stress dependence of susceptibility only in directions parallel and, in a few cases, normal to the loading axis; also, most limited their tests to a small stress range using millimeter-sized samples. *Kean et al.* (1976) were the only investigators to measure the susceptibility in directions intermediate to the stress axis, but closer examination of their experimental method raises questions about the validity of their observations.

It would be useful to the interpretation of the tectonomagnetic events to measure the stress dependence of magnetic susceptibility at intermediate orientations to the stress axis and over an expanded stress range. This might give a better understanding of the total process involved in these changes. Ideally, the results of these experiments would be a generalized susceptibility tensor k_{ij} whose components are a function of applied stress, σ. This tensor permits the inversion of magnetic data to obtain stress changes when the direction of magnetization does not coincide with the compressive stress axis. This

situation is the most geologically realistic one, since the direction of the earth's field will probably not be either parallel or normal to the differential stress axis. With this rationale in mind, a series of experiments was conducted to determine the susceptibility as functions of stress and direction relative to the loading axis.

Experimental Results

Experiments were conducted on samples of the Ralston diabase, Rapidan gabbro, and Westerly granite. The results of a typical experiment on the Ralston intrusive are shown in Figure 5-1. The normalized susceptibility is plotted as a function of applied stress for four inclinations of the measuring coils with respect to the loading axis of the sample. The longitudinal (0^o) susceptibility showed the largest decrease with increasing stress and was 60% of its initial value at 180 MPa. The susceptibilities measured at values of $\theta = 15$, 25, and 35^o showed similar stress dependencies to those of the longitudinal susceptibility, but the magnitude of the decrease was progressively smaller for each orientation. The susceptibilities measured for $\theta = 15$, 25, and 35^o decreased to 62, 66, and 68% of their initial values, respectively, at 180 MPa.

The rock samples were cyclically loaded and the measurements at some orientations were repeated. The susceptibility curves were reproducible. There was slight hysteresis during the unloading of the first cycle, the susceptibility slightly exceeding its initial value by 1%.

The results of a typical experiment on the gabbro are shown in Figure 5-2. The stress dependence of the gabbro was similar to that of the Ralston intrusive. The longitudinal susceptibility again showed the largest decrease and was 65% of its initial susceptibility at the peak stress. The susceptibilities 15, 25, and 35^o from the loading axis again showed stress dependencies that were similar to the longitudinal susceptibility, and the magnitude of the decrease was progressively smaller for each orientation. The susceptibilities for $\theta = 15$, 25, and 35^o decreased to 66, 68, and 72% of their initial values, respectively, at 180 MPa.

The susceptibility curves for the gabbro differed slightly from those of the Ralston intrusive: the gabbro showed a smaller decrease with increasing stress for each orientation; the intervals between the curves for the gabbro actually appear to cross one another below 60 MPa, although this is most likely the result of errors in the calibration of the machine frame applied to the data.

The results of a typical experiment on the Westerly granite are presented in Figure 5-3. The results for this rock type differed significantly from the results of the previous two. While the general shape of the susceptibility curves for the granite were similar to the curves for the Ralston intrusive and the gabbro, the longitudinal susceptibility showed the smallest decrease, 70% of its initial value, at 180 MPa. The susceptibilities measured

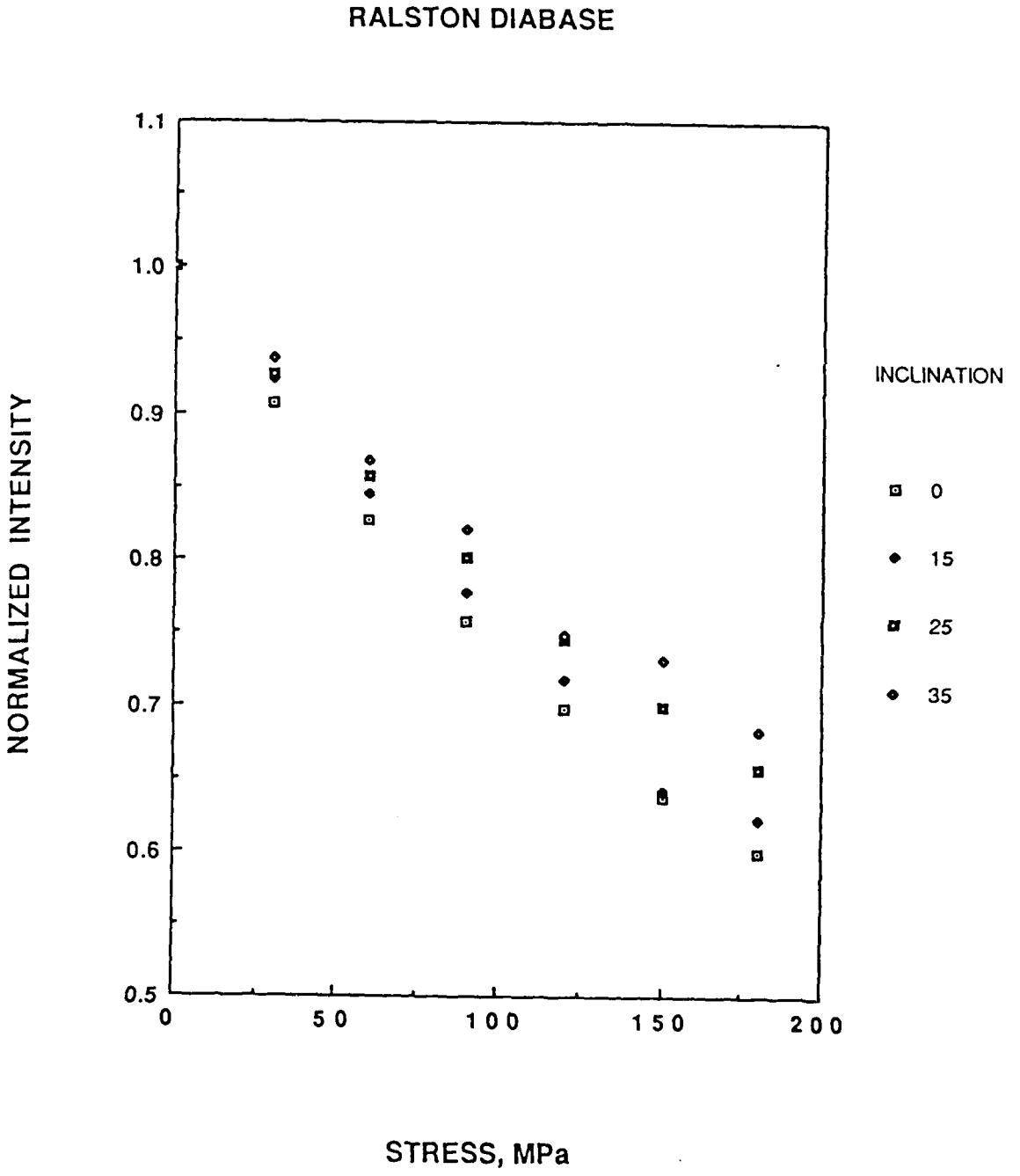

Figure 5-1. The change in normalized susceptibility is presented as a function of stress, at $\theta = 0, 15, 25$, and 35^{o}, for the Ralston intrusive. The initial susceptibility was 1.54×10^{-3} emu /g/Oe.

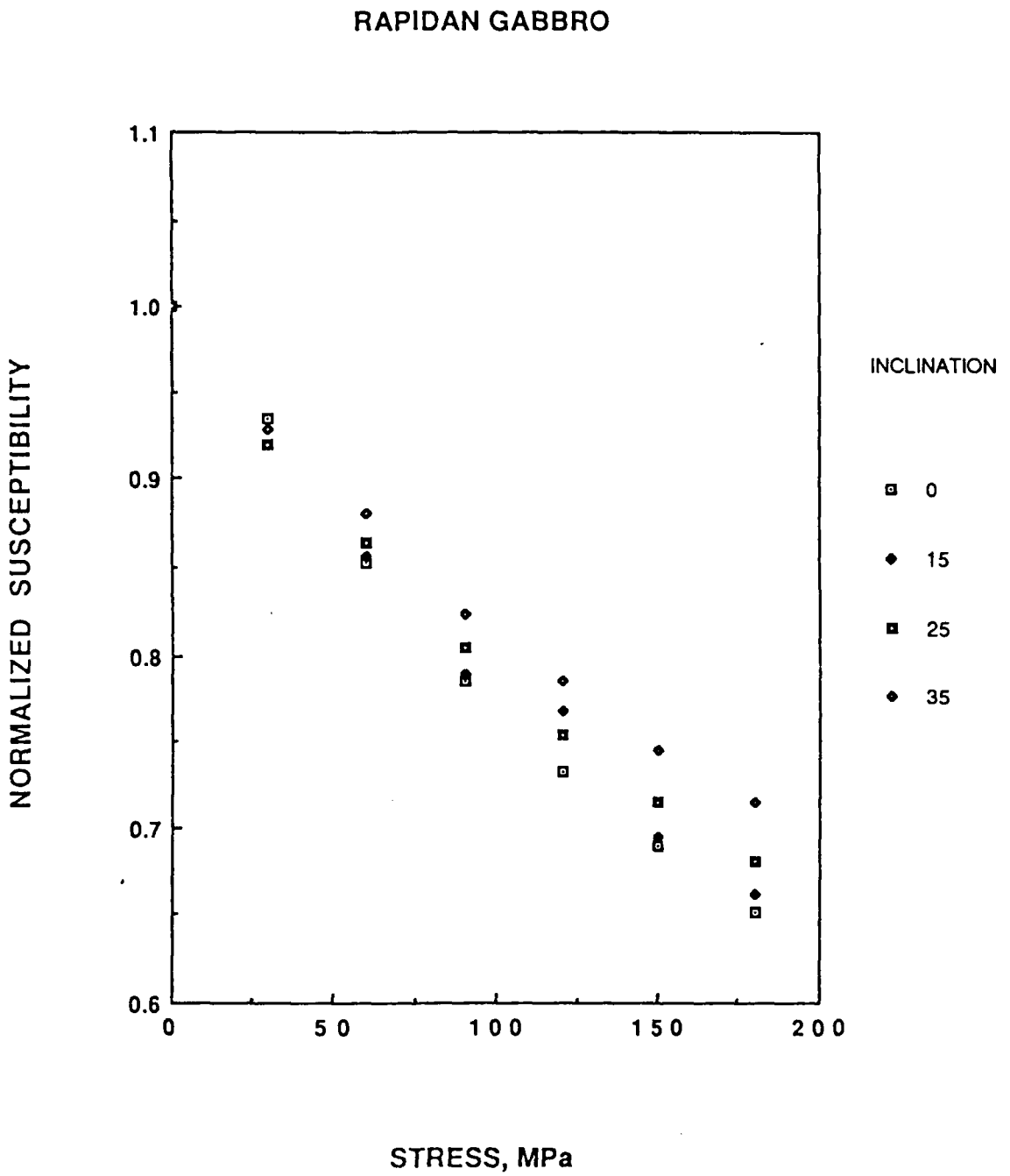

Figure 5-2. The change in normalized susceptibility is presented as a function of stress, at θ = 0, 15, 25, and 35°, for the Rapidan gabbro. The initial susceptibility was 1.79×10^{-3} emu /g/Oe..

at 15, 25, and 35° at a stress of 180 MPa were 66, 63, and 61% of their initial values. The susceptibility curves for the Westerly granite showed a reversal of order with respect to those for the previous two rock types. For both previous rock types, the longitudinal (0°) susceptibility showed the largest decrease, and the curves for θ = 15, 25, and 35° showed progressively smaller decreases. The susceptibility of the Westerly granite was smaller than that of the Ralston diabase and the gabbro (Table 1-1). For this reason, the errors in the calibration of the machine frame had relatively greater effect on the data for this rock type.

The susceptibility of all three rock types were found to be isotropic at zero stress. Then as stress was applied to the samples, they became anisotropic and the degree of anisotropy increased as the stress on the sample was increased. The magnetic susceptibility for an anisotropic mater is represented by the symmetric second-rank tensor K_{ij}, where:

$$M_i = \sum_{i=1}^{3} K_{ij} H_j \tag{7}$$

with ($K_{ij} = K_{ji}$). The susceptibility of the rock samples at each stress level was represented by a second-rank tensor. Several samples were cycled then re-positioned in the press and cycled again. The susceptibilities of these samples were symmetric with respect to the loading axis, so that the tensor had only two independent constants, K_{11} and K_{22}.

In order to derive an expression relating the susceptibility measured in a direction θ to the principal components K_{11} and K_{22} of the tensor, the sample-coil geometry must be examined in detail. This geometry is shown in Figure 5-4. The x-y coordinate system is taken to be the rock system, and the 1-2 system is the coil system. The coil system is at an angle θ to the sample system. The coaxial Helmholtz coils of the measuring transformer create a uniform field in the region occupied by the sample. This inducing field, designated $\mathbf{H}_1$, is constrained to the 1 direction of the coil system. The $\mathbf{H}_1$ field may be resolved into x and y components:

$$H_x = H_1 \cos\theta \tag{8}$$

$$H_y = H_1 \sin\theta \tag{9}$$

Because the sample is anisotropic for the fixed stress level o, the magnetization of the

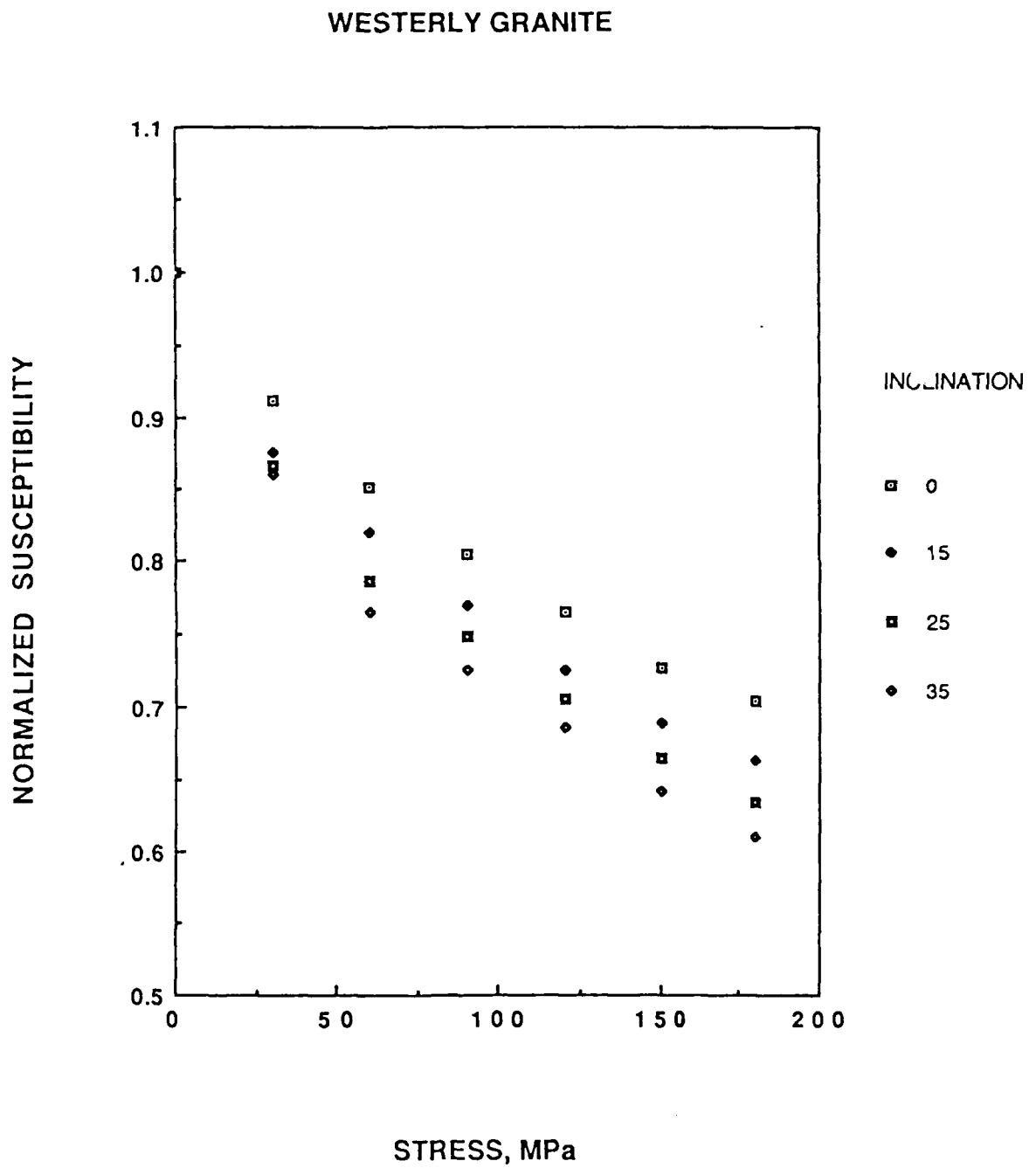

Figure 5-3. The change in normalized susceptibility is presented as a function of stress, at θ = 0, 15, 25, and 35°, for the Westerly granite. The initial susceptibility was 3.58×10^{-4} emu /g/Oe..

rock M_R, is not parallel to the inducing field H_1. The magnetization of the rock M_R, has components in the 1 and 2 directions of the coil system, M_1 and M_2, respectively. These are graphically presented in Figure 5-4. The secondary coil of the measuring transformer was assumed to be affected by only the M_1 component of magnetization. The M_2 component will, in fact, cause some response in the secondary coil. Intuition suggests that the M_2 effect will be small, and this has been verified by modelling the response in the secondary coil due to the M_2 component of magnetization. This M_1 component of magnetization may be constructed from its x and y components.

$$M_1 = M_x \cos\theta + M_y \sin\theta \tag{10}$$

The magnetization in the x-direction is equal to the susceptibility in the x-direction times the inducing field in that direction,

$$M_x = K_x H_x \tag{11}$$

similarly for the y-direction:

$$M_y = K_y H_y \tag{12}$$

Substituting (11) and (12) into (10):

$$M_1 = K_x H_x \cos\theta + K_y H_y \sin\theta \tag{13}$$

and substituting (8) and (9) into (13),

$$M_1 = K_x H_1 \cos^2\theta + K_y H_1 \sin^2\theta \tag{14}$$

This may be written as:

$$\frac{M_1}{H_1} = K_x \cos^2\theta + K_y \sin^2\theta \tag{15}$$

The quantity M_1/H_1 is defined as the effective susceptibility measured in the direction θ at the fixed stress level, σ,

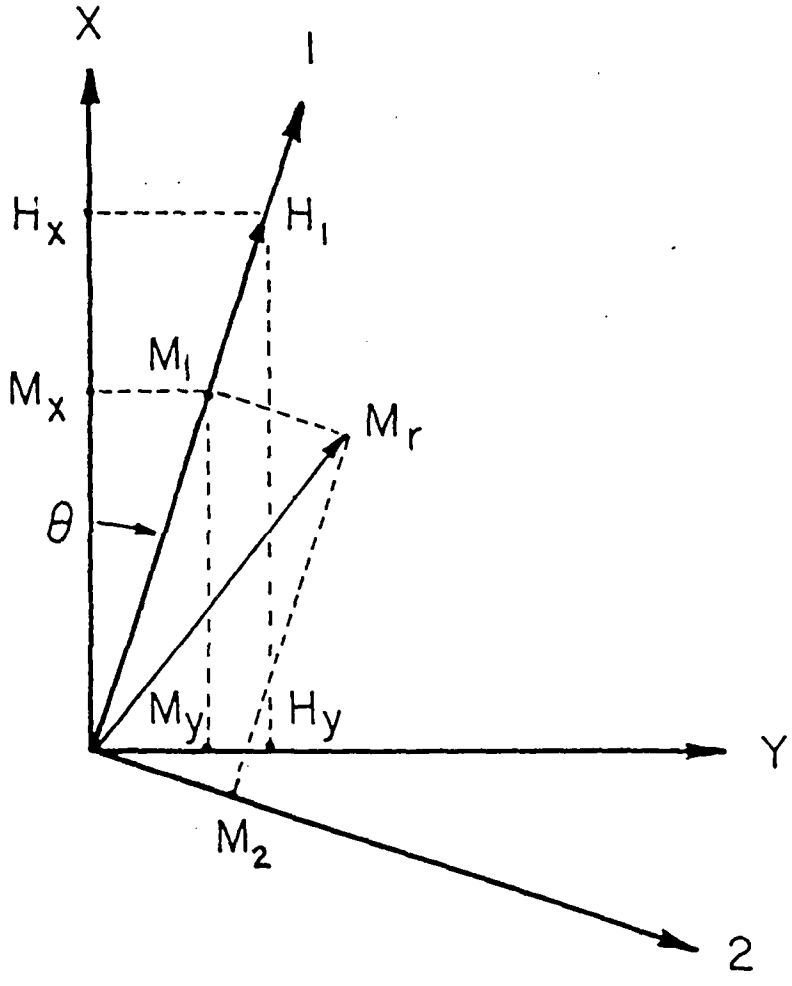

Figure 5-4. The sample-measuring transformer geometry. The x-y system is the sample system and the 1-2 system is the coil system. The coil system is rotated θ degrees with respect to the sample system. The inducing field, H, is created by the coaxial Helmholtz coils; M_r is the resulting magnetization in the rock sample.

$$K_e(\theta, \sigma)_\sigma = \frac{M_1}{H_1} \tag{16}$$

also, $K_x = K_{11}$ and $K_y = K_{22}$.

Finally, the expression relating the effective susceptibility in the θ direction to the principal components of the tensor is:

$$K_e(\theta, \sigma)_\sigma = K_{11}\cos^2\theta + K_{22}\sin^2\theta \tag{17}$$

The effective susceptibility at each stress level was determined for four values of θ. This gave, at each stress level, a set of 4 equations in the 2 unknowns (K_{11} and K_{22}). This overdetermined set of equations was inverted by least squares. The solution of the least square problem at each stress level gave the principal components of the tensor as function of stress. The K_{11} component is the susceptibility parallel to the loading axis and K_{22} is the susceptibility normal to the loading axis..

The principal components K_{11} and K_{22} at each stress level for the Ralston diabase are shown in Figure 5-5. The K_{11} component was fitted as a function of θ, by trial and error with a curve of the form:

$$K_{11} = \frac{1}{1 + \beta\sigma} \tag{18}$$

For the data shown in Figure 5-5, $\beta = 3.6 \times 10^{-5}$ MPa^{-1}. The K_{22} component was fitted by trial and error with a line:

$$K_{22} = 1 - m\sigma \tag{19}$$

The value for m is 6.4×10^{-6} MPa^{-1}.

The principal components as functions of stress for the gabbro are presented in Figure 5-6. The K_{11} and K_{22} components, as functions of stress, for this rock type were fitted by trial and error with a curve and line as was done for the Ralston intrusive using equations (18) and (19). Values of $\beta = 3.0 \times 10^{-5}$ MPa^{-1} and $m = 9.2 \times 10^{-6}$ MPa^{-1}, were computed for this data set.

The principal components for the Westerly granite, are shown in Figure 5-7. Large standard errors in the least squares solutions for this rock are due to the relatively large error in the original data (Figure 5-3). The K_{11} component for this sample was fit by

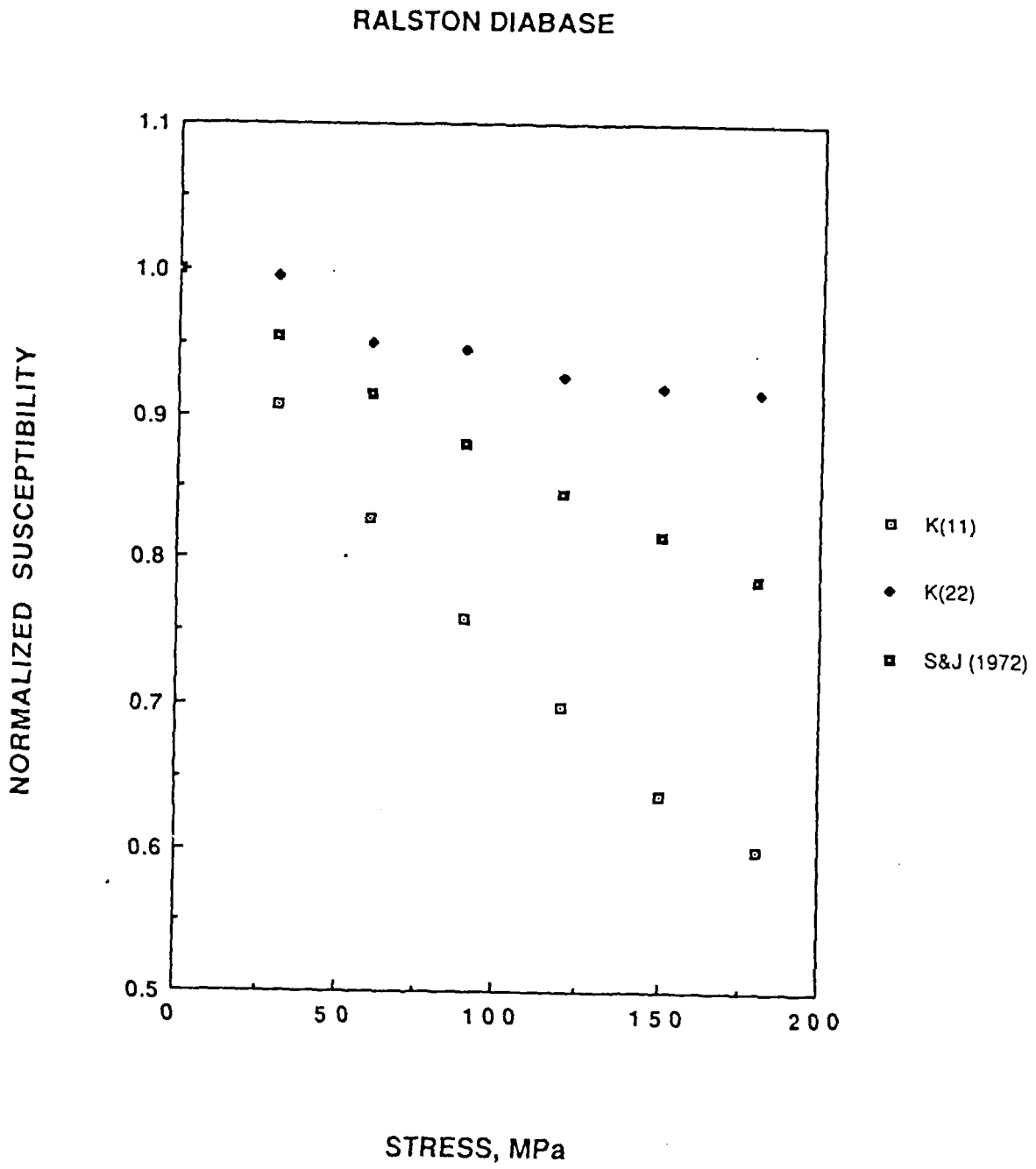

Figure 5-5. The principal components of the susceptibility tensor as functions of stress for the Ralston intrusive. The curves were fitted by trial and error to the data for the k_{11} and k_{22} components, respectively. The theoretical curve for the k_{11} component predicted by *Stacey and Johnston* (1972) is also shown.

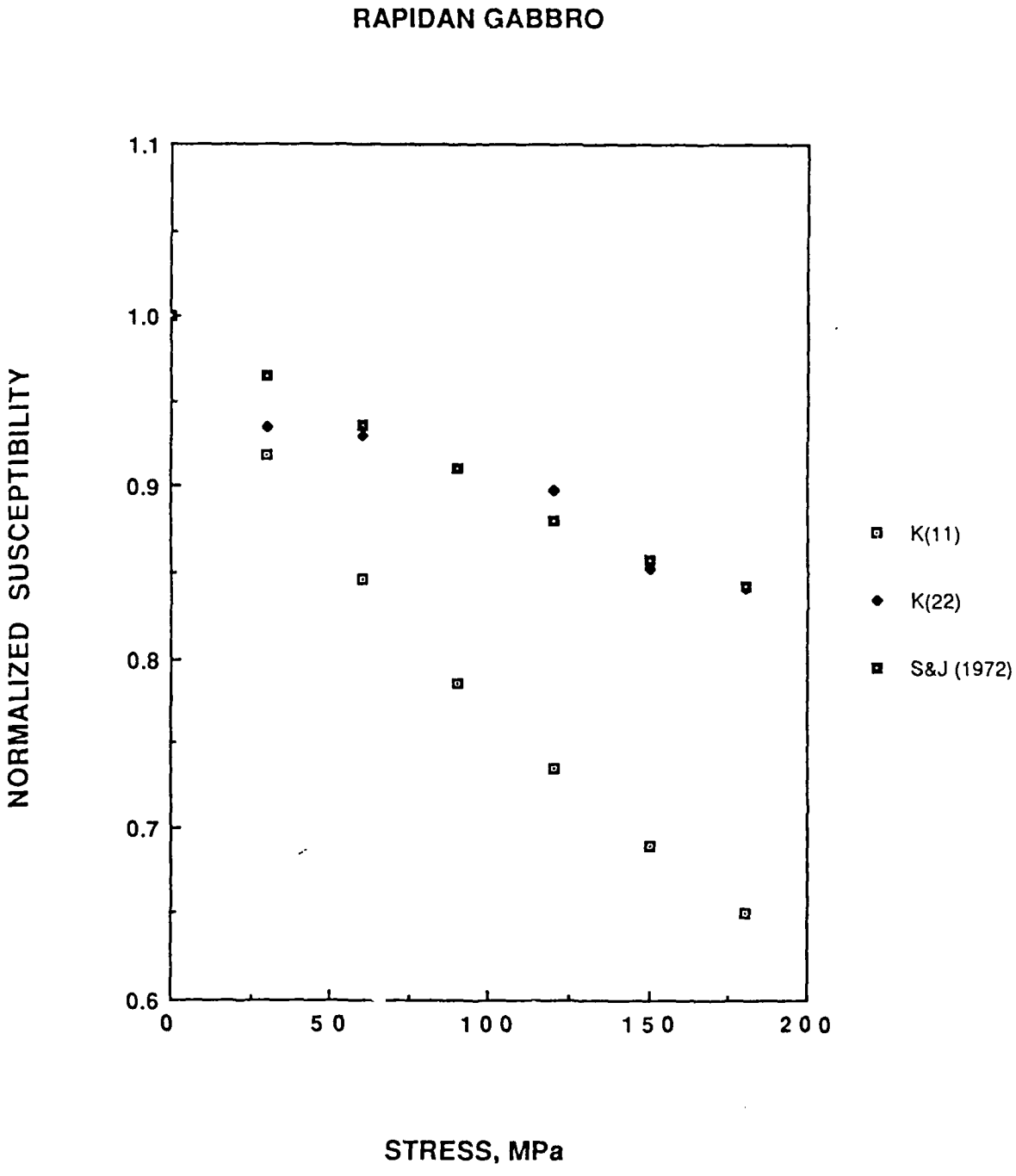

Figure 5-6. The principal components of the susceptibility tensor as functions of stress for the Rapidan gabbro. The curves were fitted by trial and error to the data for the k_{11} and k_{22} components, respectively. The theoretical curve for the k_{11} component predicted by *Stacey and Johnston* (1972) is also shown.

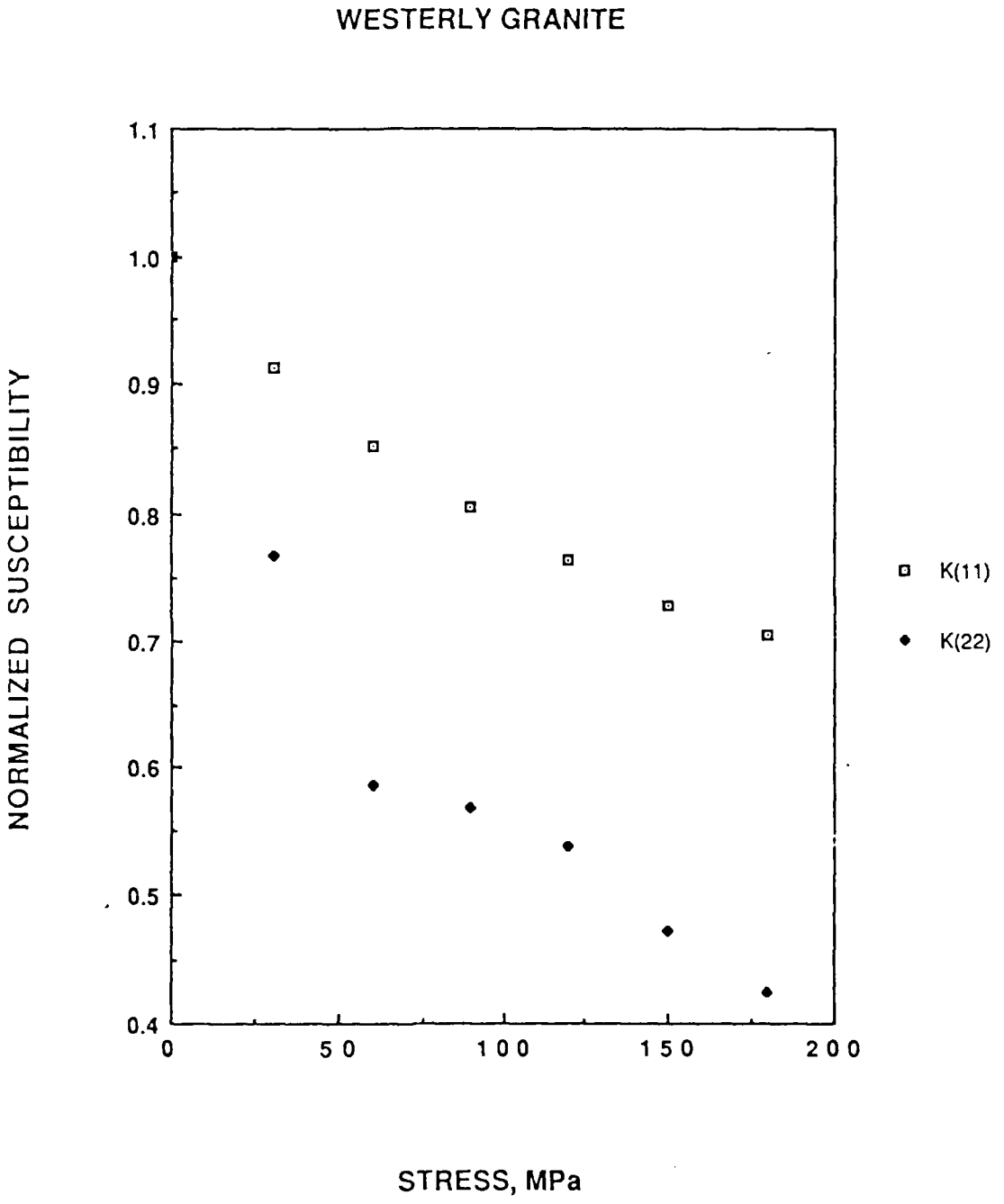

Figure 5-7. The principal components of the susceptibility tensor as functions of stress for the Westerly granite. The curve was fitted by trial and error to the k_{11} component.

error in the original data (Figure 5-3). The K_{11} component for this sample was fit by trial and error with a curve via equation (19), similar to those for the previous two rocks; the Ralston intrusive and gabbro. For the data presented in Figure 5-7, $\beta = 2.7 \times 10^{-5}$ MPa^{-1}. No curve was fitted to the K_{22} component because of the large errors in the least squares solutions.

Discussion

The susceptibility of each rock type at zero stress was isotropic ($K_{11} = K_{22}$). The susceptibility became anisotropic as stress was increased ($K_{11} \neq K_{22}$).

The effective susceptibility at a fixed stress level could be represented by the second-rank tensor k_{ij}. Further, the susceptibility was symmetric around the stress axis, so that the tensor reduced to a 2 x 2 matrix. A least squares routine was used to invert the measurements at each stress and obtain the principal components of the tensor at that stress.

The K_{11} component could be fit by a curve of the form

$$K_{11} = \frac{1}{1 + \beta\sigma} \tag{18}$$

for all three rock types tested. This was consistent with previous experimental results. The expression obtained by *Kean et al.* (1976) for the stress dependence of the longitudinal susceptibility, given by equation (3) (for $\theta = 0^{o}$), was consistent with the results of these experiments only over a greater stress range. The slope of the longitudinal susceptibility (k_{11}) as a function of stress decreased as stress was increased; the expression obtained by *Kean et al.* (1976), which is linear in stress, was found to diverge from the measured curves at high stresses.

The k_{22} component could be fit with a line of the form:

$$K_{22} = 1 - m\sigma \tag{19}$$

where m is a constant of the material, and does not appear to be related to the constant β. The approximate relationship was valid for the results on the Ralston intrusive and the gabbro, and was inconsistent with all previous experimental results. All earlier investigators, including *Kean et al.* (1976), found that the transverse susceptibility increased with stress as

$$K_{22} = 1 - \frac{\beta\sigma}{2} \tag{1}$$

where β was negative. The transverse susceptibility for the Westerly granite actually showed a larger decrease than the longitudinal susceptibility. Although no curve was fit to the data for the transverse susceptibility of this rock type because of the large error, the trend in the data was definitely real.

The effective susceptibility measured in an intermediate direction to the stress axis was given by:

$$K_e(\theta, \sigma)_\sigma = K_{11} \cos^2\theta + K_{22} \sin^2\theta \qquad (17)$$

where θ is the angle between the stress axis and the direction of the external magnetizing field and K_{11} and K_{22} are given above. As mentioned above, *Kean et al.* (1976) were the only other investigators to measure the susceptibility in intermediate directions relative to the stress axis. Their expression for the susceptibility as a function of stress and orientation, given in equation (3), did not fit the data collected in the these experiments. Specifically, their expression was linear in stress for a fixed direction of measurement while the data collected in these experiments had curvature.

The Ralston intrusive, which had a higher titanomagnetite content, showed a greater stress sensitivity than the gabbro. This was consistent with the findings of *Kean et al.* (1976). They found, for example, that an increase in the composition parameter x of the titanomagnetite in the solid solution series $xFe_2Ti_4(1\text{-}x)Fe_3O_4$ resulted in an increased stress sensitivity.

The stress cycling had no effect on the susceptibility curves after the first cycle. There was slight hysteresis during the unloading of the first cycle; the curves became reproducible for subsequent cycles.

The theoretical models for the stress sensitivity of the longitudinal and transverse susceptibilities proposed by *Stacey and Johnston* (1972), based on magnetostrictive models, failed to predict the observed stress sensitivities. The theoretically predicted curves for the longitudinal susceptibilities of the Ralston intrusive and gabbro are shown in Figures 5-5 and 5-6. These theoretical curves differed from the observed results by almost 20% at 180 MPa. The theoretical models for the stress sensitivity of the transverse susceptibility predicted an increase in the susceptibility normal to the stress axis. The results of the least-square inversion of the measurements did not show an increase in the transverse susceptibility for any of the three rock types tested.

The results of these experiments indicate that the changes in susceptibility associated with uniformly distributed differential stresses in the earth of a hundred MPa or so are going to be small even in the "best possible case" when the differential stress axis is parallel to the earth's field. The changes would be on the order of 4 or 5%. These experiments also indicate that the earth's field may make a significant angle, up to 45^o, with the differential stress axis and the change in susceptibility in that direction will not be

drastically different from the "best possible case". This result is encouraging in that a significant geomagnetic anomaly may be observed in a tectonically active region where the compressive stress axis does not coincide with the direction of the earth's magnetic field.

It is reasonable to assume that local stress concentrations may exceed tens of MPa. The presence of faults and joints in crustal rocks indicates that the local stress concentration exceed the fracture strength of the rocks. In these areas, large changes in susceptibility may be expected that would result in a significant geomagnetic anomaly.

The tensor representation for the stress-dependence of magnetic susceptibility will benefit the modelling of stress-induced geomagnetic anomalies. A possible scheme for this modelling would be as follows. First, a distribution of stress would be calculated for the geologic event of interest. Then, the direction of the compressive stress axis relative to the earth's magnetic field would be determined for the distribution of stress. The susceptibility in the direction of the earth's field, and therefore the anomalous magnetic change, could then be determined using the susceptibility tensor.

Conclusions

A suite of experiments have been carried out on a wide variety of rock types to examine the effect of pressure and stress on their magnetic properties. Specifically, the effect of loading path on thermoremanent magnetization (TRM) and magnetic susceptibility have been examined in detail. For samples with a TRM, initial loading produced a pronounced decrease in magnetization. As the specimen was unloaded, very little recovery in magnetization was observed resulting in a permanent demagnetization at the termination of the cycle. Furthermore, differential stress produced a larger demagnetization than hydrostatic pressure. For example, similar specimens with the same initial remanent intensities were loaded to 200 MPa in both pressure and uniaxial stress. Demagnetizations of approximately 20% were observed during pressurization, while the change in magnetization approached 40% of a differential stress of 200 MPa. If the specimen was reloaded over the same path to the same stress, the change in magnetization was much smaller than for the initial cycle, and only a small additional increment of demagnetization was observed at the end of the cycle. If the peak stress was augmented, once the peak stress from the previous cycle was exceeded, the stress sensitivity increased noticeably. Upon unloading, there was a pronounced hysteresis and additional permanent demagnetization at zero stress.

If the mode of deformation changed from hydrostatic to uniaxial stress, a greater stress sensitivity was observed for those cycles conducted under nonhydrostatic stress than for those carried out hydrostatically. Furthermore, for the first cycle after the transition, a permanent demagnetization was noted when the stress was removed. Additional cycles to the same peak stress became reproducible with no increase in the permanent demagnetization. If, on the other hand, the mode of deformation changed from uniaxial compression to hydrostatic, the observed stress sensitivity decreased and no permanent demagnetization occurred.

In addition to considering the total intensity of the remanent moment, specific attention was paid to the components of magnetization parallel and normal to the axis of the cylindrical specimen. For specimens where the remanent vector was parallel to the cylinder axis, the data was simply reported in terms of a change in intensity. However, as the inclination of the magnetic vector rotated away from the cylinder axis, changes in both components became more important. By continuously measuring the axial and transverse components of the remanent vector as a function of stress and pressure, it was possible to determine if significant rotations of the magnetic vector accompanied a reduction in intensity. For specimens loaded in hydrostatic compression, no rotation of the magnetic vector was evident and the rock simply demagnetized in direct proportion to the applied pressure. It is important to note that even during the first pressurization cycle, when the amount of demagnetization was large, no rotation of the vector occurred.

During uniaxial compression, however, small rotations of the magnetic moment, on the

order of three degrees, were observed during the loading portion of the initial cycle. During the unloading segment of the first cycle, changes in orientation were less than 0.25°. During subsequent cycles conducted in uniaxial compression to the same peak stress, the orientation of the vector remained stable. Only when the peak stress was increased above the peak for the previous cycle was additional rotation observed. Once again, as the specimen was unloaded, the inclination did not recover.

Since the orientation of the remanent vector with respect to the sample axis could be treated as a vector, it was of interest to see how each component transformed at various pressures and differential stresses. A series of experiments were carried out for various inclinations of the magnetic vector with respect to the axis of the specimen. For the hydrostatic case, the change in magnetization during initial loading to 200 MPa transformed according to

$$\Delta J_A = \Delta J_{200} \cos \theta$$

$$\Delta J_R = \Delta J_{200} \sin \theta$$

where ΔJ_A and ΔJ_R are the components of the remanent vector measured with respect to the sample geometry, θ is the inclination of the magnetic vector with respect to the sample axis, and ΔJ_{200} is the change in remanent intensity at a pressure of 200 MPa. An examination of the data presented in Figure 3-3 shows that the remanent moment at a fixed pressure transforms as a vector.

A series of experiments carried out in uniaxial compression on gabbro specimens for inclinations of the magnetic vector between 4° and 78° also transformed according to a similar relationship. The components of magnetization with respect to the sample axis measured at a differential stress of 200 MPa could be related according to the following equations.

$$\Delta J_A = (d_{111} \cos \theta + d_{211} \sin \theta)\, \Delta \sigma_{11}$$

$$\Delta J_R = (d_{211} \cos \theta + d_{111} \sin \theta)\, \Delta \sigma_{11}$$

where θ is the inclination of the magnetic vector, d_{111} and d_{211} are components of a proposed piezomagnetic tensor, and $\Delta \sigma_{11}$ is the change in stress. The coefficients were computed using the data set collected on the specimen at an inclination of 4° and the transformation predicted using these values. This prediction is shown with solid lines in Figure 3-8. The data scatters very closely about the predicted behavior for both components.

Based on this transformation, it was anticipated that the change in remanent magnetization with stress could be treated as a quasi-third rank tensor. However, since the change in magnetization with pressure or stress was nonlinear and markedly hysteretic, the strict formulation could not be pursued. Consequently, a straightforward characterization of the piezoremanent behavior cannot be characterized using a third rank tensor. The sensitivity of TRM to loading path, as well as previous stress history, suggests that each situation must be treated independently.

Magnetic susceptibility relates the observed magnetization with the inducing field. Typically this relationship can be represented with an equation of the form

$$J_i = K_{ij} H_j$$

where J_i is the observed magnetism, K_{ij} is the magnetic susceptibility, and H_j is the external magnetic field. For a rock in the presence of a fixed field, uniaxial stress produces a decrease in magnetization. Since the field is constant, the change in magnetization is directly proportional to the change in susceptibility. Consequently, in most discussions, susceptibility is discussed rather than the induced magnetization. This is particularly convenient when both remanent magnetization and induced magnetization are discussed in treating the total magnetic effect.

Differential stress causes magnetic susceptibility to decrease monotonically with increasing load. The changes are much greater at low stresses than they are at higher stresses. At stresses approaching 1,000 MPa, the stress sensitivity for susceptibility becomes very small and in the limit tends to approach zero. *Kern (1961)* and *Stacey and Johnston (1962)* developed a theory for the change in magnetic susceptibility due to stress based on the magnetostrictive constants of the magnetic minerals. The general form of the equation they developed is consistent with the observed results. However, significant deviations occur, often by as much as 50%. This is most likely due to imperfections in the grains that make up the rock while the magnetostrictive coefficients are typically determined on large relatively pure crystals.

Several experiments were carried out to examine the effect of hydrostatic pressure on susceptibility. The results of these tests clearly indicate that hydrostatic pressure does not influence magnetic susceptibility. This observation was predicted by *Kern (1961)* based upon his analysis.

Most susceptibility experiments are carried out for geometries where the inducing field is parallel to the greatest principal stress direction. For this arrangement, only one component of magnetic susceptibility can be obtained. Given that most rocks are isotropic at zero stress, the susceptibility is independent of orientation. However, with the application of load, an anisotropy is introduced into the rock, and the

transverse component of susceptibility must be considered. In order to examine this behavior, a suite of experiments was carried out where the inclination of the inducing field was not coincident with the uniaxial stress axis. The results of these tests show that the two components of magnetization could be determined by analyzing the observed magnetization as a function of sample geometry. It was found that the axial component of susceptibility, K_{11} could be fit by an equation of the form

$$K_{11} = \frac{1}{1 + \beta\sigma}$$

where β is the stress sensitivity and σ is the applied stress. This equation could also be fitted to the data collected when the inducing field was parallel to the stress axis. The transverse component, K_{22}, was fitted to an equation of the form

$$K_{22} = 1 - m\sigma$$

where m is a constant and σ is the stress. For three rocks studied, the transverse component of magnetization decreased with increasing stress, but at a much smaller rate than the axial. *Kean et al (1976)* found that the transverse component showed a slight increase with increasing stress. Since different rock types were used, it is definitely possible that for some titanomagnetite composition and grain sizes, the transverse component can increase with stress. Once both components of susceptibility are known, the magnetization for all intermediate inclinations of the principal stress direction with respect to the inducing field can be calculated.

The experimental results may be interpreted in terms of domain characteristics. Direct observation of domain behavior during cyclic loading has been carried out by *Boyd et al.*,(1984). They studied the motion and nucleation of magnetic domains as a function of applied stress. Tests on pseudosingle domain magnetite titanomagnetite assemblages showed that at very low stresses walls were nucleated. As the stress was augmented, additional domains nucleated and the domains adjusted to achieve a lower energy configuration. When the stress was removed, the domain pattern was irreversibly changed. *Halgedahl and Fuller* (1983) observed a similar effect due to the application of large magnetic fields. As the inducing field was increased, domains nucleated and the spacial distribution of preexisting domains was altered. When the direction of the field was reversed, the domain pattern did not exhibit a reversible behavior but showed a pronounced hysteresis.

The results reported by *Boyd et al.*(1984) and *Halgedahl and Fuller* (1983) clearly demonstrate that the nucleation and motion of domain walls adequately explain the

observed changes in magnetization due to the application of stress or the magnetic hysteresis observed as the inducing field is varied in a cyclic fashion. The nucleation sites are most likely high energy regions within the grain. As the stress increases, the energy barrier for nucleation is exceeded and the domain migrates to reduce its free energy. From this point of view it is relatively easy to understand why hydrostatic pressure produces a lower stress sensitivity than non-hydrostatic stress. Shear stress is much more efficient in moving imperfections such as dislocations or vacancies within the particle than hydrostatic pressure. The first loading cycle on a specimen with undisturbed remanence produces permanent demagnetization. Most likely the initial remanence is unstable at room temperature and elevated pressure and readjusts to a more stable configuration. This produces a permanent change. Repeated application over the same path does not produce any further permanent variation.

In contrast with the effect of stress on remanent magnetization where the experiments were carried out in zero field, induced magnetization only exists in the presence of a field. Consequently, at zero stress, the domain structure is in an equilibrium configuration with respect to the applied field. As differential stress is applied to the system, the domains nucleate and distort in response to the change in energy. At extremely high stresses, the nucleation and rotation reaches a point at which it can no longer sustain further motion. Consequently, the change in susceptibility exhibits an extremely low stress dependence. This is analogous to the situation where the field on a crystal is increased until magnetic saturation occurs. In fact a very simple calculation for several of the rocks studied here shows that the strain energy of the magnetic mineralogy at 1,000 MPa is of the same order as the work done on a titanomagnetite crystal by an external field at saturation. It has already been pointed out by *Halgedahl and Fuller (1983)* that differential stress produces domain distortions and nucleations very similar to those observed with the application of stress. In light of this observation, it is reasonable to assume that there is an equivalence between the energy developed in a crystal due to the application of large fields, and the strain energy at high stresses. Therefore, it appears that the stress sensitivity is controlled by the domain state in the magnetic carrier. Furthermore, saturation magnetization should occur at lower field strengths as the stress on the magnetic assemblage increases.

The application of the piezomagnetic effect to real problems has occurred in several ways. Magnetic anomalies have been observed prior to a number of earthquakes. *Smith and Johnston (1976)* observed a 1.8 gamma anomaly prior to the 1975 Thanksgiving Day earthquake near Hollister, CA. Numerous other events have been reported worldwide prior to and concomitant with major tectonic events. Since it has been shown that changes in rock magnetization, in the absence of fluid flow, are directly related to the change in stress applied to a rock body with a defined magnetization, it is reasonable to assume that the observed magnetic anomalies reflect a change in stress in the fault zone. In order to calculate the change in stress associated with a particular anomaly, an inversion of the data must be carried

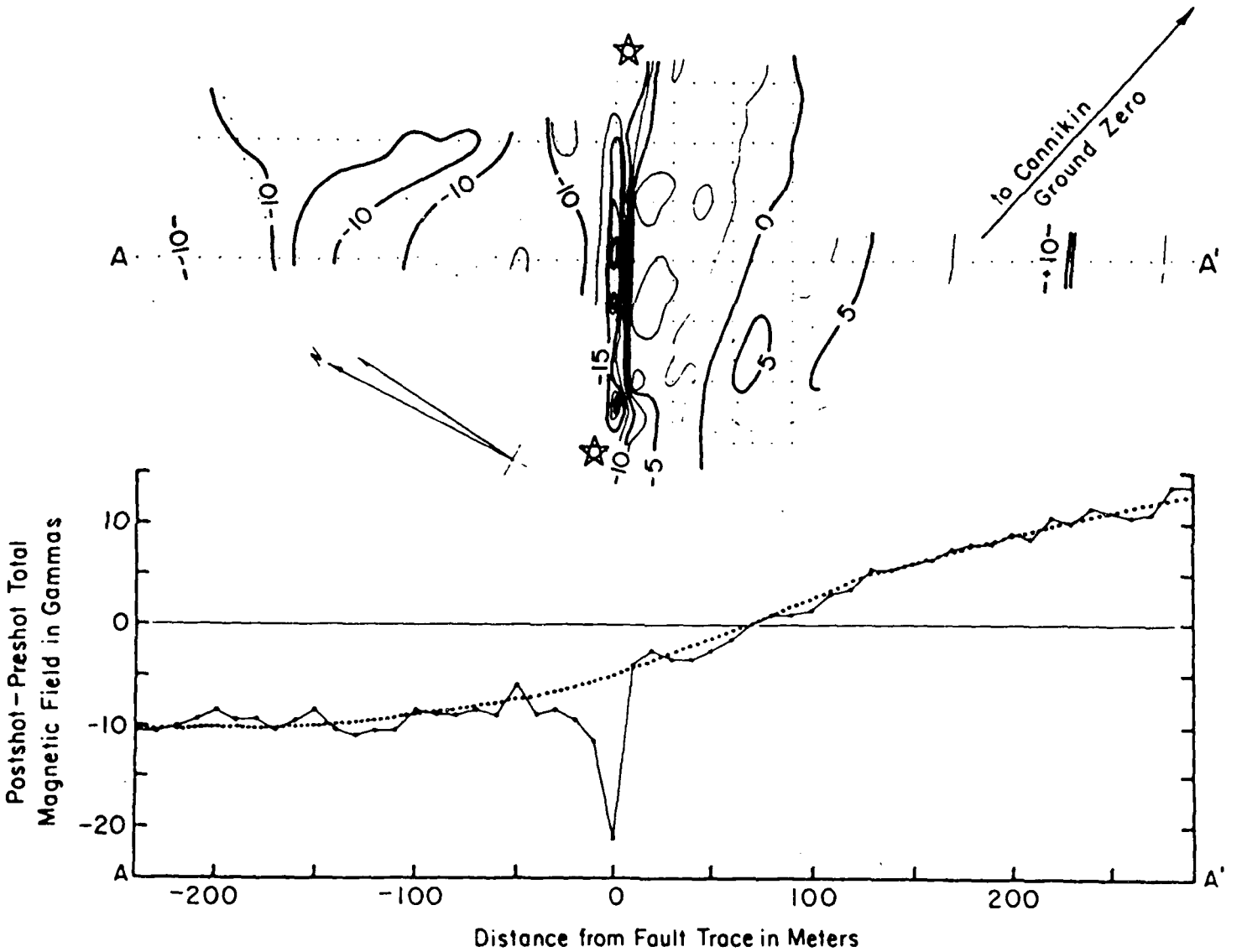

Figure 6-1 Postshot-minus-preshot differences in total magnetic field in the fault study area. Contour interval is 2.5 gammas, and station spacing is 10 m. Surface trace of Teal Creek Fault passes through starred positions on map. Profile is drawn southeasterly along longest line of array from A to A'.

out. In most cases, there is only a single station, or at most a small array of stations, that record the anomalous behavior. Based on such a limited data set, the inversion is not well constrained and the results are ambiguous.

One well defined magnetic anomaly does exist. In 1971, a detailed magnetic survey was carried out along the Teal Creek Fault, Amchitka Island, before and after the detonation of the CANNIKAN nuclear event *(Hasbrouk and Allen, 1972)*. The results of this survey are shown in Figure 6-1. A cross section normal to the fault shows a definite magnetic anomaly in the region around the fault with a 30 gamma spike centered directly over the fault zone. In this case, there was certainly enough information to carry out a detailed inversion of the magnetic data to obtain the change in stress along the fault associated with the explosion.

In order to evaluate this problem, a group of rock cores were obtained from the geologists who originally mapped in the vicinity of the Teal Creek Fault. Oriented specimens were prepared from these rocks. Then, the a series of piezomagnetic experiments were carried out to determine the influence of deviatoric stress on the natural remanent magnetization (NRM) and magnetic susceptibility. Next, an inversion was carried out to determine the change in magnetization, at depth, to produce the observed anomalous behavior. A simple dislocation fault model was chosen for the analysis, and the magnetic anomaly was developed in terms of changes in magnetization along the fault zone required to produce the magnetic signature observed in Figure 6-1. Since the problem was well constrained, the only assumption was that the orientation of the current magnetic field was parallel to the field that produced the NRM in the basalt cut by the fault. Preliminary results for this area indicate that the average shear stress acting along the Teal Creek Fault changed by 0.8 MPa due to the CANNIKAN event *(Narbut, Martin, and Greenfield, manuscript in preparation)*. This work is ongoing, and should be completed within the next year.

A much more constrained experiment was carried out during the high explosive test, ONE TON, at the Nevada test site. A series of rock cores were fielded in the vicinity of the working point to test the applicability of using decreases in rock magnetization to measure peak stress. In principle, the technique was extremely simple. Laboratory studies have demonstrated that during initial loading of rock samples, the remanent magnetization decreases. Upon unloading, a permanent demagnetization was observed. Furthermore, the magnitude of the decrease in remanent intensity was proportional to the peak stress experienced by the rock. Based on this observation, a series of rock cores with known magnetic properties were grouted along the tuff-grout interface of the access drift to ONE TON at selected distances from the working point in order to test the piezomagnetic effect as a passive stress sensor.

After the test the samples were retrieved; nearly all the samples were recovered intact. Next, the permanent demagnetization of each sample was computed (Figure 6-2). The magnitude of the change in remanent intensity was then correlated with the stress required to produce the same amount of demagnetization in laboratory samples of the same rock type (Figure 6-3). In this way, the peak stress developed by the change was obtained as a

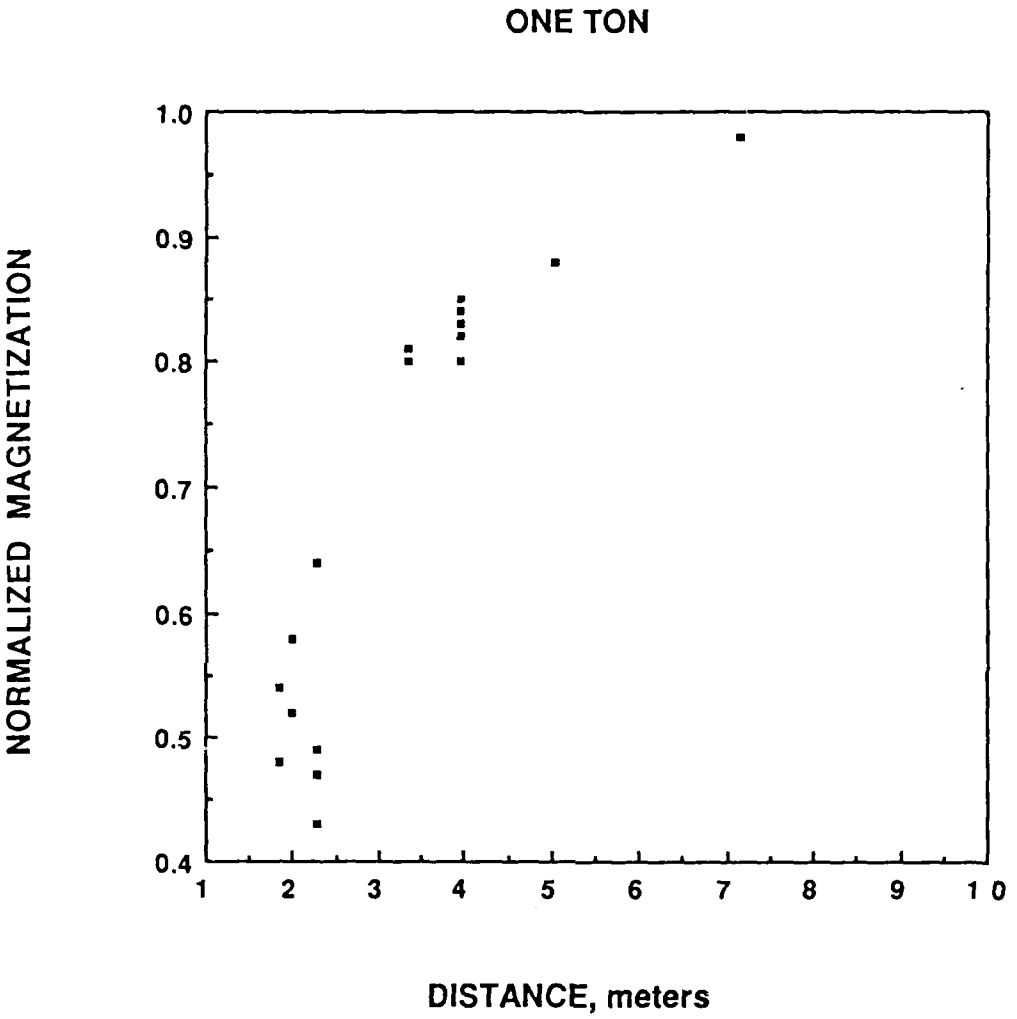

Figure 6-2 The postshot / preshot remanent magnetization is shown as a function of range for specimens of Rapidan gabbro recovered after the detonation of the ONE TON experiment.

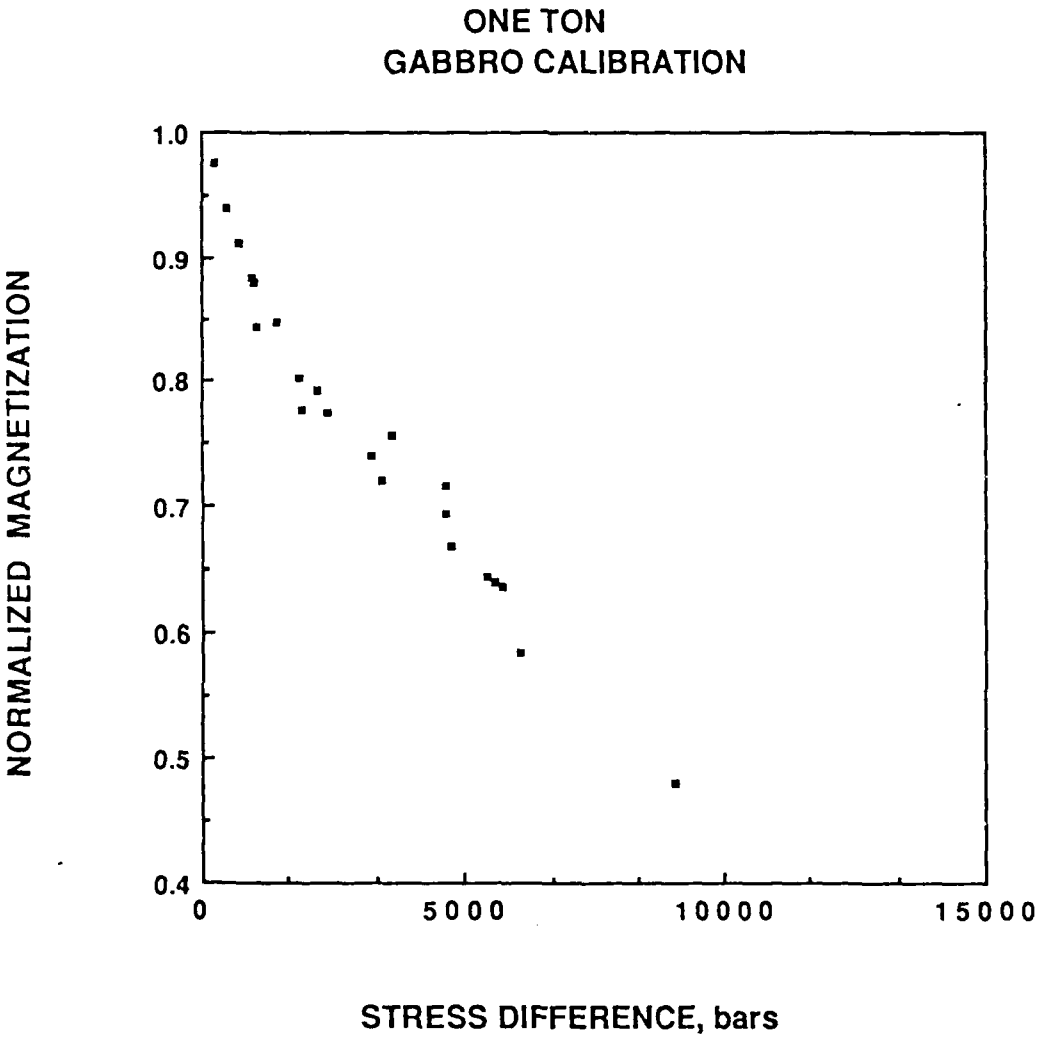

Figure 6-3 The postcycle, zero stress magnetization of gabbro specimens normalized to their initial TRM intensity are plotted as a function of the maximum differential stress experienced by the sample during a series of cyclic loading experiments. The tests were conducted in confined compression at confining pressures to 1500 bars (150 MPa). The initial TRM intensity was $3.50 \pm 0.10 \times 10^{-2}$ emu/cm^3.

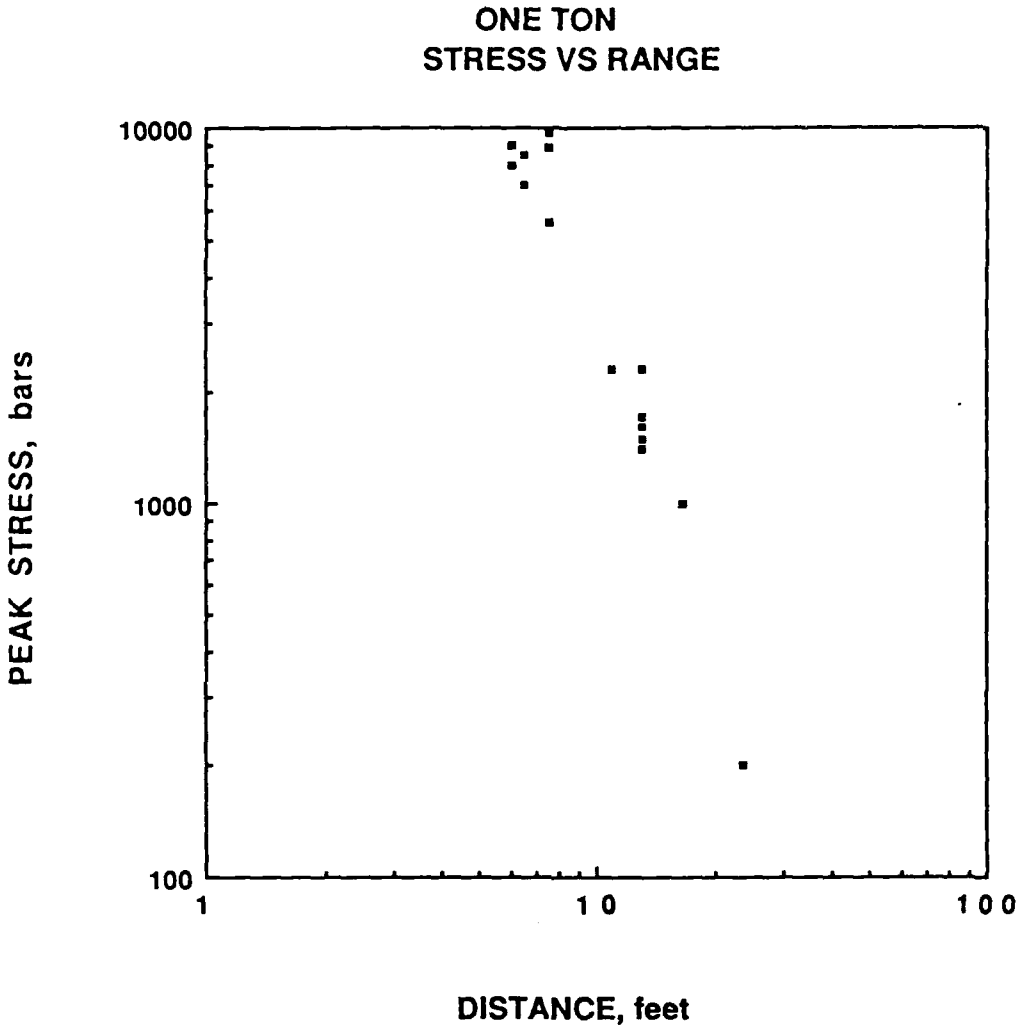

Figure 6-4 The inferred peak stress determined from the demagnetization of the Rapidan gabbro specimens is plotted as a function of distance from the working point on ONE TON.

function of range (Figure 6-4). These measurements are in very good agreement with the empirical equation relating peak stress to range which is used by Sandia National Laboratories. This experiment was carried out in 1983 and has been reinterpreted in terms of the results obtained in the study. Originally the data was reduced assuming that the remanent demagnetization was proportional to the axial stress. However, results obtained here indicate that magnetic changes respond primarily to differential stress. Consequently, the calibration shown in Figure 6-3 has a greater stress sensitivity, particularly at higher stresses, than was previously postulated. The net result of this correction was to reduce the peak stress in the vicinity of the working point by as much as 1,500 bars (150 MPa).

In conclusion, changes in rock magnetization due to pressure and differential stress follow a very characteristic pattern. When only susceptibility is considered, theoretical models adequately explain many of the observations. However, with regard to remanent magnetization, while the mechanisms governing the piezomagnetic effect are the same as those observed for susceptibility, the results are not as conducive to rigorous theoretical development. For this situation, only an empirical representation is possible and each rock type must be considered separately.

References

Boyd, J.R., M. Fuller, and S. Halgedahl, Domain wall nucleation as a controlling factor in the behavior of fine magnetic particles in rocks, *Geophys. Res. Letters, II (3)* 193-196, 1984.

Carmichael, R.S., Stress control of magnetization in magnetite and nickel and implications for rock magnetism, *J. Geomag. Geoelect., 20,* 187-196, 1968.

Christie, K.W. and D.T.A. Symons, Apparatus for measuring magnetic susceptibility and its anisotropy, *Geol. Survey of Canada Paper,* 69-41. 1969.

Day, R., TRM and its variation with grain size, *Origin of Thermoremanent Magnetization, Center for Academic Publication, Japan,* 1977.

Domen, H., Piezo-remanent magnetism in rock and its field evidence, *J. Geomag. Geoelect., 13,* 66-72, 1962.

Dunlop, D.J., Thermoremanent magnetization in submicroscope magnetite, *J. Geophys. Res. 78,* 1780, 1973.

Fuller, M.D., Geophysical aspects of paleomagnetism, in *CRC Critical Reviews in Solid State Sciences,* 137-218, Chemical Rubber Publishing, Cleveland, Ohio, 1970.

Halgedahl, S. and M. Fuller, The dependence of magnetic domain structure upon magnetization state with emphasis upon nucleation as a mechanism for pseudo-single domain behavior, *J. Geophys. Res., 86,* 6505-6522, 1983.

Hall, J.M. and R.N. Neale, Stress effects on thermo-remanent magnetization, *Nature, 188,* 805-806, 1960.

Hasbrouck, W.P. and J.H. Allen, Quasi-static magnetic field changes associated with the Cannikin nuclear explosion, *Bull. Seism. Soc. Amer., 62,* 1479-1487, 1972.

Ishido, T. and H. Mizutani, Experimental and theoretical basis of electrokinetic phenomena in rock-water systems and its applications to geophysics, *J. Geophys. Res., 86,* 1763-1775, 1981.

Jelenska, M., Stress Dependence on the magnetization and magnetic properties of igneous rocks, *Pure Appl. Geophys., 113,* 635-649, 1975.

Kato, Y. and S. Utashiro, On the changes in the terrestrial magnetic field accompanying the great Nankaido earthquake in 1946, *Sci. Rep. Tohoku Imp. Univ. Ser., 5,* 40-43, 1949.

Kean, W.R., R. Day, M. Fuller, and V.A. Schmidt, The effect of uniaxial compression on the initial susceptibility of rocks as a function of grain size and composition of their constituent titanomagnetites, *J. Geophys. Res., 81,* 861-872, 1976.

Lanham, M. and M. Fuller, Weak field control of remanent magnetization changes produced by uniaxial stress cycling, *Geophys. Res. Lett., 15, (5),* 511-513, 1988.

Larson, E.E., R.P. Hoblitt, and D.E. Watson, Gas-mixing techniques in thermomagnetic analysis, *Geophys. J. R. astr. Soc.,* 1-14, 1975.

Pike, S.J., T.L. Henyey, J. Revol, and M.D. Fuller, High-pressure aparatus for use with a cryogenic magnetometer, *J. Geomag. Geoelectr., 33,* 449-466, 1981.

Martin, R.J., III and J.S. Noel, The influence of stress path on thermoremanent magnetization, *Geophys. Res. Lett., 15 (5),* 507-510, 1988.

Martin, R.J., III and M. Wyss, Magnetism of rocks and volumetric strain in uniaxial failure tests, *Pure Appl. Geophys., 113,* 51-61 and 169-182, 1975.

Martin, R.J., III, R.E. Habermann, and M. Wyss, The effect of stress cycling and inelastic volumetric strain on remanent magnetization, *J. Geophys. Res. 83 (B7),* 3485-3496, 1978.

Martin, R.J., III, R.W. Haupt, and R.J. Greenfield, The effect of fluid flow in the magnetic field in low porosity crystalline rock, *Geophys. Res. Lett., 9,* 1301-1304, 1982.

Martin, R.J., III, Is piezomagnetism influenced by microcracks during cyclic loading?, *J. Geomag. Geoelectr., 32,* 741-755, 1980.

Mizutani, H. and T. Ishido, A new interpretation of magnetic field variation associated with the Matsushiro earthquakes, *J. Geomag. Geoelectr., 28,* 179-186, 1976.

Nagata, T., Tectonomagnetism, *Bull. Int. Ass. Geomagn. Aeron., 27,* 12-43, 1969.

Nagata, T. and B.J. Carleton, Notes of Piezo-remanent magnetization of Igneous Rocks, III,
J. Geomagn. Geoelect., 21, 623-645, 1969.

Ohnaka, M., Stability of remanent magnetization of rocks under compression--Its relation to grain size of rock forming ferromagnetic minerals, *J. Geomagn. Geoelect., 21,* 495-505, 1969.

Ohnaka, M. and H. Kinoshita, Effects of uniaxial compression on remanent magnetization, *J. Geomagn. Geoelect., 20,* 93-99, 1968.

Powell, D.W., Stress dependent magnetization in some quartz-dolerites, *Nature, 187,* 225, 1960.

Revol, J.R., R. Day, and M.D. Fuller, Magnetic behavior of magnetite and rocks stressed to failure-relation to earthquake prediction, *Earth Planet. Sci. Lett., 37,* 296-306, 1977.

Rikitake, T., Geomagnetism and earthquake prediction, *Tectonophysics, 6,* 59-68, 1968.

Smith, B.E. and M.J. S. JOhnston, A tectonomagnetic effect observed before a magnitude 5.2 earthquake near Hollister, California, *J. Geophys. Res., 81,* 3556-3560, 1976.

Stacey, F.D. and M.J. S. Johnston, Theory of the piezomagnetic effect in titanomagnitite-bearing rocks, *Pure Appl. Geophys., 97*, 146-155, 1972.

Tazima, M., Accuracy of recent magnetic survey and locally anomalous behavior of the geomagnetic secular variation in Japan, Thesis, University of Tokyo, 1966.